Impact of Biochar Amendment, Hydraulic Retention Time, and Influent Concentration on N and P Removal in Horizontal Flow-Through Bioreactors

Brady Steward Leigh Coleman

Thesis submitted to the faculty of the Virginia Polytechnic Institute and State University in partial fulfillment of the requirements for the degree of

Master of Science
In
Biological Systems Engineering

Zachary M. Easton, Chair
Stephen K. Stephenson
David J. Sample

November 10, 2017
Blacksburg, VA

Keywords: denitrifying bioreactor, DNBR, biochar, denitrification, nitrate, phosphate, Best Management Practice, BMP

Impact of Biochar Amendment, Hydraulic Retention Time, and Influent Concentration on N and P Removal in Horizontal Flow-Through Bioreactors

Brady Steward Leigh Coleman

Abstract

The advent of industrial, fertilizer-intensive agriculture during the 20th century has promoted export of anthropogenic nutrients, spurring degradation of ecosystem biodiversity and water quality. Exported nitrogen and phosphorus are recognized drivers of this deterioration, and require management. In the mid-1990s, denitrifying bioreactors (DNBRs), a subsurface, edge-of-field best management practice (BMP) that intercepts and treats agricultural drainage by supporting nitrate-attenuating denitrification with a saturated carbon substrate, were developed. Since then, their utility has expanded, and recent studies have unearthed biochar's capability to stimulate simultaneous nitrate (NO_3^--N) and phosphate (PO_4^{3-}-P) removal in DNBRs.

This study investigated biochar's potential as an amendment to the traditional woodchip media during nine, five-day trials on twelve laboratory-scale, horizontal flow-through DNBR columns. Three media types were tested: woodchips (W), 90% woodchips and 10% biochar (B_{10}), and 70% woodchips and 30% biochar (B_{30}). Simulated agricultural drainage with four unique concentration combinations of 16.1 and 4.5 mg L^{-1} NO_3^--N and 1.9 and 0.6 mg L^{-1} PO_4^{3-}-P was delivered at hydraulic retention times (HRTs) of 3, 6, and 12 h.

Mean NO_3^--N removal efficiencies ranged from 16.9%-93.7%, and media type was insignificant at low influent NO_3^--N concentrations, but B_{30} was the most effective at high influent NO_3^--N concentrations. Mean PO_4^{3-}-P removal efficiencies ranged from -122.0%-74.9%, with B_{10} and B_{30} significantly worse than W at removing PO_4^{3-}-P.

These findings corroborate previous work indicating boosted NO_3^--N removal with biochar, but contradict studies upholding PO_4^{3-}-P-removing capabilities.

Impact of Biochar Amendment, Hydraulic Retention Time, and Influent Concentration on N and P Removal in Horizontal Flow-Through Bioreactors

Brady Steward Leigh Coleman

General Audience Abstract

Nitrogen and phosphorus-containing nutrients are applied to agricultural fields for supporting higher crop yields, and once these nutrients are exported they can negatively impact ecosystem biodiversity and water quality. These nutrients therefore require management. Denitrifying bioreactors (DNBRs) are subsurface engineered structures that intercept and treat agricultural drainage by supporting nitrate-removing denitrification with a carbon substrate. Recent studies have unearthed the potential of biochar, which is a type of charcoal typically used for soil amendment, as a substrate for promoting simultaneous removal of nitrogen and phosphorus.

This study investigated biochar's potential as an amendment to the traditional DNBR woodchip media using laboratory-scale DNBRs that were subjected to different hydraulic retention times and influent nutrient concentrations.

Results revealed that the biochar did not significantly enhance nitrate removal under low influent nitrate concentrations, but did significantly improve nitrate removal at high influent nitrate concentrations. The biochar-amended treatments were significantly worse than the woodchip treatments at supporting phosphate removal.

These findings suggest that biochar may indeed boost nitrate removal, but may not improve phosphate removal.

I dedicate this work to my family, whose unrivaled compassion and vitality are a constant inspiration.

Acknowledgements

Thank you to my mother, **Beverly Coleman**, whose unrivaled compassion, tenacity, and brilliance never cease to amaze me. Thank you to my father, **Dillard Coleman**, for instilling my love of nature and the environment, and for the support you have provided over the years. My siblings, **Ashley Lucckese**, **Raleigh Coleman**, and **Dabney Coleman**, and siblings-in-laws, **Dan Lucckese** and **Allison Coleman**, exhibit superlative intelligence, kindness, and personality, and I am forever grateful that I have such strong role models as family members and as close friends. My nephew and nieces, **Hurley**, **Paisley**, **Hattie**, and **Lucy**, are beacons of light in my life; I am thankful for every encounter with them, and I look forward to watching their lives blossom. My grandparents, **Steward Leigh Hottinger** and **Mary Alice Hottinger**, and their exceptional moral character and family values, form the robust foundation that our family was built upon. I treasure their company and guidance. Thank you to **Jeff Stockton** for always being there for my mother, and for my entire family, and for your exemplary work ethic and generosity. Thank you to **Eddie**, **Michelle**, **Howard**, **Lindsey**, **Amy**, **Dale**, **Julia**, the **Chiles family**, the **Bayless family**, **Connie**, **Steve**, and all of the **other family members and friends that I have not named here**.

My advisor, **Zachary Easton**, inspired me to traverse into academia over four years ago, and the opportunities he has presented to me over the years are a testament to his outstanding character. I am grateful to have been witness to his peerless work ethic, intelligence, and patience. **Kurt Stephenson** and **David Sample**, thank you for your valued guidance as members of my committee. **Emily Bock**'s contributions to this project, whether it be in the form of countless hours of Lachat operation and troubleshooting, or considerate guidance and advice, were pivotal for progression, and I am grateful for her friendship. Thank you to **Martin Davis** for your contributions during the experimental design process and to **Casey Schrading**, **Colby Dechiara**, and **Justin Haber** for your assistance with the intense sampling required for this project. **Dumitru Branisteanu**'s input during preparation for the project was invaluable, and I am grateful that I had such an experienced, persistent, and personable companion to guide me through my arduous setup. Thank you to **Laura Lehmann** and **Denton Yoder**

for your support, to **Durelle Scott** for allowing me to borrow lab equipment for the project, to **Mary Leigh Wolfe** for your contributions as the department head, and to the rest of the **faculty, staff, and students of the BSE department**. Thank you to **Vinit Seghal**, **Tyler Keys**, **Jay Dixit**, **Pritam Solanki**, and **members of the BSE graduate student body** for your companionship during hiking trips.

Thank you to **Chuck Bailey**, **Rowan Lockwood**, **Brent Owens**, **Linda Morse**, and all the rest of the **faculty and staff of the College & William & Mary's Geology Department**, for providing me with an extraordinary undergraduate education, and encouraging me to pursue higher education.

Table of Contents

List of Figures

List of Tables

1 Introduction

Recent intensive agricultural practices, including excessive application of fertilizers for higher crop yields and the use of artificial subsurface drainage to improve cropland functionality, are threatening downgradient ecosystems, particularly those that are marine in nature. The inevitable transport of anthropogenic nutrients to receiving bodies of water has stirred eutrophication and the subsequent development of hypoxic and anoxic zones, in addition to a host of other adverse impacts, including, but not limited to, alteration of ecosystem biodiversity and productivity, the production of tropospheric ozone and aerosols, and methemoglobinemia, thyroid dysfunction, colon cancer, and ovarian cancer in humans (Sadeq et al., 2008; Powlson et al., 2008).

A 52-yr record of dissolved oxygen in the Chesapeake Bay from 1950 to 2001 revealed a drastic increase in the total volume of mild hypoxic, severe hypoxic, and anoxic water, a trend that was positively correlated with NO_3^--N loading in the Susquehanna River during the same time period (Hagy et al., 2004). These problems are mirrored in the Midwest, where artificial agricultural drainage has been in place for over 100 years (Dinnes et al., 2002), and, depending on soil type and N fertilizer applications rates, NO_3^-- N loss from agricultural fields can range from 25-40 hg ha^{-1}, and NO_3^--N concentrations in surrounding water bodies often exceed the EPA's maximum contaminant level (MCL) of 10 mg N L^{-1} (Jaynes et al., 2001). Mississippi River Basin nutrient loading has been causally linked and hypoxic zone formation in the Gulf of Mexico (Turner and Rabalais, 1994; Rabalais et al., 1996; Gulf Hypoxia Action Plan 2008), prompting the EPA's 2001 goal to reduce nutrient loads by 30% by 2015 (Mississippi River/Gulf of Mexico Watershed Nutrient Task Force, 2001).

Indeed, these realities have sparked great concern, and the cutback of nutrient export was deemed a principal environmental and engineering challenge in the 21st century (Galloway et al., 2008; Seitzinger et al., 2006). Denitrification management, the encouragement of reactive nitrogen removal, has been increasingly recognized as a preventative measure to combat the problem of increased nutrient loading. Denitrifying

bioreactors (DNBRs), a type of Best Management Practice (BMP), have shown great promise as a means to intercept and treat agricultural drainage; the carbon medium housed within these subsurface chambers facilitates natural nutrient removing processes, such as NO_3^--N removal through denitrification. Traditionally, woodchips have been used as a carbon substrate for supporting denitrifying microbes; their cheap cost, widespread availability, hydraulic properties, and extensive half-life make them an optimal choice for use in DNBRs. This is despite of a potentially significant drawback: failure to maintain an anaerobic environment within DNBRs can result in incomplete denitrification and the production of N_2O, a potent greenhouse gas. This has driven the search for alternative carbon sources, and recent studies have supported the potential of biochar, a substance formed through the pyrolysis of biomass, as a beneficial supplement to the well-established woodchip medium (Bock et al., 2015; Bock et al., 2016; Easton et al., 2015). Research on biochar, however, is still incipient in nature, especially in denitrifying bioreactors, and mechanisms behind its performance are still unclear.

This study assesses biochar's promise as a means to attenuate NO_3^--N and PO_4^{3-}-P, as there is still significant need to study biochar-amended media under a range of environments; the processes influencing NO_3^--N and PO_4^{3-}-P removal are complex and misunderstood, and further examination of treatment is required to optimize DNBR management practices. The recent need to identify mechanisms for "pollution swapping," the coinciding of contaminant production with DNBR nutrient removal, including greenhouse gas (GHG) emissions, organic C export, etc. has also surfaced (Fenton et al., 2014; Healy et al., 2012; Schipper et al., 2010b), warranting examinations of processes in controlled settings. The need for continued research on DNBR column studies has been stressed in the literature, especially those that investigate NO_3^-- N removal in concert with other relevant processes and phenomena, such a PO_4^{3-}-P removal and GHG emissions (Addy et al., 2016).

2 Literature Review

Of the elements essential for life (nitrogen (N), carbon (C), phosphorus (P), oxygen (O), and sulfur (S)), N is the most abundant on Earth, with an estimated global mass of ~4 x 10^{21} g, exceeding the combined masses of the other four crucial elements, and comprising approximately 78% of the atmosphere (Galloway et al., 2003). Nitrogen's importance should not be understated; it plays a key role in the synthesis of the two most indispensable polymers for the existence of life: nucleic acids and proteins (Canfield et al., 2010). N also has remarkable versatility, spanning seven oxidation states. Despite its abundance, importance, and versatility, N is ironically the least biologically available of the elements essential for life (Galloway et al., 2003; Moir, 2011). A key reason for this is that the vast majority of this N is manifested in its molecular form, N_2, a compound that is inert, and cannot be used by most organisms. As such, N_2 is labeled as nonreactive nitrogen, whereas all biologically, photochemically, and radiatively active N compounds within Earth's biosphere and atmosphere are classified as reactive nitrogen (N_r) (Galloway et al., 2003).

2.1 The N Cycle: Its Modern Incarnation, Gradual Evolution, and Future State

Whether N is reactive or nonreactive is dictated by the biogeochemical N cycle, a series of reduction-oxidation reactions that are crucial for all life, be it for energy production, waste excretion, or biosynthesis. These complex reactions, primarily controlled by microorganisms, currently play the largest role in the biogeochemistry of the N cycle, as well as interactions within the geosphere (Canfield et al., 2010).

2.1.1 The Modern Global N Cycle

The oxidation-reduction reactions of the modern global N cycle are represented in Figure 1, and will be referenced in the step-by-step walkthrough of the active processes. Equations for each step will be listed in respective sections.

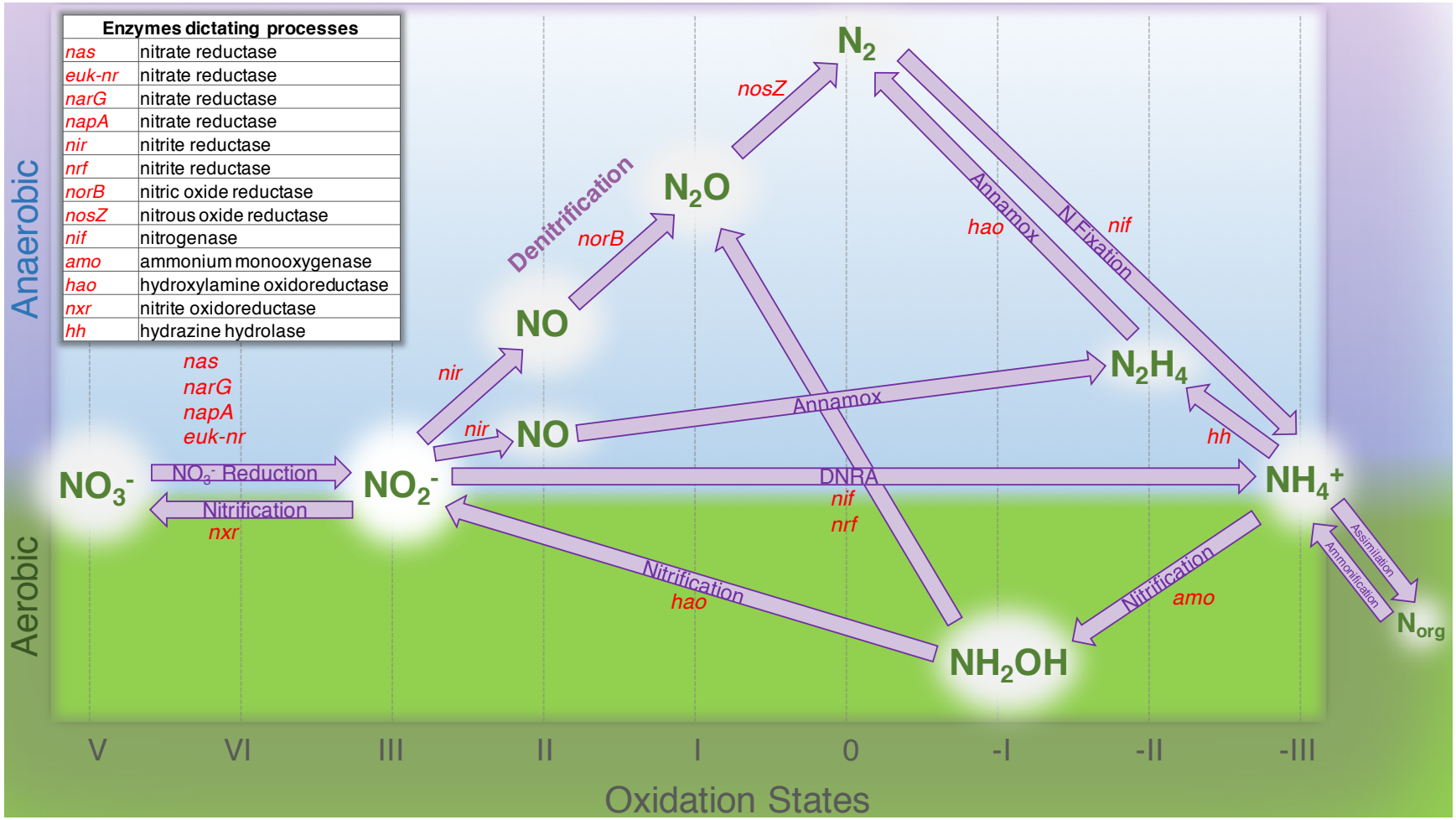

Figure 1 Graphical representation of the modern global N cycle, with oxidation states for N compounds on the x-axis, and aerobic vs. anaerobic designation indicated on the y-axis. N compounds are in green, and purple arrows indicate the process by which N is transformed. The enzymes dictating processes are in red. Inspired by Canfield et al. (2010).

2.1.1.1 Nitrogen Fixation

Nitrogen fixation is the conversion of atmospheric, inert nitrogen, N_2, to reactive ammonia, NH_3.

$$N_2 + 8H^+ + 8\ e^- \rightarrow 2NH_3 + H_2$$

The triple bond binding two N atoms together requires a significant amount of energy to break, requiring a catalyst to overcome the substantial energy barrier (Galloway et al., 2003; Canfield et al., 2010), and nitrogenase (nif), an iron-containing, heterodimeric enzyme complex, fills this role (Zumft, 1997; Canfield et al., 2010). Prokaryotes of the bacterial and archaeal domains, such as *Rhizobia* and *Bradyrhizobia* in root modules (Easton and Lassiter, 2013) and ubiquitous, free-living *Azotobacter,* commonly possess nitrogenase, and are able to perform N fixation. Some eukaryotes (termites, legumes, etc.) can also mediate this process through symbiotic relationships with nitrogen-fixing prokaryotes (Canfield et al., 2010). Certain abiotic processes can also fix nitrogen, including atmospheric fixation via lightning and industrial fixation via the Haber Bosch process, which employs high temperatures and pressures to convert nitrogen gas and either petroleum or natural gas into ammonia. This process is essential for all life, without which the biosynthesis of nucleotides for DNA and RNA and amino acids for proteins would not be possible.

2.1.1.2 Assimilation

Nitrogen assimilation is the formation of organic nitrogen compounds like amino acids from inorganic nitrogen compounds present in the environment. Organisms like plants, fungi and certain bacteria that cannot fix nitrogen gas (N_2) depend on the ability to assimilate NO_3^--N or ammonia for their needs. Other organisms, like animals, depend entirely on organic nitrogen from their food.

2.1.1.3 Ammonification

When organisms die or produce waste, the organic N in their biomass or expelled material is returned to the environment, and ammonifying bacteria, such as *Bacillus*, *Clostridium*, *Proteus*, *Pseudomonas*, and *Streptomyces*, attack internal proteins to produce polypeptides and amino acids. The amino acids are then stripped of their amino groups, bearing ammonia, NH_3, which eventually dissolves in contact with water to form ammonium ions, NH_4^+. Other inherent compounds, such as nucleic acids, urea, and uric acid, are subject to ammonification as well, and this process is of the utmost importance, as most autotrophs are incapable of assimilating these organic compounds for their own benefit.

2.1.1.4 Ammonia Volatilization

Ammonia volatilization is the conversion of ammonia gas, NH_3, to the dissolved ion ammonium, NH_4^+, which typically occurs in soils with pHs above 7.5, high soil moisture content, and high soil temperatures (Rochette et al., 2014; Jones et al., 2013).

$$NH_4^+ + OH^- \leftrightarrow H_2O + NH_3$$

Ammonium is available for uptake by plants, but ammonia is not, making this pathway a major contributor to N losses from agricultural soils worldwide, especially in areas where ammonium-based fertilizer is in use.

2.1.1.5 Nitrification

Nitrification is the stepwise microbial oxidation of NH_4^+, ammonium, or NH_3, ammonia, to NO_3^-- N , typically in aerobic soils. Historically, nitrification has been divided into two steps, with two separate groups of bacteria mediating each (Winogradsky, 1892). The first step, the conversion of NH_3 or NH_4^+ to NO_2^-, is most commonly enacted by soil bacteria of genus *Nitrosomonas*, which derive energy from the conversion, using CO_2 as a carbon source. Genera *Nitrosococcus* and *Nitrosospira*, as well as subgenera *Nitrosolobus* and *Nitrosovibrio*, are also capable of autotrophically oxidizing ammonia to

nitrite (Watson et al., 1981). The second step, the conversion of NO_2^- to NO_3^-, is promoted by the genus *Nitrobacter*, which acquire their energy from the previous nitrite oxidation process. While *Nitrobacter* is the main contributor for the second step, other genera, including *Nitrospina*, *Nitrococcus*, and *Nitrospira* can also convert nitrite to nitrate. A few kinds of heterotrophic bacteria and fungi are also capable of performing nitrification, albeit at a sluggish pace relative to the autotrophic organisms mentioned above (Watson et al., 1981; Verstraete and Alexander, 1973). Under anaerobic conditions, greenhouse gases N_2O and NO can be released as byproducts, contributing a significant source of atmospheric N_2O (Oertel et al., 2016).

Ammonium to Nitrate:

$$2NH_4^+ + 3O_2 \rightarrow 2NO_2^- + H_2O + 4H^+$$

$$2NO_2^- + O_2 \rightarrow 2NO_3^-$$

Ammonia to Nitrate:

$$NH_3 + O_2 \rightarrow NO_2^- + 3H$$

$$NO_2^- + H_2O \rightarrow NO_3^- + 2H^+$$

Recently, a single type of microorganism, referred to as complete ammonia oxidizers (comammox), was discovered that is capable of oxidizing ammonia all the way to nitrate. The existence of a comammox-performing microorganisms was predicted in 2006 (Costa et al., 2006), but the culprits, two species of *Nitrospira,* were not identified until over a decade later (van Kessel, 2015; Daims et al., 2015).

2.1.1.6 DNRA

DNRA is the first of three microbial processes in the N cycle that involve a fundamental competition for nitrate. Much like in denitrification, under anaerobic conditions, chemoorganoheterotrophic microbes can use NO_3^-- N as a respiratory electron acceptor, rather than oxygen, coupled with the anaerobic oxidation of an organic carbon source, reducing it to NO_2^-, and then NH_4^+, in a process known as dissimilatory nitrate reduction to ammonium (DNRA). Unlike the nonreactive N_2 gas

produced by denitrification, the nitrogen species produced by DNRA, NH_4^+, is still bioavailable. This process is most commonly initiated by prokaryotes, but certain eukaryotic microorganisms are capable of performing DNRA as well.

The exact mechanisms dictating whether denitrification or DNRA occurs in natural and manufactured environments are still not entirely clear (Kraft et al., 2011), and are likely the outcome of many complicated environmental factors that are still under investigation, including pH, electron donor complexity and type, and sulfide concentrations (van den Berg et al., 2017). Two known significant factors in the microbial competition for nitrate are (1) the ratio of available electron donors and available electron acceptors (van den Berg et al., 2016) and (2) the COD:N ratio. Whatever the causal mechanisms actually are, DNRA's contribution to nitrate removal should not be ignored; a recent study by Giblin et al. (2013) revealed that, at 26 sites of 55 coastal sites, more than 30% of the NO_3^-N reduced was attributed to DNRA, and that DNRA was the dominant mechanism at more than one third of the sites.

2.1.1.7 Denitrification

Denitrification is the microbially-induced stepwise reduction of NO_3^--N to nitrogen gas, N_2, and requires (1) the presence of N oxides to serve as electron acceptors, (2) denitrifying bacteria, (3) a labile carbon source, and (4) sufficiently low dissolved oxygen concentrations (Korom, 1992).

$$NO_3^- \rightarrow NO_2^- \rightarrow NO + N_2O \rightarrow N_{2(g)}$$

$$5C + 4NO_3^- + 2H_2O \rightarrow 2N_2 + 4HCO_3^- + CO_2$$

When oxygen, a generally more convenient electron acceptor, becomes depleted from environments, bacteria are forced to turn to alternatives for respiration; under anoxic conditions, facultative anaerobic bacteria use oxyanions (NO_3^-, NO_2^-) or oxides (NO, N_2O) as terminal, respiratory electron acceptors, coupled with the anaerobic oxidation of an organic carbon source, producing N_2 (Easton and Lassiter, 2013). N_2 is then free to diffuse out of soils and aquatic environments and into the atmosphere,

removing it from the reactive nitrogen pool. The extent to which DO levels can limit denitrifying varies amongst denitrifying organisms (Korom, 1992), but denitrification can be hindered at DO concentrations as low as 0.2 mg L^{-1} (Metcalf and Eddy, 2003).

The effects of denitrification are ubiquitous, impacting biogeochemical cycles and ecosystems at local, regional, and global scales (Seitzinger, 1988; Codispoti and Richards, 1976; Nixon et al., 1996). N_2O is an intermediate during this process, and the escape of N_2O gas is inevitable, making denitrification a significant source of atmospheric N_2O. CO_2 and H_2O are also produced. Certain heterotrophic bacteria are the dominant denitrifiers, but a few autotrophic denitrifiers have been identified as well. In fact, denitrifiers have been identified in all of the main phylogenetic groups of bacteria (Zumft, 1997), and many species of bacteria contribute to full denitrification under multiple enzymatic pathways (Atlas and Barthas, 1992). Other than DNRA, denitrification is the is the only way to permanently remove reactive nitrogen from both soils and aquatic environments, and establishing the required conditions is relatively straightforward, making the process ripe for exploitation as a means to attenuate reactive N. It should be mentioned that in the event that NO_3^- becomes depleted, obligate anaerobes can utilize sulfate (SO_4^{2-}), manganese (Mn (IV)), and iron (Fe(III)) as electron acceptors in place on NO_3^- (Korom, 1992), and reaction priority is dictated the energy supplied by each reaction; denitrification releases the most energy, and is, of these reactions, therefore always the reaction of highest priority, given the presence of NO_3^- (Metcalf and Eddy, 2003).

2.1.1.8 Anammox

N_r can also be converted back to N_2 through the process of anammox (anaerobic ammonium oxidation), which involves the coupling of NH_4^+ oxidation with NO_2^- reduction, producing N_2 and H_2O.

$$NH_4^+ + NO_2^- \rightarrow N_2 + 2H_2O$$

Anammox is mediated by bacteria known as planctomycetes (Canfield et al., 2010), and is common in marine environments, producing harmless N_2 while having the advantage of no N_2O production. Like denitrification, anammox requires anoxic conditions, and is an effective method of attenuating N from soil and marine environments. Even though this process occurs in a variety of different environments, and is responsible for 30-50% of the N_2 produced in the oceans (Devol, 2003), it was not discovered until relatively recently.

For many decades in the mid-1900s, a multitude of studies suggested that a microbe remained unidentified that had the ability to anaerobically oxidize ammonium, and that the N cycle contained more reactions than was previously thought (Broda, 1977; Richards, 1965; Hamm and Thompson, 1941). Field studies on water bodies revealed that there was a disparity between the expected ammonium concentrations based on Redfield stoichiometry and thermodynamic calculations, and the actual, observed ammonium concentrations (Trimmer et al., 2013). In 1995, experimental indications of this arcane process were discovered in an anoxic fluidized-bed bioreactor at the Gist-Bro-cades yeast factory in the Netherlands (Mulder et al., 1995), and the mechanism for this phenomenon was unearthed when the bacteria responsible were finally identified (van de Graaf et al., 1995; Strous et al., 1999). These bacteria, forming a monophyletic group *Brocadiales* within the *Planctomycete* phylum (Jetten et al., 2010), opposed conventional microbiological concepts, sharing features of all three domains (Bacteria, Archea, and Eukarya) and raising intriguing questions about their evolutionary context (van Niftrik and Jetten, 2012). Since their discovery, their atypical metabolism has been exploited for wastewater applications, and their fascinating characteristics continue to elicit a hotbed of research in the field of microbial ecology.

Denitrification and anammox complete the N cycle by ending with replenishing N_2. These reactions have not always been present, but instead developed through time, and understanding the N cycle's past is key to understanding its future.

2.1.2 The Ancient Global N Cycle

The modern global N cycle is the result of billions of years of gradual evolution , and is likely much different from its ancient incarnation. Some of the ancient events shaping the evolution of the modern global N cycle are shown in Figure 2.

Atmospheric reactions and slow geologic processes played a large role in controlling the primordial N cycle, prior to the development of the biotic N cycle. During this time, before 2.7 billion years ago, the N cycle was governed by reduced forms of N supplied by planetary accretion (solid NH_3, amino acids, and other basic organics), their rates of accretion, and the continual development of a secondary atmosphere through the rampant, pervasive volcanism that plagued early Earth (Canfield et al., 2010). The immense heat resulting from this volcanism caused upper mantle transition elements, such as iron, to react with the accreted, reduced forms of N, forming outgassed atmospheric N_2 (Mikhail and Sverjensky, 2014). These abiotic processes are still at play in the modern N cycle, but they are much slower in comparison to biotic contributors, with abiotic processes having an approximate turnover rate of roughly one billion years (Berner, 2006).

The lightning (Walker et al., 1981; Chameides and Walker, 1981) and meteor impacts (Kasting, 1990) that frequented early Earth are also believed to have played a role in the early N cycle, producing NO, which would have been converted to NO_3^-- N, NO_3^-, and nitrite, NO_2^-, through a series of photochemical and aqueous phase reactions (Mancinelli and McKay, 1988). These abiotic, heat shock processes also probably promoted nitrogen fixation, the conversion of N_2 to NH_3, albeit at rates about 50 to 5000 times slower compared to the rates of the modern oceans (Gruber and Galloway, 2008). At the time, the only believed mechanism for NH_4^+ production was reduction via reactions with Fe^{2+}, and this was likely a prevalent phenomenon because of the widespread abundance of Fe^{2+} in early Earth's oceans (Holland, 1984). N_2 was the dominant form of nitrogen in the atmosphere, and ammonium, and possibly NO_3^-- N, were ubiquitous in the ancient seas.

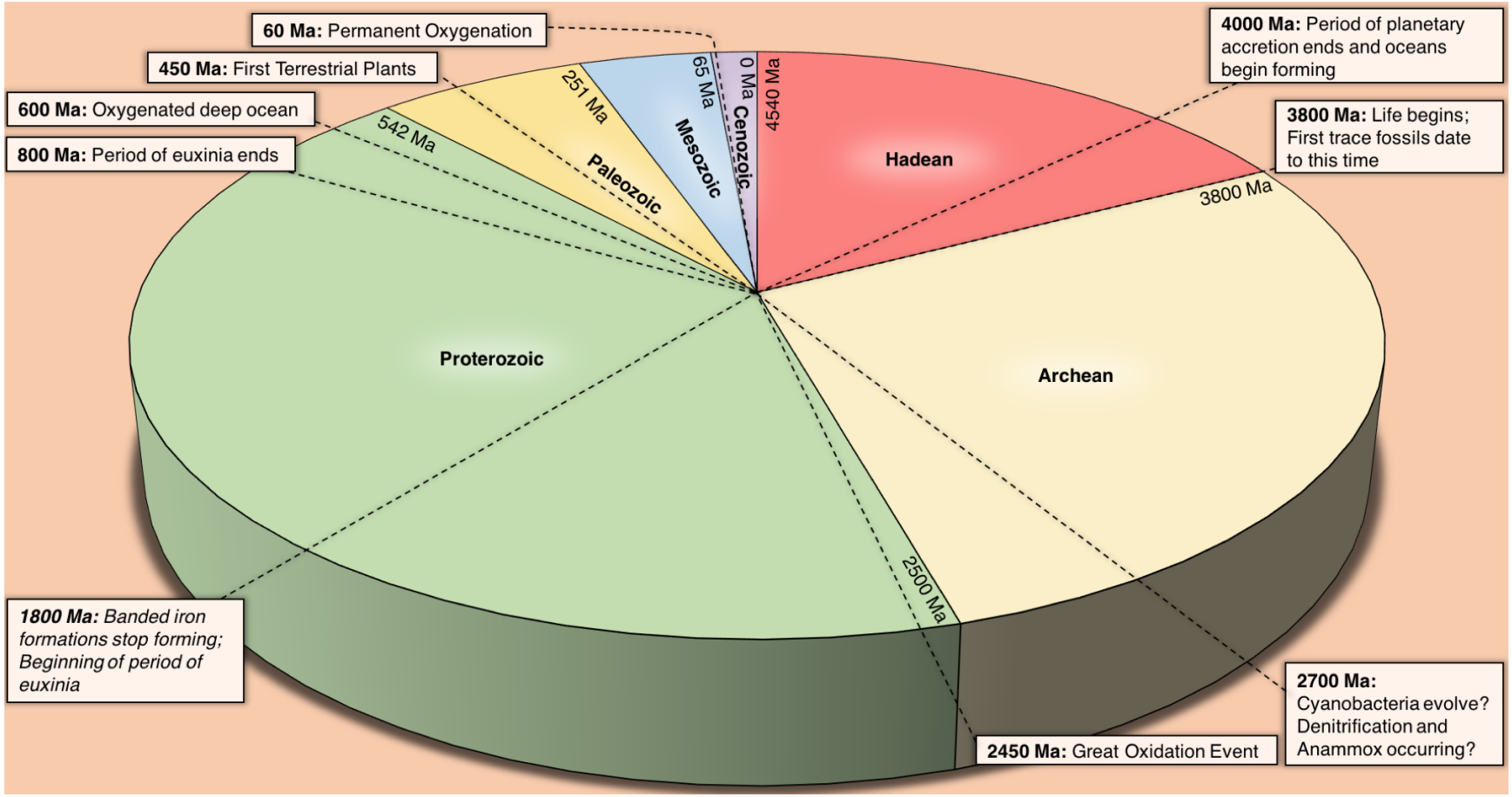

Figure 2 Timeline of known major events that shaped the global N cycle, with clockwise rotation representing the progression of time, from the formation of earth, approximately 4540 Ma, to the present, 0 Ma. The wedges represent the Cenozoic, Mesozoic, and Paleozoic Eras, and the Hadean, Archean, and Proterozoic Eons of the Precambrian Era.

Early life on Earth probably derived energy from chemically reduced compounds, likely H_2, of the planet's interior, and because H_2 was in short supply, primary productivity was severely limited in comparison to modern production (Canfield et al., 2006). Anoxygenic photosynthetic organisms evolved soon after biological evolution began, and this ultimately resulted in the limiting of inorganic N in the earliest pre-photosynthetic biosphere, forcing the evolution of biological N_2 fixation, probably amongst anaerobic photoautotrophs (Canfield et al., 2010). The advent of anoxygenic photosynthesis sparked widespread stratification of the early oceans, with the development of a photic zone with primary productivity comparable to that of today's oceans and a continued pervasiveness of Fe^{2+}. This widespread Fe^{2+} availability prior to ~2.5 Ga likely heavily influenced the ancient N cycle; some N fixers possess paralogous genes that can encode two alternative nitrogenases, with V or Fe replacing the more efficient Mo. While the Fe form is less efficient, it is probable that the low oxygen, Fe^{2+}-dominated oceans during this time lacked soluble Mo, forcing the alternative form. The Mo form probably didn't prosper until around 500 to 600 Ma, when widespread oxygenation of oceans would have increased dissolved Mo (Scott et al., 2008).

Recent isotopic fractionation analyses of N^{14} and N^{15} in Archean shales (Godfrey and Falkowski, 2009) suggest that denitrification or anammox was widespread in the upper oceans, but not anywhere else, at least 2.67 Ga (Falkowski and Godfrey, 2008). The origins of these processes are difficult to trace, and they may have evolved prior to the onset of photosynthesis and subsequent oxygen production by cyanobacteria (Canfield et al., 2010). One thing is for certain, though: if these processes did evolve before cyanobacteria, they were probably not pertinent, and only became relevant with the emergence of cyanobacteria (Canfield et al., 2010). This is almost certain because nitrification, the biological production of NO_3^- and integral aerobic process of the N cycle, requires molecular oxygen, and once nitrification evolved, probably around 2.5 Ga, the modern N cycle began. The timing of cyanobacterial evolution is somewhat unclear; there were spurts of oxygenation approximately 2.7-2.6 Ga, and a significant period of oxygenation 2.45-2.3 Ga, coinciding with the mass extinction of many organisms ill-equipped to handle rising O_2, and either of these could be the result of the

expansion of these cyanobacteria (Farquhar et al., 2000; Frei et al., 2009; Anbar et al., 2007). Whatever the case, oceanic cyanobacteria were certainly around before 2.3 Ga, and Earth's oxygen levels gradually rose for hundreds of millions of years.

Around 600 million years ago, oxygenation finally reached deep ocean environments (Scott et al., 2008, Canfield et al., 1998; Canfield et al., 2008), resulting in a significant shift in ocean stratification, with a Fe^{2+} and H_2S zone sandwiched between a surface water O_2 zone and the newly formed, deep water O_2 zone (Canfield et al., 2010). These conditions were probably much like the present-day Black Sea, and primary productivity skyrocketed during this time. Over the past 600 million years, oxygen levels have risen to their modern day levels, aided by the rise of terrestrial plants approximately 450 Ma (Berner, 2004). The oceans' interiors finally became oxygenated, eventually bringing the N cycle to its pre-industrial state, with land primary production balanced with sea primary production (Field et al., 1998), and N cycles in the land and sea also roughly balanced (Gruber and Galloway, 2008).

2.1.3 The Future of the Global N Cycle

Understanding the evolution of the modern global N cycle is key to understanding its current state and future; evolution was not rapid, but was the gradual progression across billions of years, and the recent influence of human activities may be the most significant stressors the N cycle has encountered since its inception approximately 2.5 billion years ago (Canfield et al., 2010). Because the changes imposed by human behavior are so drastic and swift, occurring within a microscopic fraction of the geologic time scale, actions may have volatile, unpredictable consequences. Over many decades, microbes may be able to adapt to anthropogenic influences through natural feedback mechanisms. Perhaps a new steady state could be achieved, where microbes are able to remove the excessive input of nutrients at the same rates that they are applied, but this best-case scenario is a long shot.

2.2 The Reality of Increased Reactive Nitrogen Production

N_r creation has increased substantially over the course of human history, and this is directly attributed to anthropogenic activity. Figure 3 shows the major events impacting the global N cycle during the 20th century, and the primary stressors are discussed below.

2.2.1 Agriculture's Imperative Role in Feeding a Burgeoning Global Human Population

Over 99.99% of the global human food supply sources from cropland (FAO, 2002), the surface area of which occupies 40-50% of the Earth's land surface (IPCC, 2007). The agriculture performed on this land is directly responsible for roughly 24% of the world's economic output (FAO, 2003), employing approximately one third of the global human population, and this fraction is comprised primarily of people from developing countries (UNEP, 2007; ILO, 2007). This extreme dependency on agriculture can be expected to increase; current projections show that there is an 80% probability that the global human population, currently at ~7.5 billion, will increase to between 9.6 and 12.3 billion by 2100 (Gerland et al., 2014). Even today, with these substantial rates of agricultural productivity, food production is insufficient in supplying the global human population; in 2006, approximately 3.7 billion people, or ~56% of the global population, suffered from malnourishment (Pimental and Pimental, 2006). These significant problems will need to be addressed in the future, and highlight agriculture's importance by virtue of innovation.

This global dependency on agriculture was made possible by a multitude of key innovations, but the most relevant development is the application of reactive N fertilizers for improved crop yields. By supplying biologically available nitrogen to cropland, farmers can circumvent the potential shortcomings of natural nutrient supply, which are often insufficient for substantial yields. The need for the development of fertilizers for improved agriculture is a primary stressor facing the Global N Cycle.

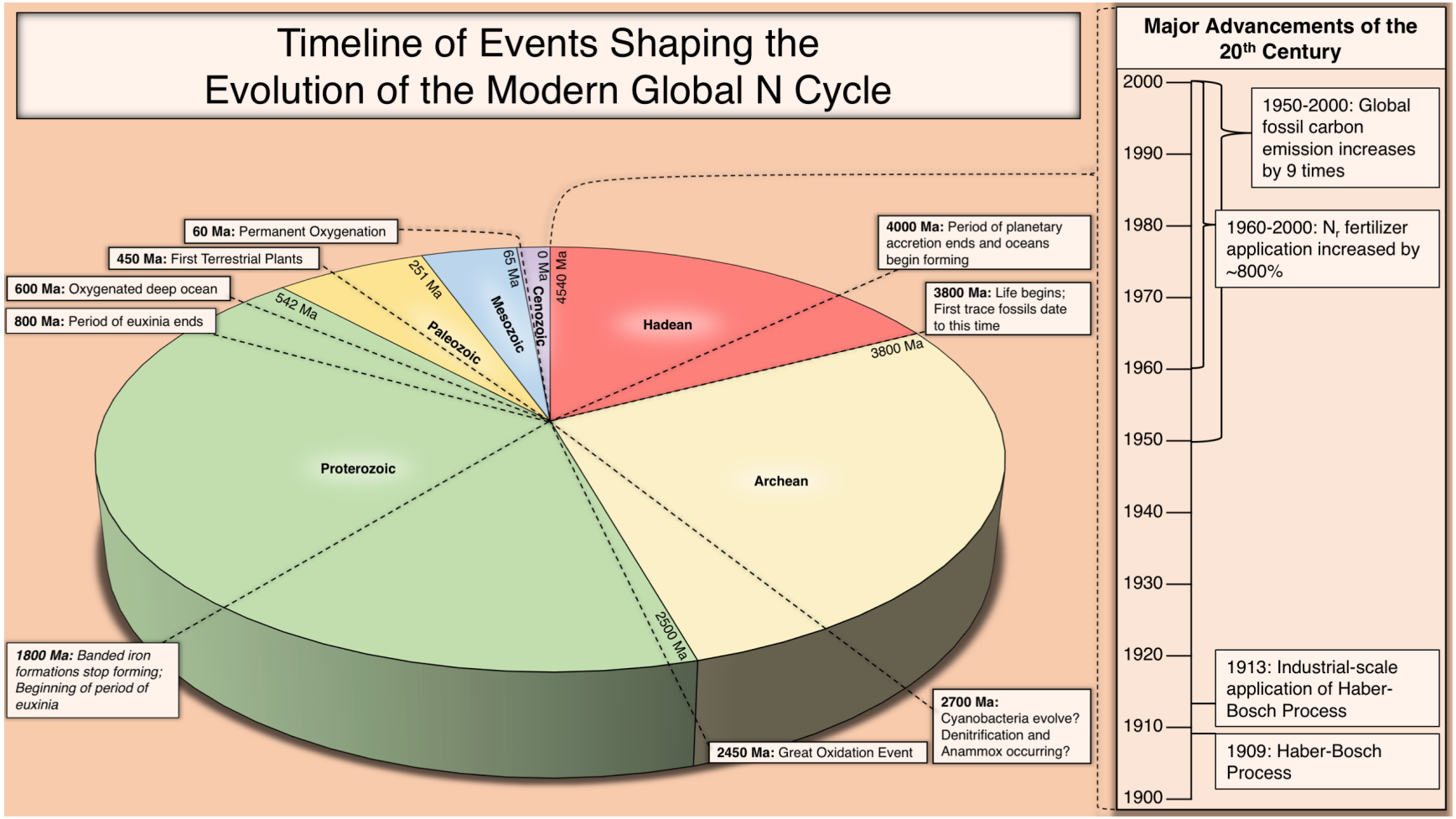

Figure 3 Continuation of the timeline presented in Figure 2, with an added section showing advancements in N_r creation during the 20th century, attributed to fertilizer production and application and the burning of fossil fuels, emphasizing how the modern stresses to the N cycle are occurring in a snapshot of geologic time.

2.2.2 Anthropogenic Reactive Nitrogen Production

Prior to the influence of humans on the N Cycle, lightning and biological nitrogen fixation (BNF) were the two primary mechanisms for converting N_2 to N_r, and the total global mass of this naturally-produced nitrogen was approximately 100 Tg, a number that has remained relatively constant since industrialization began (Galloway et al., 1995) (Figure 4). Microbial N fixation and denitrification were balanced prior to anthropogenic influences, keeping nitrogen reservoirs at equilibrium (Ayres et al., 1994).

Since the emergence of anthropogenic means for creating reactive nitrogen, reactive nitrogen creation has grown from ~15 Tg N yr^{-1} in 1860 to 156 Tg N yr^{-1} in 1995 to 187 Tg N yr^{-1} in 2005, a reality resulting from: (1) the development of new methods of N_r creation, such as the Haber-Bosch process, (2) the significant increase in cultivation of legumes, rice, and other crops that promote BNF, and (3) the widespread burning of fossil fuels (Galloway et al., 2008; Galloway et al., 2003). Of the N_r created by human activity, 15% of it is produced through the burning of fossil fuels, 75% is applied to agroecosystems, and 10% is used in industrial processes (Galloway et al., 2003). Altogether, these anthropogenic sources provide roughly 45% of the annually produced fixed nitrogen on Earth (Canfield et al., 2010). N_r creation through the combustion of fossil fuels does not have any benefits, whereas N_r creation through the Haber-Bosch process and through BNF are largely beneficial due to their potential to feed massive numbers of humans. These means of production have had a drastic effect on the global N cycle (Vitousek et al., 1997), and the means for production are discussed next.

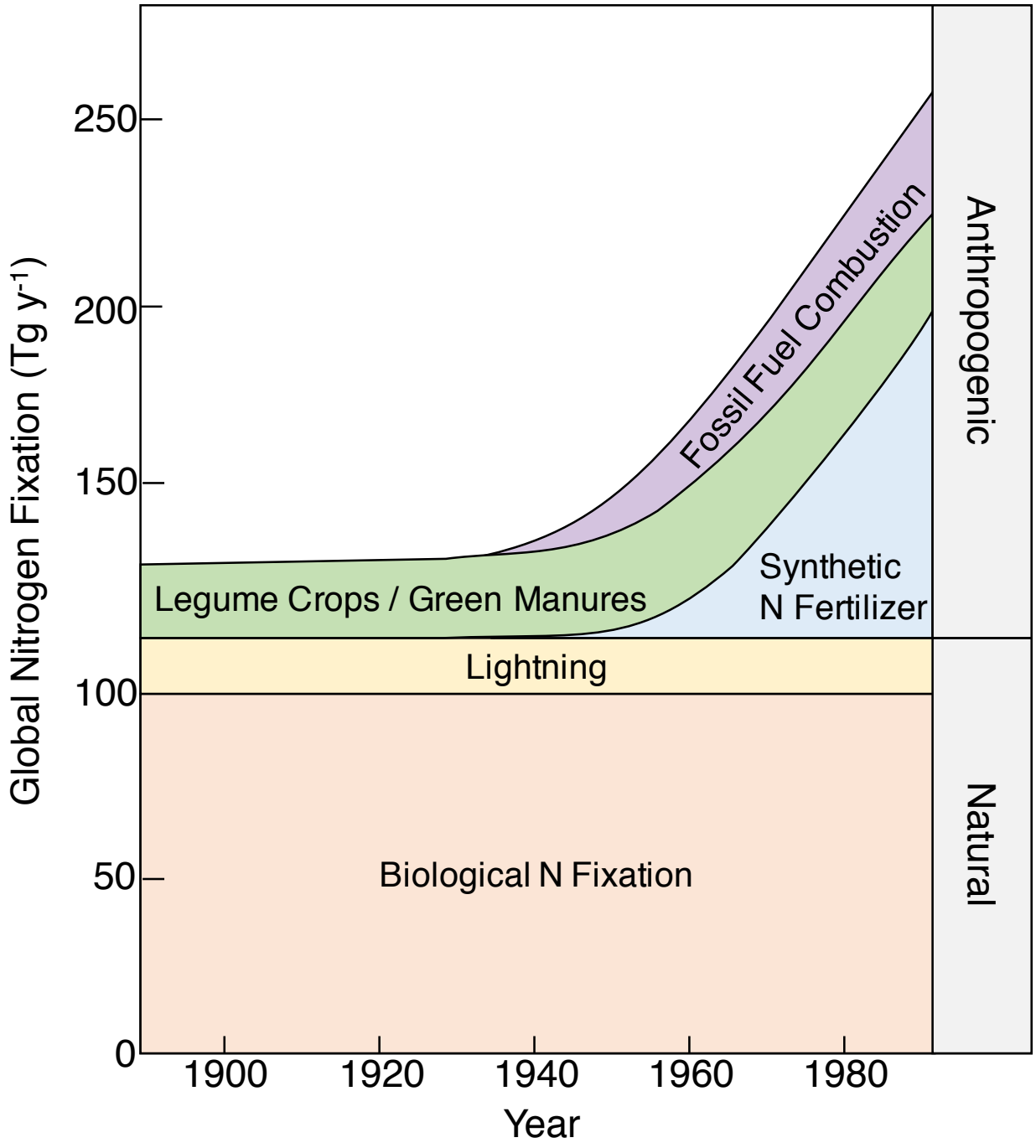

Figure 4 Graph of global nitrogen fixation in Tg yr^{-1}, highlighting the shift from pre-industrial N_r creation rates to post-industrialization, recent rates. Modified from Vitousek and Matson (1993).

2.2.2.1 The Haber-Bosch Process: Its Inception, Intended Outcomes, and Unanticipated Consequences

The Haber-Bosch process is an industrial procedure for converting atmospheric dinitrogen, N_2, to ammonia, NH_3, via a high temperature and pressure reaction with H_2 and a metal catalyst.

$$N_2 + 3H_2 \rightarrow 2NH_3$$

Throughout the 1800s, there was significant pressure placed on discovering methods for producing reactive nitrogen, especially for use as applied fertilizers and key components of explosives. The main naturally-occurring reservoirs of these materials, such as Chilean saltpeter, Peruvian guano, and sal ammonia derived from coal (Erisman et al., 2008), were being rapidly depleted, and could not keep pace with an exploding human population. Early methods for artificial nitrogen fixation, such as the Birkeland-Eyde process (Birkeland, 1906; Eyde,1909) and the Frank-Caro process, were highly inefficient, making mass ammonia production difficult. Despite its chemically and biologically unusable form, the clear candidate for possible conversion was N_2; if a viable method for transformation presented itself, its widespread availability made it ripe for exploitative purposes. In 1909, German scientist Fritz Haber was the first to synthesize chemically reactive ammonia from hydrogen, using the presence of iron at high temperature and pressures at the laboratory scale (Erisman et al., 2008). However, the production rates of Haber's setup were extraordinarily slow, yielding only about 125 mL NH_3 hr^{-1}. Carl Bosch, a scientist working under the German chemical company BASF remedied this shortcoming by scaling the process up to the industrial scale, which was achieved in 1913. The efforts of Haber and Bosch earned each of them Nobel Peace prizes in 1918 and 1931, respectively.

The Haber-Bosch process had a major influence on international conflicts; much of the reactive nitrogen developed through the Haber-Bosch process would be used to make explosives for both World Wars. Haber, a German patriot, believed that his key

role in the development of explosives and other chemical weapons was moral, as he speculated that they would shorten the war (Stoltzenberg, 2005). The Haber-Bosch process provided Germany with an indigenous supply of ammonia that was oxidized to nitric acid, via the Ostwald process (Wilhelm, 1902; Wilhelm, 1903) and then used to create nitroglycerine, ammonium NO_3^-- N, TNT, and other reactive nitrogen-containing explosives, a source that would ironically prolong both World Wars and result in many more casualties (Erisman et al., 2008). Since those days, synthetic reactive nitrogen production for lethal purposes has not slackened, and the majority of the world's ammunition sources from the Haber-Bosch process. Haber and Bosch's discoveries are therefore unintentionally responsible for 100-150 million deaths resulting from armed conflicts during the 20th century (White, 2011). Thus, even discounting the momentous impacts that the Haber-Bosch process had on agriculture, the importance of this process cannot be understated, and these developments changed the course of history.

Haber's primary intention for creating synthesized reactive nitrogen, though, was to satisfy the hunger of a skyrocketing global human population, an obstacle that he predicted would only burgeon with time (Haber, 1920). His goals quickly became realized; the discovery of the Haber-Bosch process introduced widespread synthetic fertilizer usage, ushering in a new age, one in which agricultural productivity dramatically increased in most regions of the world (Stewart et al., 2005). By the mid-1900s, the Haber- Bosch process was being used in full force, and Haber and Bosch's contributions set the stage for the Green Revolution, a blossoming of agricultural technologies, such as utilizing fertilizers and agrochemicals in conjunction with newly developed, high-yielding crops, new cultivation methods, and new irrigation practices (Pingali, 2012).

Today, the worldwide use of reactive nitrogen fertilizer has surpassed 100 Tg N yr^{-1}, and estimates suggest that between 1908 and 2008, the number of humans supported per hectare of cropland has grown from 1.9 to 4.3 persons (Erisman et al., 2008). While many factors contributed to this, the Haber-Bosch process is the main source; by the end of the twentieth century, fertilizer inputs supported roughly 40% of the world's population (Smil, 2002), and 30-50% of increased crop yields were attributed

to N_r application via mineral fertilizers (Stewart et al., 2005). Currently, roughly 80% of the total N introduced by the Haber-Bosch process is being used to bolster higher crop yields via fertilizer application (Galloway et al., 2008). Indeed, Bosch's initial reflections regarding the urgent need to seek out a means to improve food production were correct; since his discoveries, the human population has grown overly dependent on N_r for fertilizer application and subsequent food production.

N fertilizer application increased by ~800% from 1960 to 2000 (Fixen and West, 2002). ~50% of this fertilizer is used on wheat, rice, and maize, and this is problematic because the nitrogen use efficiency for these crops is less than 40%, meaning that more than 60% of applied N is lost through runoff or to the atmosphere before it is used by crops (Canfield et al., 2010). The most common form of N fertilizer applied to crops is NH_4^+, which is readily converted by nitrifying bacteria to NO_3^-, which is highly mobile and will inevitably leach into water bodies. Often, the chemicals used for fertilizer application are NO_3^--N-bearing, supplying more NO_3^- than necessary for the promotion of efficient crop growth. Indeed, the intentional, excessive application of fertilizers and pesticides has resulted in the unavoidable export of constituent, surplus inorganic and organic chemicals.

2.2.2.2 The Widespread Cultivation of Crops Promoting Biological Nitrogen Fixation

The universal farming of legumes, rice, and other crops that promote the process of biological nitrogen fixation has become a significant source of N_r; nonnative leguminous crops have symbiotic relationships with N fixing *Rhizobium* bacteria, resulting in the production of far more N_r than would be the case for native plant communities occupying the same space (Smil, 1999). Throughout history, mankind has exploited leguminous crops for improving soil fertility, but cultivation of these crops now results in N_r creation that exceeds rates of N_r consumption. Between 1860 and 2000, cultivation-induced N_r production increased from 15 Tg N yr^{-1} to 33 Tg N yr^{-1} (Galloway et al., 2003).

2.2.2.3 Combustion of Fossil Fuels

The combustion of fossil fuels contributes a substantial amount of the N_r produced each year; atmospheric N and the N in fossils is burned, releasing N oxides into the atmosphere (Galloway, 2003). In the U.S., a substantial portion of emitted N oxides are directly sourced from the transportation and industry-associated burning of fossils fuels (EPA, 2017). Between 1860 and 2000, N_r production via fossil fuel combustion increased from less than 1 Tg N yr^{-1} to 25 Tg N yr^{-1} (Galloway et al., 2003).

2.2.3 The Nitrogen Cascade

The problems associated with these extreme N_r production rates are largely a result of the environment's inability to handle the inordinate N_r supply; if the reactive nitrogen being produced was being sufficiently denitrified, as was the case prior to industrial methods, many of the nitrogen-related adverse consequences facing the world today would be nonexistent. Galloway et al. (2003) addressed this phenomenon, referring to it as the "nitrogen cascade," describing the ecological and health effects of N_r as it transitions between different environmental systems, and the tendency for N_r to accumulate in the environment due to production rates that are greater than NO_3^--N removal through denitrification. The accumulations at each transition, and their effects on the atmosphere, environment, and human health, are described in detail in Chapter 2.3 and are represented in Figure 5. Addressing the problem of human alteration to the N cycle is critical, and will require a multifaceted approach, drawing from many different disciplines and targeting the N cycle at links where the most N transformation and/or transportation is occurring (Galloway et al., 2008; Galloway et al., 2003), and potential solutions will be discussed in Chapter 2.4.

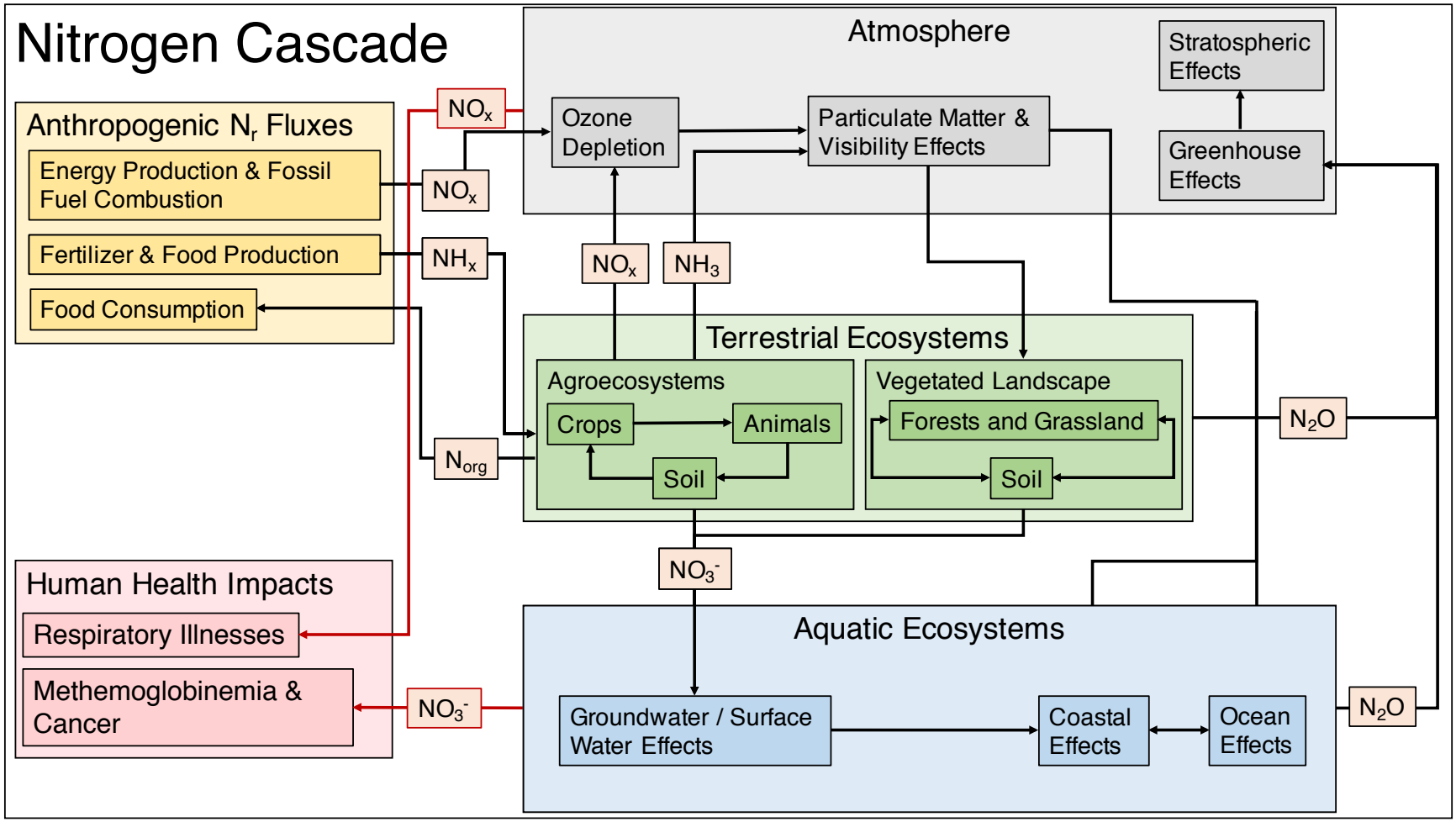

Figure 5 Flow diagram of the nitrogen cascade, with the N-containing, natural systems on the right and the anthropogenic fluxes that affect those environments in yellow, as well as the resulting human health impacts in red. Arrows with N species represent fluxes to other systems. Inspired by Galloway et al. (2003).

2.3 Implications Consequences of Anthropogenic Reactive Nitrogen Export

A large proportion of the excessive amounts of N_r and P fertilizer that humans are producing and applying to agricultural fields is lost to the environment; Smil (1999) estimates that of the ~170 Tg N_r added to agroecosystems in 1995, only ~12% was directly fed to humans, and the rest was left to be distributed throughout the environment (Galloway et al., 2003). These nutrients are exported from applied areas at rates that far exceed their natural production (Galloway and Cowling, 2002; Foley et al., 2005), and this problem is magnified by the widespread presence of artificial, subsurface agricultural drainage. While these water management practice improve crop production efficiency (Fausey et al., 1995), making field operations more efficient and improving soil functionality by removing excess water from the soil profile in poorly drained field via perforated conduits (Skaggs and van Schilfgaarde, 1999; Skaggs et al., 2012; Hua et al., 2016), recent phenomena have revealed that these practices do not come without their significant drawbacks; artificial drainage effectively modifies the nitrogen and hydrologic cycles (Sims et al., 1998; Jaynes et al., 2001), rapidly exporting drainage water and reducing the amount of time for denitrification to take place (Kellman, 2005), as well as playing a role in phosphorus transport (Smith et al., 2015). Once these nutrients are released to surface water bodies and/or underlying aquifers, they have the potential to promote a host of adverse repercussions, including eutrophication, global acidification, stratospheric ozone depletion, and deleterious human health conditions (Howarth et al., 2000; Howarth, 2008; Erisman et al., 2013; Galloway et al., 2003).

2.3.1 Impacts on Aquatic Ecosystems

N_r is a particularly pernicious nutrient in aquatic ecosystems, especially when it is introduced in excess, promoting processes such as eutrophication and global acidification, discussed in detail below.

2.3.1.1 Eutrophication: Impacts on Ecosystem Biodiversity and Productivity

Eutrophication, defined as an increase in the rate of supply of organic matter and subsequent increase in primary production (Nixon, 1995; Rabalais, et al., 2009), has been identified as a significant problem in many coastal ecosystems (Boesch et al., 2000; Duarte, 2009), and has many implications for ecosystem biodiversity and productivity. While the phenomenon of eutrophication is not inherently bad, as nutrients are essential for growth, it becomes problematic when receiving environments become supersaturated with respect to certain nutrients, resulting in inordinate primary production. Primary production is facilitated by nutrients N and P, and in soils and water bodies, there is usually a limiting nutrient, but the overabundance of nutrients due to recent anthropogenic practices has introduced far more N and P than is necessary for primary production, particularly in aquatic systems, resulting in a multitude of adverse consequences (Rabalais, et al., 2009). As nutrients are continually delivered to downstream aquatic environments, the phytoplankton capable of assimilating them are increasingly favored over other species that depend on a variety of other factors for survival (Erisman et al., 2013). This success of a narrow selection of organisms results in low-diversity algal or cyanobacterial blooms and depleted oxygen levels in surface waters. Higher trophic levels, such as fish and invertebrates, suffer as a result (Camargo and Alonso, 2006; Rabalais et al., 2002).

The problems associated with modern eutrophication are further complicated when we consider global climate change and its impact on eutrophication. Increasing temperatures will result in pycnoclines, stratigraphic patterns in water columns whereby water density variation occurs in response to temperature and salinity (Gnanadesikan, 1999). This is especially the case in coastal and estuarine waters, with abnormally low surface salinities resulting from high freshwater runoff inputs (Milliman and Meade, 1983). The development of pycnoclines will complicate oxygen diffusion, making lower portions of the water column less oxygenated; a problem that is already associated with eutrophication will be greatly exacerbated, and biological communities will suffer (Diaz and Rosenberg, 1995; Diaz and Rosenberg, 2008). Climate change will result in changing wind patterns, and this will likely have an impact on eutrophication, with the

potential to either enhance oxygenation problems (Grantham et al., 2004), or even solve them (Rabalais et al., 2009). The impact of changing hurricane and tropical storm frequency, intensity, and duration will also inevitably impact eutrophication, but these changes will be highly unpredictable, as there is still discord over whether climate change will increase frequency/intensity (Hoyos et al., 2006; Kerr, 2006) or decrease frequency/intensity (Knutson et al., 2007; Kerr, 2008). Projected sea level rise threatens coastal wetland areas, which play a key role in removing reactive nitrogen before it reaches water bodies (Galloway and Cowling, 2002). Perhaps the biggest eutrophication catalyst resulting from global climate change, however, will be the disruption of the hydrological cycle; due to expected increased precipitation in certain areas, more water, sediments, and nutrients will reach coastal waters (Cloern, 2001; Rabalais, 2004), or, conversely, reduced precipitation in other areas will deliver fewer nutrients, resulting in oligotrophication and reduced fisheries productivity (Nixon, 2003).

2.3.1.2 Global Acidification

Delivery of NO_3^--N to water bodies is resulting in a net input of acidity in the form of nitric acid. Acidification of water bodies is increasing in certain parts of North America and Europe (Wright et al., 2001; Allott et al., 1995), decreasing acid neutralizing capacity (Erisman et al., 2013). This has a tremendous negative impact on aquatic ecosystem productivity and biodiversity, shifting species composition to more acid-tolerant organisms. Many organisms at the base of the food chain, including incipient stages of fish and aquatic invertebrates, and even some higher level predators, including benthic invertebrates, zooplankton, amphibians, and birds (Ormerod and Durance, 2009), will be phased out to make way for simpler organisms. These simpler organisms include certain types of macrophytes and phytoplankton. Additionally, atmospheric deposition of reactive N and S is disrupting aquatic ecosystems, particularly those that are freshwater in nature, which have especially low acid neutralizing capacities. And while sulfur emissions have declined significantly, beginning in the mid-1980s, reactive N has become a major component of acidic deposition,

particularly in North America, Europe, and some developing countries (Erisman et al., 2013).

2.3.2 Implications for Global Climate Change

N_r application has significant implications for climate change; the overall enhanced agricultural productivity associated with synthetic fertilizer application spurs elevated denitrification, nitrification, and DNRA rates, resulting in the inherent, subsequent release of nitrous oxide. In fact, roughly 40% of total N_2O emissions are a direct result of anthropogenic activities, including agriculture, industrial activities, and transportation (EPA, 2017). A significant portion of this 40% is attributed to application of synthetic fertilizers to agricultural soils, contributing ~75% of the total United States N_2O emissions in 2015 (USEPA, 2017). On top of this, tropospheric concentrations are increasing at a rate of ~0.25% per year (Galloway et al., 2003). These emissions have significant implications for global climate change.

2.3.2.1 Nitrous Oxide's Potential as a Greenhouse Gas

Nitrous oxide is a potent greenhouse gas with roughly 298 times the 100-yr global warming potential of carbon dioxide, and a residence time in the atmosphere of approximately 114 years (EPA, 2017). While nitrous oxide still contributes less to the greenhouse gas effect than do carbon dioxide, water vapor, and methane, due to the presence of those gases at higher concentrations in the atmosphere, current trends and future projections for N_2O-attributed global warming warrant great concern. Early models projected global emissions of 25.7 Tg N yr^{-1} by 2100, up from 12.7 Tg N yr^{-1} in 1990, and emissions would need to be cut by 80% to meet environmentally desirable climate goals (Kroeze, 1994). Unfortunately, nitrous oxide's ability to impact global warming doesn't end there; recent developments have unveiled nitrous oxide's complicated consequences for the ozone layer.

2.3.2.2 Stratospheric Ozone Depletion

The destruction of the stratospheric ozone layer has been labelled as one of the major environmental issues of the 20th century, with higher production rates of ozone-depleting substances (ODSs) being the catalyst for recent elevated depletion rates (Portmann et al., 2012). Historically, stratospheric chlorine and bromine loading associates with anthropogenic chlorofluorocarbons (CFCs) has been been deemed the primary ODS (Molina & Rowland, 1974; Stolarski and Cicerone, 1974), but recently, a new culprit's potency has been revealed; N_2O currently contributes more to ozone destruction than any other gas emitted as a result of human activities (Ravishankara et al., 2009). N_2O shares many qualities with CFCs, being highly nonreactive in the troposphere, but volatile once it reaches the stratosphere, where it is broken down via photolysis, releasing nitrogen oxides, NO_x:

$$N_2O + h\nu \rightarrow N_2 + O(^1D)$$
$$N_2O + O(^1D) \rightarrow N_2 + O_2$$
$$N_2O + O(^1D) \rightarrow 2NO$$

Ultimately, approximately 10% of N_2O reacts to form these N oxides (NO_x = NO + NO_2), which are known to catalyze reactions that result in the destruction of ozone via the following reactions (Crutzen, 1970; Johnston, 1971):

$$NO + O_3 \rightarrow NO_2 + O_2$$
$$O + NO_2 \rightarrow NO + O_2$$
$$\text{Net: } O + O_3 \rightarrow 2O_2$$

Unlike with CFCs, N_2O has natural sources, the primary contributors being nitrification and denitrification in soils, but, as discussed in previous sections, anthropogenic, intensive agriculture is causing N_2O to be emitted at excessive, unnatural rates. The literature overwhelmingly suggests that these agricultural practices

will continue to be a primary culprit for ozone depletion in the recent future (Ravishankara et al., 2009; Portmann et al., 2012; Revell et al., 2012a; Revell et al., 2012b). However, some sources suggest that the negative effects of these N_2O emissions may ironically be offset by projected increased CO_2 emissions and associated radiative cooling (Rosenfield et al., 2015; Stolarski et al., 2015). Moving forward, controlling and monitoring stratospheric ozone levels will require significant consideration of N_r application and related N_2O emissions, as well as CO_2 emissions (Stolarski et al., 2015).

2.3.3 Human Health Repercussions

N_r production and application also present serious ramifications for human health, be it through interaction with aqueous or gaseous varieties. The known human health repercussions, including respiratory illnesses, methemoglobinemia, and cancer, are discussed in detail below.

2.3.3.1 Respiratory Illnesses

The NO_x compounds produced in the stratosphere, depleting the ozone layer, are having dire consequences for human health. If inhaled, NO_2 can cause severe damage to the lungs, and high indoor concentrations can induce a variety of respiratory illnesses, as well as coughing and a burning sensation inside the lungs (WHO, 2003). Children subjected to continuous exposure are more likely to develop reduced breathing efficiency and certain respiratory diseases (WHO, 2003). High NO_2 concentrations are also indicative of the potential presence of other toxic pollutants produced by the same source, and it is easily measureable, making it useful as a surrogate for the entire pollutant mixture (WHO, 2006).

Apart from the dangers inherent to NO_x production, its subsequent impacts, when released into the lower atmosphere and allowed to react, can increase tropospheric ozone (O_3), smog, particulate matter, and aerosol formation. Tropospheric O_3 is pernicious in that inhalation can cause coughing, asthma, a temporary decline in lung function, and chronic respiratory disease (von Mutius, 2000). A recent study by the

World Health Organization revealed that increasing levels of O_3 in the environment caused a clear rise in mortality and respiratory morbidity (WHO, 2008). The formation of particulate matter is especially concerning, affecting people worldwide; a recent study by the European Environment Agency reveal that there fine particles are responsible for over 455,000 premature deaths in the EU27 states every year (de Leeuw and Horálek, 2009).

2.3.3.2 Methemoglobinemia

The environmental problems inherent to excessive eutrophication are complicated by significant implications for human health; ingesting too much NO_3^- can cause a serious condition known as Methemoglobinemia (MetHb). Methemoglobinemia is a blood disorder involving the abnormally high production of methemoglobin, a type of hemoglobin that contains ferric iron (Fe^{3+}). Hemoglobin is the protein responsible for transporting and distributing oxygen to body tissues via red blood cells, an essential, niche bodily function. Methemoglobin in humans without MetHb is typically below levels of 1%, but individuals with MetHb can, in worst case scenarios, exhibit levels over 70%. Symptoms of mild methemoglobinemia, characterized by methemoglobin levels above 1%, can include headaches, dizziness, shortness of breath, and cyanosis, a condition involving the bluish discoloration of skin membranes (Mansouri and Lurie, 1993). Individuals with severe methemoglobinemia can be prone to seizures (levels greater than 50%), comas, and death (>70%).

At the fundamental level, MetHb takes root when defensive mechanisms in the blood for responding to imbalances in reactive oxygen are rendered less effective, and the ferrous iron (Fe^{2+}) of the heme group in the hemoglobin molecule becomes oxidized to its ferric state, essentially converting hemoglobin to methemoglobin. The unusual abundance of ferric iron results in a relative disproportion in oxygen affinity amongst heme sites in the blood; humans with MetHb have hemoglobin that can transport oxygen, but not in a way that is effective for releasing oxygen, to be uptaken by body tissues, often resulting in tissue hypoxia. MetHb can be inherited from parents carrying the recessive gene for the disorder, and it can also be acquired via exposure to a few

drugs, including certain antibiotics, analine dyes, bromates, chlorates, etc. But the catalyst of particular concern is exposure to NO_3^--N-containing compounds. The recent problem of exported NO_3^--N from excess agricultural fertilizers is of particular concern because infants under the age of six months are especially at risk of MetHb because their red blood cells have lower levels of a crucial methemoglobin reduction enzyme. For this reason, the EPA set a MCL of 10 ppm NO_3^-- N for drinking water.

2.3.3.3 Cancer

The NO_3^--N inherent to nitrogen pollution has been implicated as a precursor and indirect source of nitrosamines, a commonly carcinogenic chemical compound. Nitrate, if ingested, can be resorbed in the gastrointestinal tract and secreted in saliva, where oral bacteria convert approximately 20% of this NO_3^-- N to nitrite (Spiegelhalder et al., 1976; Stephany and Schuller, 1980). Substances included in consumed foods and drugs can then react with this nitrite to form nitrosamines, which are carcinogenic (Magee et al., 1976); in 1984, more than 90% of the 300 different N-nitroso compounds caused carcinogenic activity (Pruessmann, 1984). N-nitroso compounds have been linked to cancer in about 40 animal species, proving to be carcinogenic for many different organs in animals (Bogovski and Bogovski, 1981). Indeed, high exposure to nitrates can increase risk for cancer, especially including esophageal, colon, nasopharyngeal, and gastal cancers (Correa et al., 1975; Hagmar et al., 1991; Tricker and Preussmann, 1991; Mirvish, 1995; Loh et al., 2011), highlighting the need to stifle the delivery of agricultural effluent to nearby water bodies.

2.4 Denitrification Management

As the excessive application of reactive nitrogen (N_r) continues to grow, so does the need to develop strategies for managing its application and eventual, inevitable transportation (Galloway et al., 2008). Many such strategies exist for reducing nitrate leaching from agricultural croplands, including the simple adaptation of nutrient management plans (NMPs), but even with these measures in place, N, P, and other

nutrients are inevitably transported when the water table intersects the root zone (Lassiter and Easton, 2013). And while nitrate leaching from land treatment systems can be inhibited by several other mechanisms, including plant harvesting (Cameron et al., 1997) and N immobilization into the organic matter pool (Degens et al., 2000), the only permanent removal of nitrate is denitrification (Averill and Tiedje, 1982). For this reason, denitrification has been targeted and exploited for its ability to permanently remove nitrate, by designing systems for use in the environment that encourage denitrification, termed “denitrification management.” Two traditional systems for denitrification management are represented in Figure 6 and are discussed below: riparian zones and constructed wetlands.

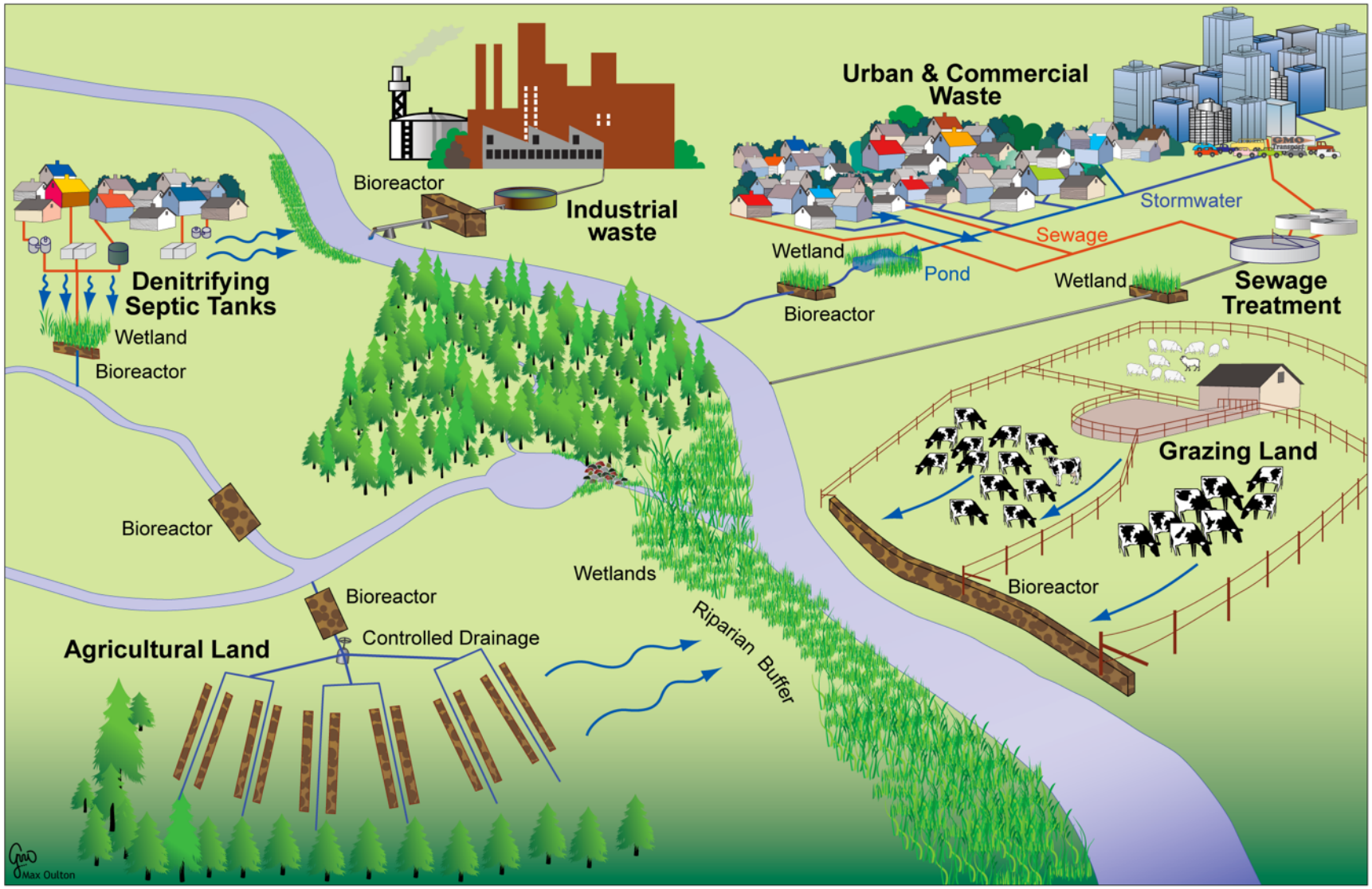

Figure 6 Illustration of denitrification management options, including riparian zones, wetlands, and denitrifying bioreactors. Borrowed from WaiBER (2012).

2.4.1 Riparian zones

Riparian zones are uncultivated, narrow strips of land sandwiched between rivers or streams and adjacent lands, and they are typically covered in dense vegetation, including trees, shrubs, and grasses. Because of their position at the interface of terrestrial and aquatic ecosystems, and the biotic, hydrologic, and geomorphic processes that occur there, these zones have been lauded for their facilitation of pollutant removal, acting as a last-ditch effort to mitigate nutrient pollution in groundwater discharge, before it feeds into downgradient streams (Peterjohn and Correll, 1984; Haycock and Pinay, 1993; Cey et al., 1999). While nitrogen attenuation in riparian zones is still not well understood (Ranalli and Macalady, 2014), there are several known mechanisms that contribute to riparian zones' ability to function as filters, including uptake of nutrients by vegetation (Lowrance, 1992), denitrification (Tiedje, 1988; Jacobs and Gilliam, 1985; Hill, 1996; Cooper, 1990; Hill et al., 2014), and dilution (Altman and Parizek, 1995). Pollutants in sediments can also potentially be removed in ponds, which are commonly formed at upslope edges of riparian buffer zones, allowing these contaminants to settle out of the water column (Muscutt et al., 1993), but the processes following the infiltration of overland flow are the primary pollutant removal mechanisms (Gharabaghi et al., 2002). The thick vegetation that typically surrounds water bodies increases surface roughness and slows overland flow, allowing for drainage to infiltrate into the buffers, and inherent processes filtrate drainage. Because of these slower flow rates, riparian buffers also allow nearby rivers and streams to more adequately handle significant floods and higher flow events.

Riparian zones are currently facing a significant number of anthropogenic stressors, including land use changes, climate change, atmospheric N deposition, and wildfire, and there is therefore added need to fully understand the mechanisms contributing to N attenuation in these zones (Ranalli and Macalady, 2014). Currently, soils are being altered by the stressors, resulting in groundwater passage through mineral soils that are not as favorable for promoting denitrification (Cooper, 1990), thereby making these zones less effective for enhancing N attenuation through the

promotion of “riparian bypass,” Flewelling et al., 2011). Furthermore, returning these organic soils to their denitrification-inducing state can take decades (Downes et al., 1997), highlighting the need to develop alternatives for removing nitrate from groundwater.

2.4.2 Constructed Wetlands

Constructed wetlands are engineered systems that simulate natural wetlands, strategically installed for land reclamation following ecological disturbances, and for biofiltering targeted pollutants that are inherent to industrial wastewater, urban stormwater, etc. (Kadlec and Wallace, 2009). The vegetation, soil, and organisms in these wetlands act in concert to support physical, chemical, and biological processes, removing sediment and/or pollutants, all while contributing to a functional, productive wildlife habitat (Mitsch et al., 2015). Constructed wetlands have shown promise as an effective means for removing a significant number of pollutants, including N (illyas and Masih, 2017a), P, and heavy metals (Khan et al., 2009), from incoming drainage, with dissolved oxygen, organic loading rate, and specific surface area deemed as the most important determinants for pollutant removal (Ilyas and Masih, 2017a), but nitrate is the pollutant of most relevance. In fact, in ordinary, natural wetlands, which are typically dominated by carbon rich and anaerobic environments, it is not uncommon for there to be complete NO_3^--N removal, suggesting that denitrification rates are primarily limited by influent NO_3^--N concentrations (Reddy and Patrick, 1984).

A significant downside to installing constructed wetlands for denitrification management is the fact that they require a significant amount of land for occupation (Ilyas and Masih, 2017b); more often than not, farmers are not keen on using valuable land on remediation, rather than more the more lucrative, fruitful purpose of agricultural production. There have been attempts to develop modified constructed wetlands, such as stack designs or aeration methods (Ilyas and Masih, 2017b), but there is still a need to search for alternative means of denitrification management. One such alternative is the denitrifying bioreactor.

2.5 Denitrifying Bioreactors

Denitrifying bioreactors have emerged as an effective edge-of-field BMP for intercepting agricultural wastewater, and removing excess NO_3^--N from agricultural drainage before releasing it to nearby water bodies and/or underlying aquifers (Blowes et al., 1994; Greenan et al., 2006; van Driel et al., 2006; Jaynes et al., 2008; Schipper et al., 2010; Christianson et al., 2011a).

2.5.1 What are Denitrifying Bioreactors?

Denitrifying bioreactors are subsurface BMPs typically used as an edge-of-field practice for removing nitrate from agricultural drainage, housing organic matter and maintaining an anaerobic environment. The carbon substrate within these bioreactors supports the process of chemoheterotrophic denitrification, the most cost effective and environmentally sound method for removing nitrate from drinking water (Volokita et al., 1996; Lu et al., 2014). The lack of a sufficient carbon energy source can often limit nitrate removal via denitrification, particularly in groundwater, and the carbon media in DNBRs overcomes this lack of an energy source (Starr and Gillham, 1993). The cheap costs and low risk remediation of DNBRs make them implementable at large scales, and applicable to a wide variety of environmental problems, particularly in areas downgradient from significant NO_3^- contributors (Schipper and Vojvodić-Vuković, 1998). Since their inception, DNBRs have been adapted to treat a variety of pollution problems including septic systems (Robertson et al., 2000), aquaculture wastewater, etc.

2.5.2 Installation and Cost

DNBR bed installation typically begins with the excavation of a pit where the bioreactor will be positioned, followed by the placement of drainage control structures where inflow is directed into the bioreactor, and where outflow will escape from the bioreactor (Woli et al., 2010). This can involve the placement of bypass flow structures (discussed later in this chapter), which may be worthwhile if overwhelming flows are expected at the site. The pit should then be lined with a geosynthetic fabric, which will

prevent drainage from escaping from anywhere but the outflow structure. The bioreactor can then be filled with the chosen media, and, while filling the pit, it may be convenient to add piezometers for sampling convenience and water level monitoring. Finally, once the bioreactor is filled with media, the top should be lined with more geosynthetic fabric and/or a soil cover, which may potentially reduce nitrous oxide emissions (Woli et al., 2010). DNBR installations reported in the literature have cost $4400 to $11800, treating a wide variety of drainage areas (12 ha to over 40 ha) (Christianson et al., 2012b). Most cost between $7000 and $9000, with the fill media and contractor fees typically comprising the majority of the costs (Christianson et al., 2012a). The most traditional DNBR substrate of woodchips costs ~$25 m^{-3}, and it is important to remember that costs are also not linear with respect to size (DeBoe et al., 2017).

2.5.3 Types of Denitrifying Bioreactors

Traditionally, in-field DNBRs have been divided into three categories, denitrifying layers, denitrifying walls, and denitrifying beds (Addy et al., 2016). These classifications are largely based on bioreactor geometry, as well as the nature of the pollution that that geometry is meant to enhance pollution interaction. This section delves into the different types of bioreactors, discussing their attributes, frequencies of usage, and performance, ending with a brief summary of Addy et al. (2016), a meta-analysis of DNBRs that compares types.

2.5.3.1 Denitrifying Layers

Denitrifying layers are horizontal, carbon-filled DNBR layers underlying pollution sources. Schipper and McGill (2008), one of the few studies reporting on the performance of field scale DNBR layers, evaluated a New Zealand layer treating dairy factory influent. Results revealed that the layer was unable to achieve insignificant nitrate removal from the wastewater, a finding that the authors attributed to the insufficient 100 mm thickness of the layer; the resultant shorter retention times were incapable to reducing nitrate concentrations to acceptable levels. They concluded that the thicker layers (300-500 mm) used in previous studies by Robertson et al. (2000) and

Bedessem et al. (2005) were more lucrative. Keeping the organic carbon saturated also proved to be difficult, as the potential presence of oxygen in pore spaces limited denitrification. Bypass flow was also identified as a potential limiting factor for nitrate removal rates in this bioreactor, raising concern regarding management practices.

2.5.3.2 Denitrifying Walls

Denitrifying walls are carbon medium-filled trenches that dip beneath the water table by 1 to 2 m, oriented in a direction perpendicular to groundwater flow paths, allowing groundwater to pass through the "subsurface walls" (Addy et al., 2016; Schipper and Vojvodić-Vuković, 2001). Darcian flow principles govern flow in denitrification walls, thereby typically resulting in longer HRTs and a lower nitrate flux per media volume in comparison to denitrifying beds (Schipper et al. 2010a). Denitrifying walls are relatively uncommon, with only a few known examples reported in the literature (Moorman et al., 2010; Schipper and Vojvodić-Vuković, 2000; Schmidt and Clark, 2012). During N-limiting conditions, walls may be more applicable for DNBR treatment, and Robertson and Cherry (1995) suggested using other technologies in concert with denitrifying walls, including the "funnel and gates" concept presented in Starr and Cherry (1994), which involves the use of a plume to funnel concentrated drainage to a single point of treatment, or gate, where the reactive media is contained. Schipper et al. (2010b), a review of monitored denitrifying walls reported nitrate removal rates of 0.01–3.6 g N m^{-3} d^{-1}, significantly lower than rates typically reported in beds.

2.5.3.3 Denitrifying Beds

Denitrifying beds differ from walls in that they are designed to treat concentrated drainage, typically delivered by tile drainage, ditches, or wastewaters (Addy et al., 2016), and have been adapted for treatment in stream beds (Robertson and Merkley, 2009). Beds are often acknowledged as the most effective type of DNBR (Addy et al., 2016), typically supporting nitrate removal rates of 2–22 g N m^{-3} d^{-1} (Schipper et al., (2010b). One potential limitation of denitrifying beds is that substantial bypass flow can occur during significant storm events that generate high flows (Christianson et al.,

2013a; Rosen and Christianson, 2017), and this should be taken into consideration when design and implementing these structures. Hydraulic control components can be installed to adjust for bypass flow potential, and can extend or shorten HRTs if there is need to do so (Figure 7).

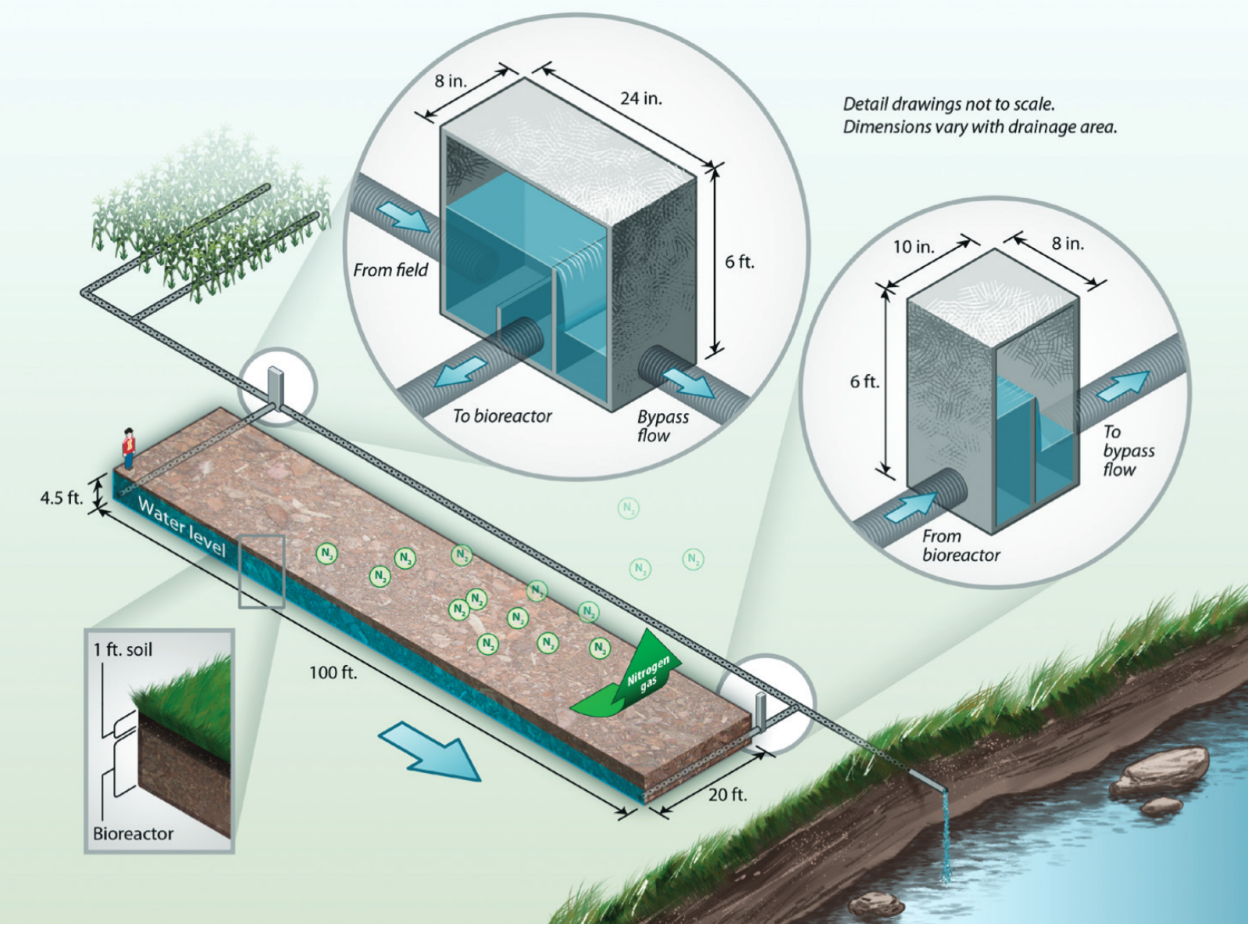

Figure 7 Diagram of an effective denitrifying bed setup, with bypass flow control structures incorporated to adjust for high flow rates and approximate goal HRTs. Borrowed from Christianson and Helmers (2011).

2.5.3.4 DNBR Columns

Unlike the previous three designs mentioned, DNBR columns are not built for in-field treatment, but are rather constructed to replicate the flow dynamics of denitrifying beds at the laboratory scale, meaning they are much smaller than typical, in-field DNBRs (Greenan et al., 2006; Healy et al., 2006). DNBR column experiments are highly

useful because, unlike in the field, the processes that DNBRs are subjected to can be controlled by the observer, and performance can be easily monitored.

2.5.3.5 Comparison

The meta-analysis techniques employed in Addy et al. (2016) to assess 57 separate DNBRs from 26 studies, revealed that while nitrate removal rates reported in bed and column studies did not differ significantly from each other, they were significantly higher than removal rates reported in wall studies. Even with these findings, there is no “one-size-fits-all” DNBR design, and the most ideal setup will vary significantly based on site-specific factors.

2.5.4 The History of Denitrifying Bioreactors: A Synopsis of Case Studies

The use of organic carbon for removing agriculturally-derived N has long been studied, and was implemented decades before the advent of DNBRs, with the first reported case in 1971 (Williford et al., 1971). In the early years, this mechanism was typically applied for treatment of agricultural and municipal wastewater through a variety of approaches (Loehr, 1984; Perry et al., 1984), including sludge sewage treatment processes (Grady and Lim, 1980), trickling-filter or fixed-film reactors (Rock et al., 1990), and methanol dosing (Sikora and Keeney, 1976). However, most of these methods were not practical because of their cost and maintenance requirements, and none of them were appropriate for convenient treatment of farm field runoff. Boussaid et al. (1988) identified the potential of solid organic carbon as a means for remediating NO_3^--contaminated drinking water through passive denitrification, confirming the findings of a septic-system effluent denitrification experiment by Stewart et al. (1979) and an experiment by Williford et al. (1971) that tested the ability of barley straw-filled trench to remove nitrate. Robertson et al. (1991) and Robertson and Cherry (1992) also measured rapid attenuation of septic system NO_3^- in two aquifer zones where solid organic carbon was in abundant supply.

These antecedent studies ushered in the early work on DNBRs, which did not begin until the mid-1990s. A laboratory experiment by Vogan (1993) recorded the ability

of sawdust, alfalfa, wheat straw, and cellulose-filled columns to support denitrification, and found that while sawdust provided the lowest nitrate removal rates, it provided the most potential for long-term removal. A landmark study by Blowes et al. (1994) documented the economical, maintenance free N removal provided by three fixed-bed bioreactors containing coarse sand, tree bark, wood chips and leaf compost. This was the first study on in-field DNBRs, marking the advent of a new, convenient BMP technology for intercepting and treating agricultural effluent.

Many studies would follow in the coming years, and at a variety of scales and locations, including another early study that examined the performance of three denitrifying layers and one denitrifying wall to treat septic system effluent at three different locations at the University of Waterloo in Ontario, Canada (Robertson and Cherry, 1995). The successful nitrate removal, ranging from 60-100%, provided by these bioreactors, containing 20% sawdust and 80% sand media, prompted extended examination, and the Waterloo bioreactors were studied for many years to come. A six-year follow-up study revealed that these bioreactors were still serving their intended purpose, yielding average removal rates of 80%, 70%, 91%, and 57% at HRTs ranging from three hours to forty days, and the authors speculated that the carbon media consumption resulted in a mass reduction of only <10-20% over that lengthy period of time (Robertson et al., 2000). Schipper and Vojvodić-Vuković (1998) expanded on the ideas presented in these in situ sawdust DNBR studies, and the “funnel and gate system” concept presented in Starr and Cherry (1994), reporting on denitrification in a sawdust DNBR wall downgradient of Bardowie Farm, North Island, New Zealand. This DNBR wall would be the site of continued study for years to come, providing a window into the long term performance of DNBRs.

In the years since, DNBRs have been installed in monitored in a vast variety of climate zones. Cooke et al. (2001) examined DNBR applications for tile drainage in Illinois, which initiated a series of subsequent tile drainage studies in Illinois that shed light on DNBR gravel amendments for lessening degree of compaction (Wildman, 2001) and the responses of different media to HRTs and temperatures (Doheny, 2002). In Iowa, a series of studies explored the impacts of carbon media, HRTs, and design

geometry on DNBR performance. A handful of field studies in Iowa and Minnesota have recorded carbon media longevity, N_2O emissions, and removal of non-nitrate compounds (Jaynes et al., 2008; Moorman et al., 2010, Christianson et al., 2012b). A growing number of in situ bioreactors have been implemented in the Chesapeake Bay Watershed (Bock, 2014; Bock et al., 2015; Bock et al., 2016; Rosen and Christianson, 2017).

DNBRs have been adopted as a final step for wastewater treatment (Oakley et al., 2010; Schipper et al., 2010), with van Driel et al. (2006) being one of the first reported cases of DNBRs directly treating drainage water effluent. Bioreactors have been implemented to target wastewater from aquaculture facilities, where controlled flow rates are more realistic than in non-point source N pollution streams (Lepine et al., 2016; von Ahnen et al., 2016), and they have been used in conjunction with other BMPs, such as constructed wetlands (Tanner et al., 2012)

DNBR application has even been expanded to treat P in addition to N. Robertson and Cherry (1995) highlighted Fe as a beneficial additive to DNBRs for limiting PO_3^-; iron and PO_3^- can react to precipitate vivianite ($Fe(PO_4^2) \cdot 8H_2O$), thereby reducing PO_3^- levels via formation of lake bottom sediments (Nriagu and Dell, 1974). Woodchip and biochar bioreactors the Delmarva Peninsula and Tidewater region of Virginia, both in situ and in laboratory column studies, have successfully supported NO_3^--N and PO_4^{3-}-P removal from tile drainage and simulated agricultural drainage, respectively (Bock, 2014; Bock et al., 2015; Bock et al., 2016). Goodwin et al. (2015), Hua et al. (2016), and Abusallout and Hua (2017) recorded the successful simultaneous removal of nitrate and phosphate from drainage water using woodchips and steel byproduct filters.

2.5.5 Factors Contributing to DNBR Performance

The many factors that influence DNBR performance are still under investigation, and much progress has been made in recent years, as DNBRs have continued to garner recognition as a means to cost-effectively attenuate nitrogen from agricultural effluent.

2.5.5.1 Carbon Media

Selecting the proper carbon source prior to DNBR installation is of utmost importance, and should involve the consideration of the many site-specific factors that will impact the ability of chosen media to perform. The most important factors to take into consideration include cost, porosity, C:N ratio, and longevity (Robertson et al., 2000; Robertson et al., 2005a; Christianson et al., 2012). Based on these considerations, and on the desired treatment goals, the most appropriate, applicable media type can change from location to location. A wide variety of carbonaceous materials have been tested for their ability to support denitrification, including woodchips (Blowes et al., 1994; Elgood et al., 2010; Long et al., 2011; Moorman et al., 2010; Robertson and Cherry, 1995; Schipper and Vojvodić-Vuković, 2001; Addy et al., 2016), biochar (Bock et al., 2015; Easton et al., 2015; Bock et al., 2016), cellulose (Boussaid et al., 1988; Vogan, 1993), raw cotton (Volokita et al., 1996a), newspaper (Volokita et al., 1996b), sawdust (Vogan, 1993; Robertson and Cherry, 1995; Schipper and Vojvodić-Vuković, 1998; Robertson and Anderson, 1999; Schipper and Vojvodić-Vuković, 2001), bark (Blowes et al., 1994), compost (Blowes et al., 1994), jute pellets (Wakatsuki et al., 1993), wheat straw (Vogan, 1993), vegetable oil (Hunter et al., 1997; Hunter, 2001), alfalfa (Vogan, 1993), and maize cobs (Cameron and Schipper, 2010).

Initial studies identified simple carbon compounds, such as ethanol, methanol, and acetate, as successful at enhancing denitrification rates. The need to find cheaper, more widely available carbon sources soon brought cellulose, a constituent of all plant materials and the most most abundant renewable resource in the world (Couglan, 1985), to the forefront of DNBR media research. Sawdust was revealed as an ideal carbon media source for its high degree of reactivity (Carmichael, 1994), ideal C:N ratio (Vogan, 1993), high permeability, and high availability. It was also common practice to use sand or excavated soil amended with woody material (typically less than 25% by volume) as a carbon source for denitrification in DNBRs (Robertson et al., 2000). These practices were voided after evaluations of long-term performance in these bioreactors and comparisons of the media, showing that the sole use of woody material sustained higher N removal rates for substantial periods of time (Robertson et al., 2000).

Traditionally, woodchips have been supported as the most common medium used in DNBRs (Blowes et al., 1994; Elgood et al., 2010; Long et al., 2011; Moorman et al., 2010; Robertson and Cherry, 1995; Schipper and Vojvodić-Vuković, 2001; Addy et al., 2016); their cheap cost, longevity, C:N ratio, and conductivity make them an ideal choice in denitrifying bioreactors. In fact, in many cases, substantial nitrate removal has been supported for over 10 years, with little to no maintenance required for operation (Blowes et al., 1994; Robertson, 2010; Christianson et al., 2011a; Cooke and Bell, 2014), and a few studies report woodchip bioreactors approaching 15 years of age still managing to remove NO_3^--N effectively (Robertson et al., 2008; Schipper et al., 2010). Moorman et al. (2010) compared woodchip matrix to a soil control, and found that denitrification potential activity was, at minimum, 31 times greater for woodchips than for the soil control, and, at maximum, 4000 times greater.

Out of the various woodchip varieties, hardwood species are typically preferred over softwood species (Addy et al., 2016). This is largely due to the fact that hardwood species are generally more reliable C sources than softwood species; the lignin in softwoods makes C-limited scenarios more likely in DNBRs (Cornwell et al., 2009). Additionally, the lower density wood in softwoods allows for more exposure to oxygen, resulting in faster decomposition, further contributing to a C-limited scenario (Cornwall et al., 2009). Indeed, softwood species often have lower C:N ratios, resulting in flushing losses and mass degradation (Gibert et al., 2008). Carmichael (1994) suggested that, in woody, carbonaceous material, denitrification occurs at the penetrable rims of particles, where NO_3^--N-rich influent can be easily diffused, thereby opposing the notion that denitrification is restricted to grain surfaces. These assertions were affirmed in long-term DNBR studies that larger wood particles featured thick, dark-colored rims, with lighter centers, whereas smaller particles appeared to be completely darkened (Robertson et al., 2000). Robertson et al. (2005b) concluded that this suggests that the water infused into the wood may also be denitrified, and Appleford et al. (2008) later confirmed this theory.

The porosity, particle size, and hydraulic conductivity of woodchips is highly variable, and will influence bioreactor hydraulic properties (Christianson et al., 2012a).

Commonly, woodchip porosities range from 0.6-0.86 (Chun et al., 2009, Robertson, 2010; Ima and Mann, 2007; Christianson et al., 2010a) and from 0.65 to 0.79 in situ (Chun et al., 2009; Woli et al., 2010; van Driel et al., 2006). Woodchip porosity decreases as moisture content (Ima and Mann, 2007) and packing density (Christianson et al., 2010) increase. While several studies have investigated chip shapes and sizes, no significant differences in nitrate removal have been reported between coarse and fine chips (Greenan et al., 2006; van Driel et al., 2006), course chips are considered preferable because of their high hydraulic conductivity (van Driel et al., 2006).

Carbon media type directly influences, bioreactor longevity, which is of obvious importance, and depends on a variety of complex factors, including the type and volume of carbon source, flow characteristics, the degree of bioreactor saturation, and certain physical changes in the media through time (Schipper et al., 2010b). The presence of oxygen plays a significant role in organic matter degradation; oxygen, like nitrate, acts as an electron acceptor, but, unlike nitrate, acts as a reactant, attacking complex organic matter and thereby causing degradation (Schink, 1999). The anaerobic decomposition of organic carbon is generally slower than the aerobic decomposition of organic carbon (Bridgham et al., 1998), so DNBRs should be designed to keep carbon media as saturated as possible, maximizing anaerobic conditions. Other consumption reactions include dissolved organic carbon (DOC) leaching and sulfate reduction (Robertson et al., 2000), and these reactions need to be considered for their promotion of pollution swapping.

The lifetime of a carbon supply supporting denitrification is difficult to estimate; denitrifiers do not directly use media as a C source, but rather the more labile organic compounds released by other anaerobic microbes (Tiedje, 1988; Beauchamp et al., 1989). The longevity of carbon in DNBRs can be predicted using stoichiometric equations of the decomposition of organic matter using nitrate as an electron acceptor, but these methods are limited in that they ignore the possibility of the anaerobic degradation of organic matter when an external electron acceptor is unavailable (Schipper and Vojvodić-Vuković, 2001). In other words, these equations assume that

denitrification is the only process responsible for the decay of organic matter, potentially resulting in inflated DNBR lifetime estimates via these methods.

Results from stoichiometric estimates of longevity are highly variable, depending on any number of site-specific factors. The first DNBR study, Blowes et al. (1994), speculated that their DNBRs would perform for over 70 years. Another early DNBR study proposed that carbon sources may potentially last over 15 years, based on estimates of the stoichiometric consumption of carbon by nitrate (Robertson and Cherry, 1995). That same bioreactor was still operating proficiently 15 years later (Robertson et al., 2008). The bioreactor discussed in Moorman et al. (2010) was fully functional after 9 years, and estimates of the saturated wood half-life yielded an expected lifetime of ~37 years. Empirical observations of the 11-year-old wall investigated in Long et al. (2011) produced a lifetime estimate of 66 years.

A handful of evaluations of the long-term performance of DNBRs suggest that these BMPs have the ability to support substantial denitrification rates for "at least a decade or longer" with no need for carbon replenishment (Robertson and Cherry, 1995; Robertson et al., 2000). An assessment of four denitrifying bioreactors in Robertson et al. (2000) found that DNBR performance did not deteriorate at a University of Waterloo bioreactor during 6 years of operation, and reported the highest removal rates of 32 mg N L^{-1} during the fourth year of operation. While the indirect measurement of hydraulic rates at the other three DNBRs made the calculation of reaction rates more difficult, and therefore it was difficult to evaluate long-term performance, these bioreactors removed significant amounts of nitrate over the 6 year period. Robertson et al. (2000) claimed that after 6-7 years of operation, carbon media in four DNBRs at the University of Waterloo had only degraded by 2-3% in each via denitrification, and <10-20% total, including other consumption reactions.

Addy et al. (2016) found media age to have a significant impact on nitrate removal; beds younger than 13 months generally supported significantly high nitrate removal rates than beds that were 13 to 24 months old and >25 months old. For these reasons, Schipper et al. (2010) and Robertson (2010) suggested that nitrate removal rates in the first year should not be expected in the long-term. There is therefore great

need for more work on long-term DNBR maintenance to provide information on performance of these bioreactors as their carbon sources continually deplete.

2.5.5.2 Influent NO_3^--N Concentration

Influent NO_3^--N concentration can have a profound impact on NO_3^--N removal rates (Barton et al., 1999), and many examples of N-limited conditions have been reported in the literature (Rosen and Christianson, 2017; Addy et al., 2016). Addy et al. (2016) compiled data from a vast variety of DNBR studies, and determined that influent NO_3^--N concentrations play a major role in nitrate removal rate; higher nitrate removal rates were observed in beds that received influent with N concentrations at >30 mg N L^{-1} than in beds that received low (<10 mg N L^{-1}) or intermediate (10-30 mg N L^{-1}) concentrations. To determine whether or not denitrification is limited by energy source or NO_3^--N concentrations, half-saturation constants (K_{in}) can be calculated (Myrold and Tiedje, 1985). Consistent, prolonged denitrification requires influent with a sufficient NO_3^- concentrations coupled with a steady C supply (Starr and Gillham, 1993). However, in NO_3^--N limited environment environments, denitrifier populations are resilient and can survive for months using slow fermentation for cell maintenance (Jørgensen and Tiedje, 1993). Therefore, DNBRs employed at locations where seasonal NO_3^--N concentration trends and fluctuations are expected may not have their denitrification performance jeopardized.

When implementing DNBRs, the potential for NO_3^--N limitation is also important to consider because the absence of an electron acceptor in a low oxygen setting can promote formation of harmful compounds, such as methyl mercury, hydrogen sulfide, and methane (Fenton et al., 2014; Schipper et al., 2010b).

2.5.5.3 Hydraulic Retention Time

Hydraulic retention times (HRTs) play a major role in bioreactor maintenance, and are governed by bioreactor flow rates, volume, and carbon media porosity. HRTs are calculated as:

$$HRT = \rho V/Q$$

Where V represents the total volume of the bioreactor, ρ is the porosity of the carbon medium, and Q is the flow rate passing through the bioreactor.

HRT is typically correlated with NO_3^--N removal rates (Christianson et al., 2012b; Woli et al., 2010); the longer the HRT, the more time a given parcel of water is subjected to processes like denitrification, removing nitrate. Therefore, brief retention times can be expected to result in minimal nitrate removal, mainly due to the aforementioned higher flow rates, but also because dissolved oxygen higher levels are usually higher, crippling the ability of denitrifying organisms to perform denitrification. On the opposite end of the spectrum, excessively long retention times can result in complete NO_3^--N removal from agricultural drainage. Chun et al. (2009) examined NO_3^--N reductions of 10 to 40% at HRTs of 5 h, and 100% removal at HRTs of 15.6 and 19.2 h. Greenan et al. (2009), presented removal efficiencies of 30 to 100% at HRTs ranging from 2.1 to 9.8 days. Addy et al. (2016) revealed that cumulative nitrate removal in beds with HRT from 6 to 20 h and >20 h was significantly greater than in beds with HRT < 6 h.

Optimal DNBR maintenance should involve control structures to establish HRTs sufficient enough to lower drainage nitrate concentrations to acceptable levels (Christianson et al., 2012). Significant bypass flow, occurring during high flows that overwhelm DNBRs, can substantially reduce DNBR effectiveness (Christianson et al., 2013; Rosen and Christianson, 2017), and has been reported as a phenomenon common to DNBR layers (Schipper and McGill, 2008). In denitrifying beds, flow control structures, strategically placed at the upstream and downstream ends of DNBRs, can easily be managed to manipulate flow rates for desired HRTs. During periods of low precipitation, stop logs within these structures can be removed to maintain appropriate retention times, and the opposite is true for periods of higher precipitation, when stop logs can be added to maintain retention times (Chun et al., 2010). As such, implementing these structures and actively managing them can vastly improve denitrifying bed performance.

2.5.5.4 Dissolved Oxygen

Because denitrification requires sufficiently low dissolved oxygen concentrations (Korom, 1992), high levels of dissolved oxygen can cripple the ability of denitrifying organisms to perform denitrification within DNBRs. When oxygen is present in high concentrations, denitrifying bacteria will generally choose oxygen over NO_3^--N as an electron acceptor, as it is generally more convenient. The extent to which DO levels can limit denitrifying varies amongst denitrifying organisms (Korom, 1992), but denitrification can be hindered at DO concentrations as low as 0.2 mg L^{-1} (Metcalf and Eddy, 2003). Therefore, maintaining a significant degree of saturation within bioreactors is ideal, keeping dissolved oxygen as low a possible.

2.5.5.5 Temperature

Denitrification is a biologically-mediated process, and high temperatures therefore generally increase denitrification rates. Many examples of improved DNBR performance in response to higher temperatures have been reported in the literature (Volokita et al., 1996; Diaz et al., 2003; Cameron and Schipper, 2010; Hoover, 2012; Bock et al., 2016). For example, Volokita et al. (1996) found that cellulose-dependent denitrification was highly impacted by temperature, with denitrification rates at 14°C being roughly one third of the rates at between 25 and 32°C. Schipper and Vojvodić-Vuković (1998) revealed a similar relationship, with NO_3^--N removal at 28°C averaging 6.5 g N m^{-3} d^{-1} and 3.6 g N m^{-3} d^{-1} at 19°C. The Q_{10} factor is an important measure for determining NO_3^--N removal rate in response to increasing temperature, and is the factor by which the reaction rate rises for every 10°C increase in temperature (Christianson et al., 2012a). In the literature, reported Q_{10}s have ranged from 1 to just under 3, and most values are constrained within 2 ± 0.5 (van Driel et al., 2006a; Robertson and Merkley, 2009; Cameron and Schipper, 2010; Warneke et al., 2011a; Hoover, 2012). The meta-analysis fitted linear model of Addy et al. (2016) yielded a Q_{10} of 2.15. Addy et al. (2016) also revealed that denitrifying beds operated at temperatures less than 6°C supported lower NO_3^--N removals than did beds at intermediate temperatures (6 to 16.9°C) and high temperatures (greater than 16.9°C).

Prior to any DNBR installation, site-specific temperatures, and seasonality influences should be given significant consideration; based on expected temperatures, DNBRs can be sized for appropriate HRTs and expected influent NO_3^--N concentrations. Furthermore, it is also vital to consider how temperature will affect these inflow fluxes and NO_3^--N concentrations; during frigid seasons, when the presence of snow is more likely, periodic pulses of snow-melt can result in abnormal DNBR HRTs, drastically fluctuating in response to the pulsing flow. Warmer seasons, when flows are likely more stable, have to be accounted for as well. This is further complicated by the fact that the highest drainage NO_3^--N loads, which typically occur in the spring, are often out of sync with maximum temperatures, in the summer, and HRTs may need to be adjusted because of temperature and influent concentrations.

Further testing needs to be done regarding temperature's influence of DNBR performance, especially on the lower end of the spectrum, as most tested temperatures have only gone down to 10°C (Greenan et al., 2006; Healy et al., 2006), with one outlier study that observed NO_3^- removal at temperatures as low as 2°C to 4°C (Robertson and Merkley, 2009). Artificial increasing of DNBR temperatures is a topic of interest, even though a recent attempt using passive solar heating yielded only a 3.4°C mean bioreactor temperature increase and no significant increase in NO_3^--N removal rate (Cameron and Schipper, 2011). If temperatures can be successfully artificially increased in DNBRs, the lower reduction rates associated with colder environments may be circumvented altogether.

2.5.5.6 Microbiology

Denitrifiers are usually ubiquitous in natural environments, impacting biogeochemical cycles and ecosystems at local, regional, and global scales (Seitzinger, 1988; Codispoti and Richards, 1976; Nixon et al., 1996). Denitrifying enzyme activity (DEA), the measure of functional denitrifying enzymes in soil, indicates how suitable an environment is for supporting denitrification (Tiedje et al.,1989), and therefore is an effective means of assessing microbiology within bioreactors. Despite denitrifier ubiquity, DEA can be highly variable, and the microbial communities within bioreactors

vary with depth, flow direction, season (Schipper and Vojvodić-Vuković, 2001). Inoculation has typically not been required in the maintenance of DNBRs (Schipper et al., 2010a; Christianson et al., 2012), although small volumes of soil have been supplemented in a few cases (Blowes et al., 1994; Christianson et al., 2011c). Sometimes, microbial communities grow slowly after start-up (Wildman, 2001; Bock et al., 2016), and these are situations where inoculation may be warranted. The inoculation of optimal denitrifiers species to support maximum denitrification rates is worth exploring in future research (Andrus, 2011).

Non-denitrifying bacteria present within DNBRs have the potential to promote clogging if biofilm forms (Chun et al., 2009). Occasional flushing by removing stop logs may solve this issue (Wildman, 2001; van Driel et al., 2006), although high flows could potentially wash out denitrifiers (Volokita et al., 1996).

2.5.5.7 Bioreactor Dimensions and Geometry

Despite guidelines provided in NCRS (2009) and spreadsheets that calculate sufficient dimensions for bioreactors (Iowa Natural Resource Conservation Service, 2016), there is still no consensus on the optimal designs for DNBRs (Christianson et al., 2012a), mainly because these designs will be highly site specific, and will change based on many factors. Little work has been done to assess the impact of DNBR geometry on function, except for a lone study by Christianson et al. (2010), which evaluated the impact of different cross-section shapes in pilot-scale DNBRs, and found no significant differences. There is the potential for bioreactors to be undersized (Rosen and Christianson, 2013), which can result in insufficient treatment and bypass flow, and there is therefore significant need to consider dimensions.

2.5.6 Pollution Swapping

“Pollution swapping” refers to the unintended creation of soluble or gaseous contaminants, including GHGs, organic C, or metals, by DNBRs (Fenton et al., 2014; Warneke et al., 2011c; Schipper et al., 2010b). Obviously, this is an undesirable outcome to system installed with the best of intentions, and, as such, preventing these

consequences is ideal. Some of the potential routes of pollution swapping are discussed below, and include sulfate reduction, the flushing of dissolved organic carbon, and nitrous oxide emission

2.5.6.1 Sulfate Reduction

Sulfate reduction is the conversion of sulfate (SO_4^{2-}) to hydrogen sulfide (H_2S) by sulfate reducing bacteria or archaea via anaerobic respiration. This process is problematic because it can result in (1) C depletion, (2) hydrogen sulfide production through anaerobic digestion, and (3) methylation of mercury. Carbon media depletion is obviously undesirable because denitrifiers will have less of an energy source. Hydrogen sulfide, H_2S, is a corrosive, poisonous, and flammable gas that is colorless and has a rotten egg odor. Methyl-mercury is a bioaccumulative environmental toxicant that is highly toxic to humans and aquatic systems (Compeau and Bartha, 1985). Bioaccumulation can result in developmental issues in children, including decreased memory function, loss of IQ points, and adverse impacts on language skills (Rice et al., 2003), and elevated risk of cardiovascular disease and heart attacks in adults (Choi et al., 2009).

While high denitrifying bioreactor HRTs and/or low influent nitrate concentrations can result in complete NO_3^--N removal, they can also support sulfate reduction. This is especially likely at high temperatures, which make sulfate reduction a more probable outcome (Blowes et al., 1994; Robertson and Cherry, 1995; van Driel et al., 2006; Robertson and Merkley, 2009; Shih et al., 2011). In conditions where N is limited and reduced conditions exceeding -300 mV ORPs, DNBRs can support sulfate reduction, and these conditions are typically most common in bioreactors that are set for longer HRT treatments with close to 100% nitrate removal efficiencies (Lepine et al., 2016).

In order to minimize sulfate reduction, bioreactors should be designed and managed to maintain low nitrate effluent concentrations of no less than ~0.5 mg NO_3^--N L^{-1} (Robertson and Merkley, 2009; Shih et al., 2011), and if the presence of hydrogen sulfide is detected, stop logs should be removed in flow control structures to decrease

the HRT, and therefore lessen the likelihood of complete nitrate removal and subsequent sulfate reduction (Christianson and Helmers, 2011).

2.5.6.2 Flushing of Dissolved Organic Carbon

The flushing of dissolved organic carbon (DOC) from DNBRs has long been a concern in DNBR maintenance (Schipper et al., 2010b; Healy et al., 2012; Fenton et al., 2014; Bell et al., 2015; Abusallout and Hua, 2017). DOC exported from DNBRs can potentially encourage downstream microbial activity, resulting in oxygen depletion; installing these bioreactors can, in some cases, ironically support the development of hypoxic zones (Schmidt and Clark, 2012). The DOC leached during the bioreactor start-up period is the result of mass transfer across the liquid film encapsulating wood particles, whereas long-term leach rates, which are lower and more consistent, are a response to sustained microbial and chemical degradation rates of the medium and intra-particle diffusion (McLaughlan and Al-Mashaqbeh, 2009). Woodchip leachate is commonly brown in color, due to the presence of tannins, lignins, and other phenolic substances, and this can reduce sunlight penetration through the water column, potentially reducing primary productivity downstream (Svensson et al., 2014; Svensson, 2014). This leachate can also contain organic matter that is highly reactive with chlorine, possibly resulting in the formation of haloacetic acids (HAAs), trihalomethanes (THMs), and total organic halogen (TOX) (Golea et al., 2017). There is also the potential for humic substances to promote the formation of disinfection byproducts (DBPs) during the process of drinking water disinfection (Hua et al., 2014). Oxidized steel byproduct filters have been proven as a valuable addition to DNBRs for their ability to attenuate DOC from woodchip leachate, with the two-phase bioreactor in Abusallout and Hua (2017) reducing DOC export by 44%. Recent evidence also suggests that weather carbon mediums are preferable to fresh carbon mediums for their lower rates of C export (Hoover et al., 2016).

2.5.6.3 Nitrous Oxide Emission

N_2O is a GHG, and its increased emission due to widespread agricultural practices is of great concern; N_2O has 300 times the radiative forcing of carbon dioxide (CO_2), and it also reacts with and depletes essential stratospheric ozone (O_3). Current estimates suggest that human activities are responsible for about 30% of the atmosphere's N_2O (Mosier et al., 1998), and there is therefore serious need to stifle nitrous oxide emissions from agricultural systems. Unfortunately, nitrous oxide has been observed from denitrifying bioreactors (Warneke et al., 2011b; Moorman et al., 2010; Elgood et al., 2010; Easton et al., 2015; Bock et al., 2015; David, 2014; Eldyasti et al., 2014a; Eldyasti et al., 2014b), which typically occurs when incomplete denitrification is supported.

2.5.7 Phosphorus Removal Potential

Historically, denitrification has been the primary process promoted in denitrifying bioreactors (Greenan et al., 2009), and as a result, there is a tendency to direct all focus towards N treatment. However, in recent years, growing attention has been directed towards these reactors as potential systems for removing phosphorus (P), a nutrient that is typically naturally limited in natural ecosystems, but, with the onset of modern agricultural practices, is being exported at much higher rates than is natural, upsetting freshwater ecosystems. P is often coupled with N in pollution directly resulting from agriculture (Groffman et al., 2006), and the discovery and application of systems that remove both N and P in conjunction is therefore highly desirable, despite the fact that the processes that promote effective N removal are fundamentally different in nature from the processes that promote P removal. Several media types have successfully promoted N and P removal in DNBRs, and these include steel byproducts (Goodwin et al., 2015; Hua et al., 2016; Christianson et al., 2017) and biochar (Bock et al., 2015; Bock, 2014), biochar being the main media of focus in this work.

2.6 The Properties of Biochar

Recently, biochar has been labeled as a promising, fruitful additive to DNBR column media (Bock, 2014; Bock et al., 2015; Easton et al., 2015; Bock et al., 2016). This section begins by discussing biochar's properties and its use as a soil amendment, and ends by discussing its place in DNBR research as a means to enhance nutrient removal from agricultural drainage and stifle nitrous oxide emissions.

2.6.1 What is Biochar?

Biochar is a carbon-rich material formed through pyrolysis, the thermal decomposition of biomass in low oxygen environments at temperatures less than 700°C (Lehmann and Joseph, 2009), hydrothermal carbonisation, the carbonisation of saturated organic matter under high pressures and temperatures between 180°C and 250°C (Libra et al., 2011), or gasification. This conversion effectively results in approximately a twofold increase in carbon content (Lehmann, 2007). Biochar production is not too unlike charcoal production, but biochar's intended use in soil improvement, waste management, climate mitigation, and energy production, warrants its unique name (Rodríguez, 2010; Lehmann and Joseph, 2009). Conversely, the term "charcoal" refers to charred biomass used for fuel, filtering, iron-making, or art.

2.6.2 A Brief History of Biochar Application

While the term "biochar" was coined relatively recently, and the use of this carbon-rich material as a soil amendment for ecological engineering is a modern advancement at the global scale, it is not foreign to particular regions, and has left its mark on recorded history. Trimble (1851) reported the success of charcoal in accelerating the growth of vegetation, Santiago and Santiago (1989) and Morley (1927) confirmed charcoal's advantageous sponge-like properties and encouraged applications in horticulture, and Young (1804) accounted the process of "paring and burning," which involved the dumping of soil onto burning organic matter for increased farming profit. Usage even precedes these early accounts in the 19th and 20th centuries; in the

Amazon Basin, patches of black soil, rich in biochar, suggest that natives of the region, present before the arrival of the Europeans, intentionally applied the material for increased soil productivity (Lehmann et al., 2006; Sombroek et al., 2003). Even today, hundreds of years later, the total C storage in these biochar-amended soils is more than double that of adjacent Amazonian soils without biochar (Glaser et al., 2002). This Amazonian biochar is, in part, responsible for sparking the recent widespread fascination with the material; the sustained fertility of the region is believed to have been instigated by biochar application, and may have promoted the success of complex civilizations there (Petersen et al., 2001).

2.6.3 Biochar in the Modern World

As this evidence of ancient usage suggests, biochar is an excellent soil amendment; it is much more efficient at enhancing soil productivity than materials like composts and manures, largely due to its physical and chemical properties. These properties include: (1) its high charge density and sorption affinity (Liang et al., 2006), making it superb for carrying and retaining nutrients (Lehmann et al., 2003; Glaser et al., 2015), attenuating certain contaminants, organic compounds, and heavy metals (Cao et al., 2009; Zheng et al., 2010; Cabera et al., 2011), and expediting soil water percolation (Rodríguez, 2010), (2) its particulate nature (Skjemstad et al., 1996; Lehmann et al., 2005), (3) its high C content, and (4) its chemical structure (Baldock and Smernik, 2002), which make it less susceptible to microbial decay in comparison to other types of organic matter (Shindo, 1991; Cheng et al, 2008). Together, these benefits make biochar highly conducive for agronomic and/or environmental management, increasing soil fertility and structure, and improving fertilizer efficiency and decreasing the likelihood of excess nutrient transport (Liang et al., 2006).

In addition to the enhanced agricultural productivity inherent to amended soils, biochar's high C content and slow decay rate make application an effective means of C sequestration, thereby combating climate change. Plant biomass typically degrades rather rapidly, but converting biomass to biochar lengthens its biological cycle (Lehmann et al., 2006; Lehmann, 2007); while biochar's storage time is still under

question, and is likely impacted by many factors, evidence suggests a lifetime on the order of centennial to millennial time scales, orders of magnitude longer than ordinary plant biomass (Lehmann et al., 2006). Additionally, biochar sequestration is far lower risk than many other sequestration options; once biochar is added to soil, it is highly unlikely that it will promote adverse reactions (Lehmann, 2007). Even under high application rates of up to 140 tons C ha^{-1}, no negative impacts have been observed, all while improving crop yields (Lehmann et al., 2006).

Of course, potential cost constraints need to be taken into consideration. Fortunately, biochar wins out here as well, being cheaper in application than many other soil amendments and C sequestration methods. A multitude of thermochemical routes can be employed to produce biochar, and any substance of biological origin can be exploited as feedstock, resulting in myriad biochar varieties that are available wherever biomass is bountiful (McLaughlin et al., 2009). Given a steady, cheap supply of biomass, the heat and pressure generated by the machinery used to execute pyrolysis costs only ~US$4 GJ^{-1} (Lehmann, 2007). This cheap cost is bolstered by the fact that biochar production makes efficient use of existing resources; even farmers in ill-equipped ecosystems can create biochar from already-existing organic residues and biomass fuels without squandering yields and returning profits (Lehmann and Joseph, 2009).

2.6.4 Nutrient Cycling Dynamics

Indeed, biochar is a cost-effective, efficient, environment-friendly soil additive that has become a hot research topic in recent years, and its utility has expanded to include enhancement of agricultural and wastewater treatment processes (Liang et al., 2014). This is largely because biochar has the potential to enhance soil-plant system N and P cycling (Gul and Whalen, 2016). Pyrolysis is generally seen as the traditional, preferred method for biochar creation, and the pH, surface area, and nutrient content are believed to dictate the cycling properties of these biochars (Brewer, 2012). Depending on the production temperatures and feedstocks that are used to create pyrolyzed biochar, pH, surface area, and nutrient content can vary significantly (Lehmann et al., 2006; Downie

et al., 2009; Brewer and Brown, 2012; Zhao et al., 2013), and this is an important, emerging component of biochar research.

The baseline nutrient content of biochars will obviously impact cycling, and therefore intended use. Organic and inorganic forms of N and P contained in biochar include NO_3^-, NH_4^+, ortho-P, and amide groups (Kookana et al.,2011; Jindo et al., 2014). Generally speaking, feedstocks like manure and crop residues will be converted to biochars with higher nutrient contents, pHs, and surface areas, and biochars produced from ligno-cellulosic feedstocks, such as wood, will typically have lower nutrient contents, pHs, and surface areas (Gul et al., 2015). The amount of biologically-available N changes based on production temperature; NH_3 volatilization at higher temperatures results in a net loss (Gul and Whalen, 2016). The dominant N species is controlled by heating temperatures; biochars produced at higher temperatures will typically contain more NO_3^-, while biochars formed at lower temperatures are characterized by a more pronounced presence of NH_4^+ (DeLuca et al., 2009). Increased production temperature also dictates biochar ortho-P concentration, with several studies revealing that higher temperatures produced biochar with lower ortho-P concentrations (Mukherjee and Zimmerman, 2013; Azuara et al., 2013), a result attributed to ortho-P crystallization with insoluble magnesic, ferric and calcic phosphates (Zornoza et al., 2016).

The following section discusses currently known mechanisms for N and P cycling alteration by biochar, largely based on the work of a review by Gul and Whalen (2016).

2.6.4.1 Mechanisms for Attenuating Reactive Nitrogen

Biochar is known to disrupt the N cycle, and its influence on denitrification is of particular interest. In soils sans biochar, denitrification is responsible for a significant portion of nitrous oxide emissions; incomplete denitrification results in the escape of intermediate N_2O, a potent greenhouse gas. Biochar has the ability to alter this process; depending on the additive influence of many arcane, misunderstood environmental conditions, biochar amendment can provoke atypical decreases (Alho et al., 2012; Saarnio et al., 2013; Cayuela et al., 2013; Bock et al., 2015; Easton et al., 2015; Dicke et al., 2015; Hüppi et al., 2015; Harter et al., 2017) or increases (Clough et al., 2010;

Yoo and Kang, 2012; Alho et al., 2012; Anderson et al., 2014; Sánchez-García et al., 2014; Davis, 2015; Obia et al., 2015; Petter et al., 2016) in expected N_2O emissions. The mechanisms responsible for these discrepancies are still under investigation, and highlight the need for continued research on biochar's impact on the N cycle. A recent review by Cayuela et al. (2014) declared that biochar impacts on N_2O emissions depend on C:N ratio, pyrolysis temperature, feedstock, and interactions with soil and N fertilizer. Together, these factors can diminish nitrous oxide emission by: (1) increasing soil pH (Gul et al., 2015), (2) promoting nosZ gene expression (Anderson et al., 2011; Harter et al., 2014), thereby increasing the likelihood that N_2O will be reduced to N_2, (3) enhancing aeration (Gul et al., 2015), and (4) promoting NO_3^- immobilization and subsequent uptake by plants (Deenik et al., 2011; Zheng et al., 2012; Maestrini et al., 2014).

2.6.4.2 Mechanisms for Attenuating Reactive Phosphorus

Biochar application also has promise for removing reactive phosphorus through sorption, a process that is highly dependent on the type of biochar feedstock (Chintala et al., 2014), and, like with N attenuation, the mechanisms behind P removal via biochar application are still not well understood. For example, Chintala et al. (2014) and Nelson et al. (2011) both reported low phosphate sorption in acidic soils, while Xu et al., (2014) observed high sorption in acidic soils. In fact, several studies have implicated that biochar has no use for attenuating P (Madiba et al., 2016; Uzoma et al., 2011). More recently, a biochar production experiment suggested that higher pyrolysis temperatures produce biochars that have decreased P availability and increased P sorption, but results were highly feedstock specific (Ngatia et al., 2017). These findings indicate that biochar application should involve careful consideration of the factors involved in biochar production. Frequently, biochar used for agricultural purposes is produced at temperatures that range from 300-500°C (Hale et al., 2013; Xu et al., 2014; Zhai et al, 2015), which, according to the conclusions drawn from Ngatia et al. (2017), may be out of range for optimizing P sorption. This trend of higher P sorption with higher production temperature biochars is believed to result from the conversion of highly labile O-alkyl C

(Spielvogel et al., 2008) to the more inert, stable aromatic C (Haumaier and Zech, 1995), thereby squandering the volatility of wood components and increasing the number of sorption sites, fixed C, and surface area (Keiluweit et al., 2009). With continued research, the factors contributing to optimal P sorption with biochar will hopefully continue to surface.

While these studies are a testament to how far our understanding of biochar has come in recent years, due to the heterogeneous nature of these findings, there is still much to uncover, and many years of further testing will be needed before biochar is sold to the masses.

3 Methods

3.1 Motivation

The primary objective of this experiment was to determine the effect of biochar media, HRT, influent NO_3^- concentration, and influent PO_4^{3-} concentration on NO_3^--N removal and PO_4^{3-}-P removal in flow through, laboratory-scale denitrifying bioreactor columns.

3.2 Experimental Design

The impact of media type, HRT, influent NO_3^--N concentration, and influent PO_4^{3-}-P concentration on NO_3^--N and PO_4^{3-}-P removal in woodchip-based and biochar-amended DNBRs was assessed using laboratory-scale columns. Nutrient removal was quantified for three media types, woodchips (W), 90% woodchips and 10% biochar (B_{10}), and 70% woodchips and 30% biochar (B_{30}). Each percentage of media type was added by volume. Each media type was subjected to four formulations of simulated agricultural drainage: all combinations of high and low influent NO_3^--N concentrations (16 and 4.5 mg L^{-1}) and high and low PO_4^{3-} concentrations (1.9 and 0.6 mg L^{-1}), which were deemed environmentally relevant based on assessments of nutrient concentrations in tile drainage and drainage ditches (Schmidt et al., 2007; Baker et al., 1975; Vadas et al., 2007). Three HRTs were selected (3, 6, and 12 h) based on several studies identifying HRT targets of 4-6 h (Hoover et al., 2016; Lepine et al., 2016; Greenan et al., 2009; Damaraju et al., 2015), 8+ h (Christianson et al., 2013b), and 12 h (Moorman et al., 2015). Each unique combination of media type, influent formulation, and HRT was tested in triplicate using independent columns (Figure 8). For each of the nine trials, twelve DNBR columns (6560 mL ± 30 mL) were filled with 5000 mL of a single medium, which was primed for one week with the formulation of nutrient solution that it was to be subjected to during the experiment. When each trial began, the four formulations of simulated agricultural drainage (Table 1) were each pumped through the four sets of three columns at a constant rate corresponding to one of the three tested

HRTs (Figure 9). Influent and effluent water samples were collected to quantify N and P removal over the course of each five-day trial.

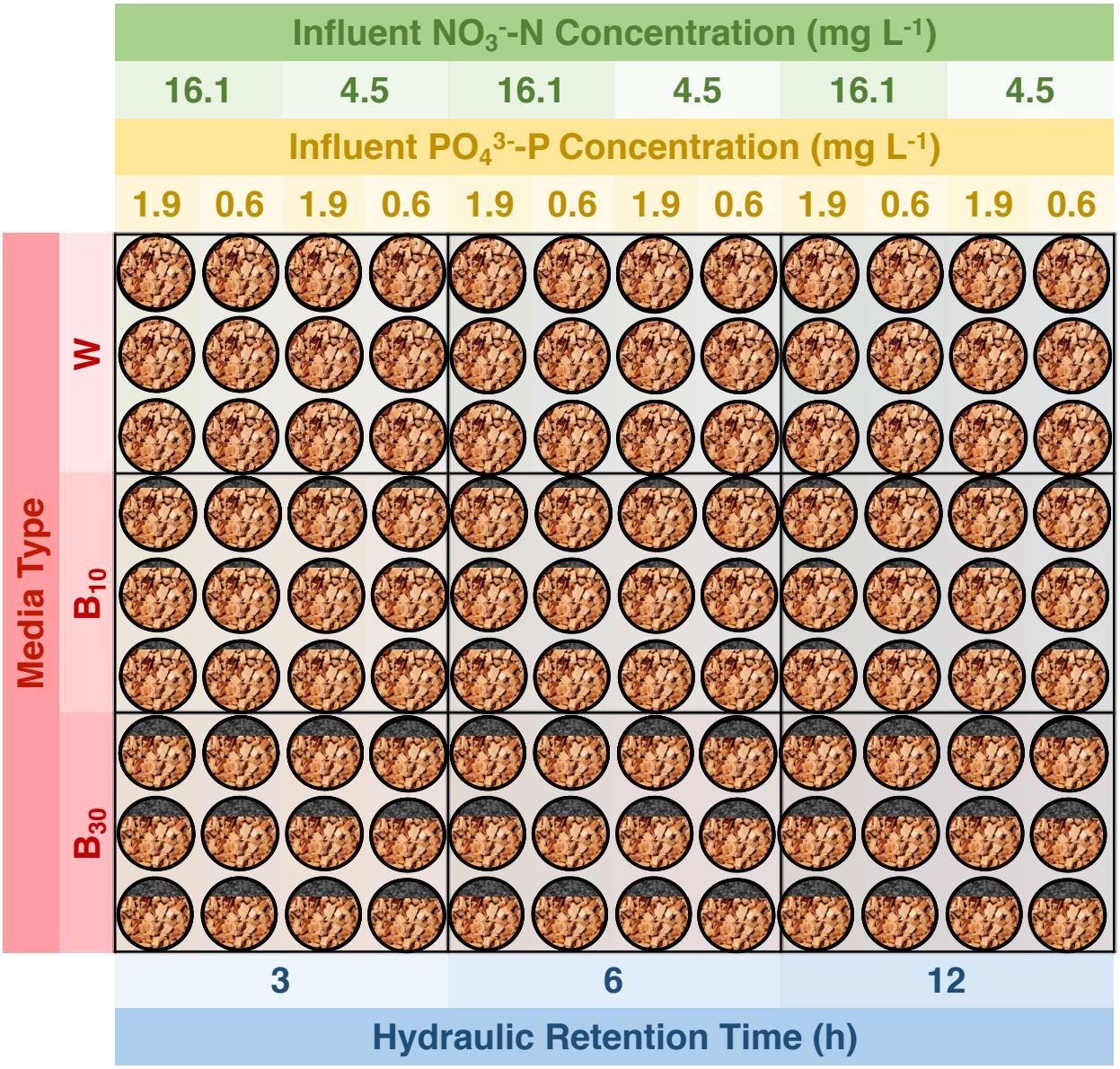

Figure 8 Schematic showing each of the nine experimental trials, with each circle representing an independent column. All unique combinations of medium type, HRT, and influent NO_3^--N and PO_4^{3-}-P concentration were tested with three independent replicates.

Combination Term	NO_3^--N Conc. (mg L^{-1})	PO_4^{3-}-P Conc. (mg L^{-1})
HH	16.1	1.9
HL	16.1	0.6
LH	4.5	1.9
LL	4.5	0.6

Table 1 The influent NO_3^--N and PO_4^{3-}-P concentration combinations used for the experiment.

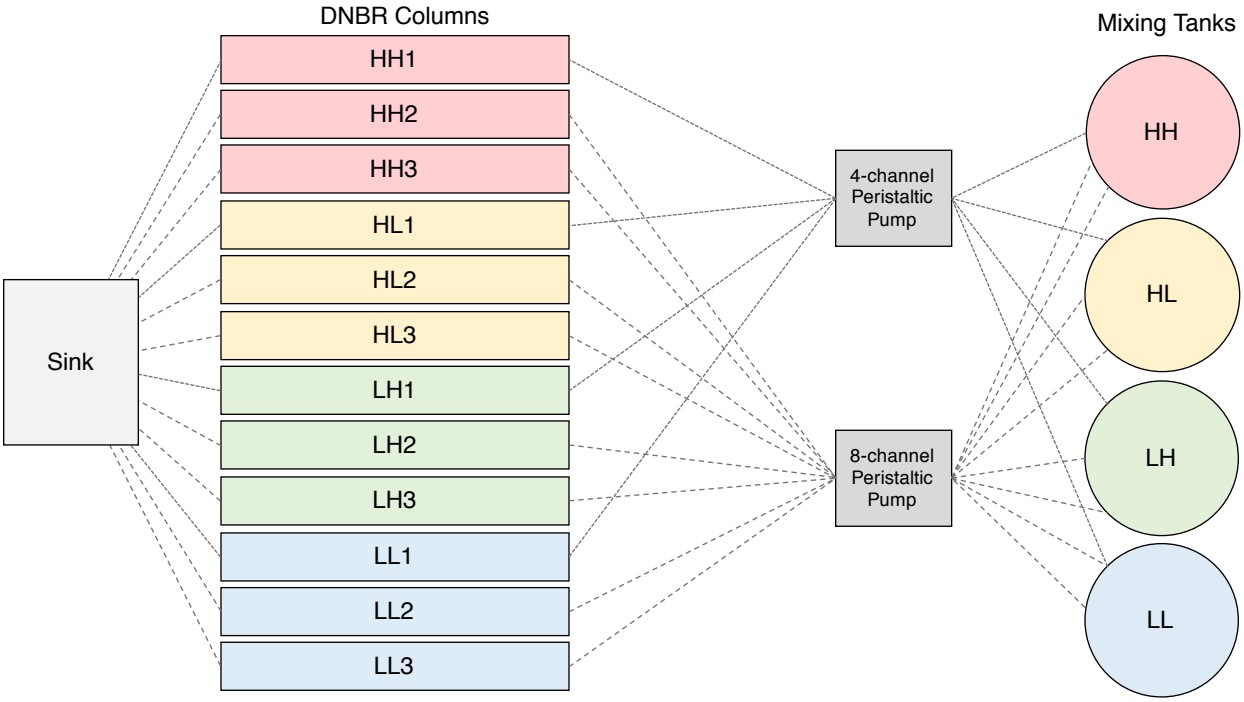

Figure 9 Diagram of the experimental setup, with flow from right to left. Using the two peristaltic pumps, simulated agricultural drainage was pumped from the mixing tanks into the individual designated DNBR columns at a flow rate corresponding to the desired HRT, and effluent is disposed. HH represents high NO_3^--N (16.1 mg L^{-1}) and high PO_4^{3-}-P (1.9 mg L^{-1}), HL represents high NO_3^--N (16.1 mg L^{-1}) and low PO_4^{3-}-P (1.9 mg L^{-1}), etc., and the numbered columns represent the replicates.

3.3 DNBR Column Design

Twelve bioreactor columns, constructed from PVC pipes (61 cm L x 10 cm i.d.) fitted on opposite ends with end caps and threaded plugs with adaptors and couplings, were used in prior, relevant laboratory-scale DNBR batch experiments (Figure 10) (Bock et al., 2015; Easton et al., 2015; Davis, 2015), during which the columns were oriented vertically. For the purposes of this study, these columns were modified for a horizontal flow-through setup to adequately simulate field-scale DNBR conditions. Prior to modification, each of the columns was thoroughly cleaned using Decon™ Contrex™ AP Powdered Labware Detergent and triple rinsed with deionized (DI) water. Each of the columns was then sawed into two pieces at approximately 20 cm from the outflow end of the columns, and PVC wye fittings were used to bridge the separated pieces of each column, increasing the original total inner volume of each column from 5660±30 mL to 6560 L ± 30 mL (Figure 11; Figure 12). PVC primer and cement was used to join the pieces. Originally, there were butyl rubber septa attached to the top of the threaded plugs, allowing for gas headspace sampling via syringe extraction, but the addition of the wye fittings to the columns allowed for a new, convenient means of gas sampling, involving the attachment of a cap connected to a Picarro G2508 Analyzer for N_2O, NH_3, H_2O, CH_4, and CO_2, purchased from Picarro, Inc. (Santa Clara, CA).

Figure 10 The original column design, which was modified for this experiment. Note that these columns were originally oriented vertically.

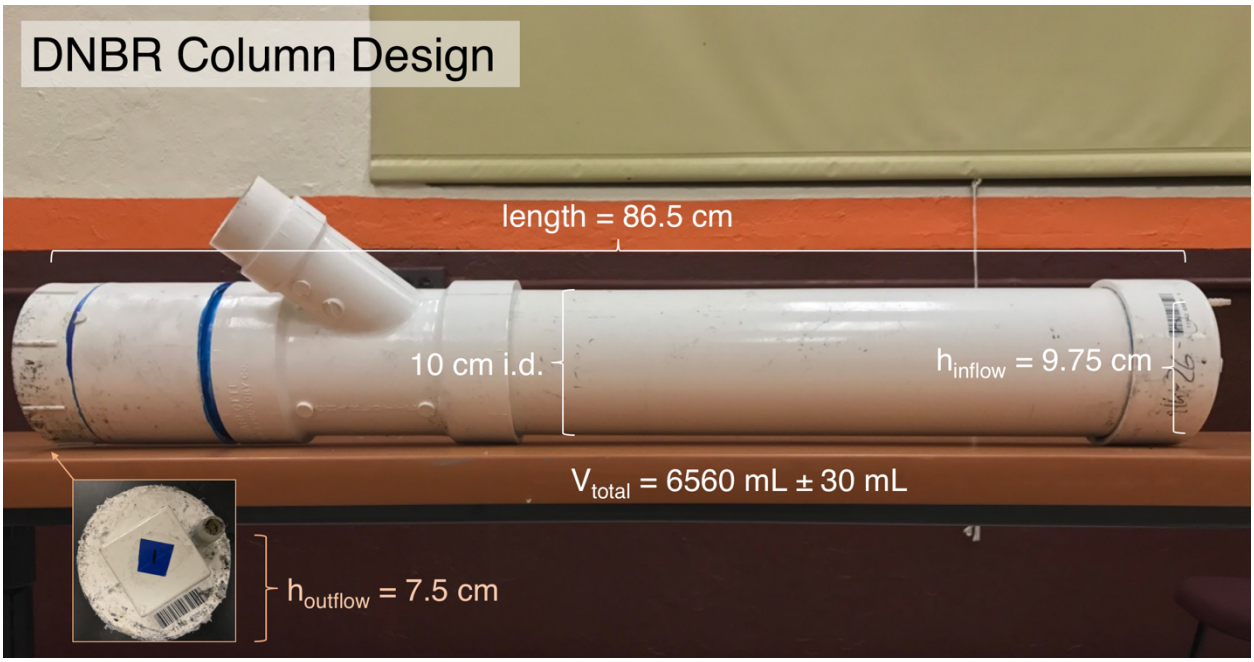

Figure 11 The modified DNBR setup used for this experiment. The wye fitting was added for the purpose of collecting gas emission measurements. The inflow adaptor was placed at the highest possible height of the horizontal column (9.75 cm). The picture in the bottom left corner is of one of the threaded plugs, which has an adaptor at a height of approximately 7.5 cm, controlling the desired height of the water table, and indicating the approximate height of the fill media.

Figure 12 Lengthwise cross-section visual of an individual DNBR column, with flow from right to left. The wire mesh was added as a means to prevent media, particularly biochar, from washing out of the columns.

The end caps were attached by using PVC-primer and cement and holes for nylon tube fitting adaptors (Thogus), ¼" NPT Male x ⅛" Barbed, were drilled in the end caps, approximately 9.75 cm from the bottom of the inner column, the highest position the hole could be placed. The adaptors were attached at this position on each column and using thread seal (teflon) tape, and served as the locations where ⅛" tubing delivered influent from a peristaltic pump. On the opposite ends of the columns, holes for nylon tube fitting adaptors (Thogus), ¼" NPT Male x ½" Barbed, were drilled in each threaded plug, 7.5 cm from the bottom of the inner diameter of each column, the approximate height of the medium within each column, and therefore the desired extent of saturation. These adaptors were also attached with thread seal, and sections of ½" tubing were attached to them, serving as the points of collection for aqueous samples. The threaded plugs were attached to the columns using thread pipe thread sealant (RectorSeal), maintaining a watertight seal. Between each trial, the authenticity of this seal was verified, since swapping the aged media for fresh media required breaking the

seal. For the duration of this study, the columns were stored in slotted wooden racks, in a room where greater than 95% of periodically collected temperatures fluctuated between 19.5°C and 22°C.

3.4 Organic Carbon Media

Woodchips purchased from Blackberry Mulch (Christiansburg, VA) were used as the control media for the experiments, and sourced from mixed hardwood species. Hardwood species were chosen for their more labile C supply than typical for softwood species (Cornwell et al., 2009), although rarely do either provide for C-limited conditions (Cameron and Schipper, 2010). The biochar was purchased from Biochar Now (Carbondale, CO), and was produced from a pine feedstock via a two-stage pyrolysis process, during which the feedstock is briefly held for <1 min at 500-700°C under low oxygen conditions, and then the temperature is reduced to 300 to 550°C and held for up to 14 min. Two size fractions are produced by passing the biochar through an auger, yielding a biochar consisting of about 80% pieces approximately 1.5 cm long by 1 cm wide by 0.5 cm and 20% as a fine dust fraction on the order of 10-100 μm. This particular biochar was chosen for its prior success in removing NO_3^--N and PO_4^{3-}-P while maintaining minimal N_2O emissions in a previous study involving batch experiments with biochar and woodchips (Bock et al., 2015).

Prior to each trial, 5000 mL of media were added to each of the columns, representing approximately 76% of the total volume of each column. This volume was chosen to leave gas headspace in the DNBR columns for gas sampling with a Picarro GHG Analyzer, which will be discussed in future works. Three media types were chosen for these experiments, and each percentage was added by volume: 100% woodchips (5000 mL), 90% woodchips (5000 mL) and 10% biochar (500 mL), and 70% woodchips (5000 mL) and 30% biochar (1500 mL). Because the biochar filled the interstitial spaces between the woodchips, the total media volume was not increased despite keeping the 5000 mL of woodchips consistent across all media types. A near uniform distribution of

the biochar-amended media was achieved by thorough mixing prior to filling the columns in between trials.

The porosity of the woodchips was determined via volumetric displacement to be 0.66 $cm^3\,cm^{-3}$, which falls within the range of 0.60-0.86 $cm^3\,cm^{-3}$ reported in the literature (Chun et al., 2009; Robertson, 2010; Ima and Mann, 2007; Christianson et al., 2010a; Woli et al., 2010; van Driel et al., 2006). The porosity for 90% biochar and 10% woodchips was determined to be 0.61 $cm^3\,cm^{-3}$ and the porosity for 70% woodchips and 30% biochar was approximately 0.52 $cm^3\,cm^{-3}$. These porosities were determined by adding the known biochar volume to the product of the woodchip porosity and woodchip volume, and dividing that number by the total media volume.

3.5 Column Dosing

Two peristaltic pumps were used to deliver simulated agricultural drainage from four separate mixing tanks, each of which contained a unique solution, to the columns. The 4-channel pump (Catalyst by Masterflex 77724-04) was used to supply the top rack of columns, and the 8-channel pump (Masterflex L/S 7535-08) was used to supply the bottom two racks. Tygon E-Food tubing links (1.57 mm i.d., Catalog No. 97100-63) were used for the 4-channel pump, and Masterflex Tygon E-LFL tubing links (1.57 mm i.d., Model No. 06447-14) were used for the 8-channel pump. Tygon ND-100-65 PVC Medical/Surgical Tubing (1/8" i.d., 1/4" o.d., Part No. S50HLTGT18-116-50) was used to connect the pumps and attached links to the mixing tanks and the DNBR columns. The links were checked often for leaks, and were switched out when air bubbles were noticeably propagating towards the columns or when solution began to drip from the pump rollers. Between trials, all tubing was thoroughly rinsed with DI water to prevent the buildup of precipitated material.

Influent was delivered to the columns with goal retention times of 3, 6, and 12 h, chosen based on a variety of studies attempting to evaluate the impact of hydraulic retention time on bioreactor performance (Hua et al, 2016; Hoover et al., 2016; Hoover, 2012; Lepine et al., 2016; Addy et al., 2016). The flow rates necessary for these

theoretical, desired HRTs were determined using estimates of media porosity, calculated using results from preliminary volumetric displacement tests on woodchip media and measured biochar media volumes (Table 2). HRTs were measured at the beginning of each trial by recording the differences between the pump starting time and times of outflow in each of the twelve columns. These early, measured HRTs were assumed to remain constant throughout each trial, since tubing link leaks were so uncommon, and so easily diagnosable.

Trial	Med	p	v_p (mL)	q (mL min^{-1})	Goal HRT (h)	Actual Mean HRT (h)
1	W	0.66	3300	4.6	12	11.77
2	W	0.66	3300	9.2	6	5.97
3	W	0.66	3300	18.3	3	3.28
4	B_{10}	0.61	3050	4.2	12	12.5
5	B_{10}	0.61	3050	8.5	6	5.78
6	B_{10}	0.61	3050	16.9	3	3.05
7	B_{30}	0.52	2600	3.6	12	13.05
8	B_{30}	0.52	2600	7.2	6	6.62
9	B_{30}	0.52	2600	14.4	3	3.43

Table 2 The porosities (p) and corresponding pore volumes (v_p) used to calculate pump flow rates (q) necessary for goal HRTs for each of the nine trials, as well as the actual, observed mean HRTs.

3.6 Simulated Agricultural Drainage: Constituents and Carbon Medium Priming Procedure

The four test solutions for each trial were prepared in four separate, graded 30 gal plastic bins. Tap water was used as the solvent for the solution, chosen over DI water for its cost, convenience of usage, and more accurate simulation of real-world conditions. Prior to the experiments, testing of the tap water revealed low N and P concentrations that did not result in significant variation after adding solute. Granular

calcium nitrate ($Ca(NO_3)_2$) was used as a source of NO_3^- and granular potassium phosphate monobasic (KH_2PO_4) was used as a source of PO_4^{3-}, and solute masses were carefully added to produce the necessary concentration combinations.

In order to promote conditions suitable for denitrification, prior to each experimental trial, fresh media was primed for one week with the test solution that it was to be subjected to during the experiment (e.g. column HH1 was primed with HH solution, column LH1 was primed with LH solution, etc.), taken directly from the mixing tanks. During the priming process, the discolored, used solution was drained from the columns three times, usually every two days, and replaced with fresh solution to reduce the impacts of DOC export from the matrix leachate during DNBR start-up (Abusallout and Hua, 2017), and to eliminate the possibility of interference during analysis of aqueous samples. After the week of priming, in an attempt to minimize the effects of the first flush of dissolved organic carbon, each of the columns was drained and washed three times with DI water. This process was repeated and used media was replaced with fresh media between each trial.

3.7 Sampling Schedule

Aqueous effluent samples and greenhouse gas (GHG) emission measurements were collected at 0, 2, 4, 6, 9, and 12 h, every 6 h for the remainder of the first two days, every 12 h on the third day, and every 24 h for the remainder of each 5-day trial (Figure 13). Sampling frequencies were selected based on preliminary testing, and on sampling frequencies used in previous column experiments of similar nature (Bock et al., 2015; Easton et al., 2015; Davis, 2015).

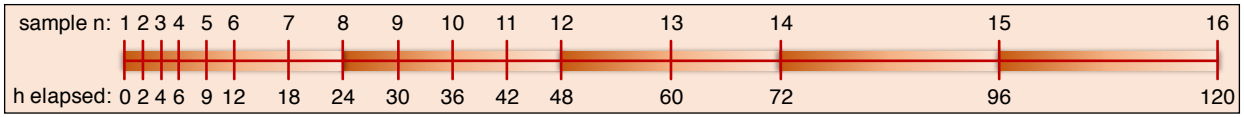

Figure 13 Timeline of aqueous and gaseous sampling for each five-day trial, with color ramp resets indicating the passage of one full day.

3.8 Aqueous Sample Collection and Analysis

Aqueous samples were collected in 50 mL acid-washed Falcon™ 50mL Conical Centrifuge Tubes by placing them in styrofoam trays and directing the proper tubing to the labeled centrifuge tubes, taking extra care to not cross-contaminate. Samples were immediately filtered through 0.45-μm nylon filters (Restek Corporation, Bellefonte, PA), and stored in a freezer until analysis was performed. Usually within three days, and always within a week, aqueous samples were analyzed using a flow injection analysis system (QuikChem® 8500, Lachat Instruments, Loveland, CO), with the cadmium reduction method for NO_3^- Lachat method 10-107-04-1-A) and the ascorbic acid method for PO_4^{3-} (Lachat method 10-115-01-1-A) (Lachat Instruments, 2012). The method detection limit ranges were 0.2-20 mg L^{-1} N and 0.02-2 mg L^{-1} P.

3.9 Statistical Analyses

Times series plots of effluent NO_3^--N and PO_4^{3-}-P concentration, and their respective removal efficiencies, were created with the ggplot2 and gridExtra packages in R (Wickham, 2009; Baptiste, 2015). Using the ggplot function, a non-parametric loess smoothing method (span = 0.35) was applied to the time series data to allow for better visualization of trends. Initially, the effects of media type, HRT, influent NO_3^--N concentration, influent PO_4^{3-}-P concentration, elapsed time, and their interactions on effluent NO_3^--N and PO_4^{3-}-P concentration were assessed through linear mixed effects (LME) modeling and breakpoint analyses. Results from these analyses indicated that time was not a significant factor in NO_3^--N or PO_4^{3-}-P removal (e.g., the columns were at steady state), and therefore the factor time was dropped during subsequent analyses. After removing three time points from the data set (72, 96, and 120 h) to avoid making the data unbalanced, four Analyses of Variance (ANOVAs) were generated using the ezANOVA function from the 'ez' package (Lawrence, 2016) in the R statistical programming environment (R Core Team, 2016). Prior to running the ANOVAs, normality was verified by graphically inspecting quantile-quantile (Q-Q) plots of the NO_3^--N and PO_4^{3-}-P experimental data sets. Homoscedasticity of variances was also verified

via Levene's Test for Homogeneity of Variance (p-value = 0.30 for the NO_3^--N data set and p-value = 0.45 for the PO_4^{3-}-P data set). Multicollinearity was not present because the independent variables of HRT, media type, influent NO_3^--N concentration, and influent PO_4^{3-}-P concentration are not intercorrelated and are independent from each other. The first two ANOVAs were used to examine NO_3^--N removal, and the second two ANOVAs were used to examine PO_4^{3-}-P removal.

3.9.1 ANOVAs: Nitrate

The first NO_3^--N ANOVA was used to determine if media type, HRT, influent NO_3^--N concentration, influent PO_4^{3-}-P concentration, and any of their interactions, had significant effects on effluent NO_3^--N concentration. Effluent NO_3^--N concentration was designated as the dependent variable, and media type, HRT, influent NO_3^--N concentration and influent PO_4^{3-}-P concentration were identified as between group independent variables. Output from this ANOVA revealed that none of the effects containing influent PO_4^{3-}-P concentration significantly affected effluent NO_3^--N concentration, so influent PO_4^{3-}-P concentration was dropped as a predictor. The second NO_3^--N ANOVA was the same as the first ANOVA, except media type was dropped from the predictors. This second ANOVA was generated to develop a clearer picture of the impact of HRT on effluent NO_3^--N concentration, and therefore on NO_3^--N removal, regardless of which media types were used.

3.9.2 ANOVAs: Phosphate

The first PO_4^{3-}-P ANOVA was used to determine if media type, HRT, influent NO_3^--N concentration and influent PO_4^{3-}-P concentration had significant effects on effluent PO_4^{3-}-P concentration. Effluent PO_4^{3-}-P concentration was designated as the dependent variable, and media type, HRT, influent NO_3^--N concentration and influent PO_4^{3-}-P concentration were identified as between group independent variables. None of the predictors were dropped from the ANOVA, since every predictor was present in a significant interaction term. The second PO_4^{3-}-P ANOVA was the same as the first ANOVA, except media type was dropped as a predictor. Like with the second NO_3^--N

ANOVA, the second PO_4^{3-}-P ANOVA was created to identify differences between PO_4^{3-}-P concentrations based on HRTs, regardless of which media types were used.

3.9.3 Tukey's HSD Tests

Tukey's Honest Significant Difference (HSD) tests were run on both sets of ANOVAs using the TukeyHSD function in the multcomp R package (Hothorn et al., 2008) to assess the significance of differences between the means of each unique treatment. Significant differences between treatment groups were displayed on interaction plots of the experimental data set, binned based on the significant ANOVA predictors.

4 Results

The results for NO_3^--N and PO_4^{3-}-P are reported separately below, with the plots of the raw time series data, output from the ANOVAs, summary statistics, and interaction plots for both data sets.

4.1 Nitrate

Times series of DNBR effluent NO_3^--N concentrations (Figure 14) and corresponding removal efficiencies (Figure 15) reveal that every possible combination of media type, HRT, and nutrient solution was successful at removing nitrate from the simulated agricultural drainage, albeit to varying degrees. Several individual treatments were even able to achieve removal efficiencies approaching 100% at steady state (Figure 14g, j, k); most of these cases involved the longest HRT of 12 h and lower influent NO_3^--N concentration of 4.5 mg L^{-1} (Figure 14g, j).

The NO_3^--N ANOVA containing all possible explanatory variables revealed that none of the interactions terms that included influent PO_4^{3-}-P concentration were significant predictors of effluent NO_3^--N concentration, suggesting that influent PO_4^{3-}-P concentration did not play a role in NO_3^--N removal in these systems. Influent PO_4^{3-}-P concentration was therefore dropped from the first ANOVA (as stated in section 3.9.1), and the resulting ANOVA output is displayed in Table 3. The highest order interaction of media type, influent NO_3^--N concentration, and HRT was significant, making interpretations of any of the lower order interactions invalid following the principle of marginality, which asserts that only the highest order significant interactions of model summaries are meaningful and worth further explanation (Nelder, 1977; Nelder, 1994). In the NO_3^--N ANOVA assessing NO_3^--N effluent concentration regardless of media type, the highest order interaction was significant as well, and output is shown in Table 4.

Based on the significant highest order interactions reported in the full NO_3^--N ANOVA, Table 5 shows the summary statistics for the significant ANOVA effects. At the low influent NO_3^--N concentration of 4.5 mg L^{-1}, treatment mean removal efficiencies

and rates ranged from 40.7-93.7% and from 4.38-11.02 g N m^{-3} d^{-1}, respectively. and from 16.9% to 58.8%, or 8.62 to 18.52 g N m^{-3} d^{-1} at the high influent NO_3^--N concentration of 16.1 mg L^{-1}. Note that while the removal efficiencies as a percent reduction in influent concentration are generally higher for lower influent NO_3^--N concentrations than for the higher influent NO_3^--N concentrations, removal rates (g N m^{-3} d^{-1}) are greater for higher influent concentrations.

The interaction plots with assignment of significant differences from Tukey's HSD test results (Figure 16) for effluent NO_3^--N concentration and media type suggest that the impact of biochar amendment on NO_3^--N removal at each HRT in these systems was dependent on influent NO_3^--N concentration. At the low influent NO_3^--N concentration of 4.5 mg L^{-1}, the W, B_{10}, and B_{30} treatments were not significantly different from one another in their ability to remove NO_3^--N at each HRT (Figure 16d, e, f). However, differences arose at the high influent nitrate concentration of 16.1 mg L^{-1}. For the 12 hour HRT, the W treatment was not significantly different from B_{30}, but the B_{10} treatment supported less NO_3^--N removal than both W and B_{10} (Figure 16a). At the 6 hour HRT, B_{30} had a clear advantage over B_{10}, but the W treatment was not significantly different from either of the biochar amendments (Figure 16b). Finally, at the 3 hour HRT, B_{30} removed more NO_3^--N than both W and B_{10}, which were not significantly different from one another (Figure 16c). Under the high influent NO_3^--N concentration of 16.1 mg L^{-1}, the B_{30} treatment was significantly better than B_{10} at removing NO_3^--N at every HRT (Figure 16a, b, c), but, interestingly enough, B_{30} only clearly outperformed W at the 3 hour HRT (Figure 16c). It should be noted that while B_{30} wasn't indicated by the Tukey's HSD tests as being significantly better at removing NO_3^--N than W at the 12 hour and 6 hour HRTs (Figure 16a, b), but mean outflow concentrations for each B_{30} column were lower than the mean outflow concentrations for W (Table 5).

Regardless of media type, the HRTs at each NO_3^--N inflow concentration resulted in NO_3^--N outflow concentrations that were significantly different from one another (Figure 17). At the high influent NO_3^--N concentration of 16.1 mg L^{-1}, the 12 hour HRT resulted in a significantly greater mean NO_3^--N removal efficiency (51.9%) than did the 6 h HRT (28.9%) and the 3 h HRT (21.1%), and the 6 h HRT efficiency was

significantly greater than the 3 hour HRT efficiency. The same pattern in efficiencies was present at the low influent NO_3^--N concentration of 4.5 mg L^{-1} (89.9% for the 12 h HRT, 70.2% for the 6 h HRT, and 42.8% for the 3 h HRT). However, the reverse of this pattern was noted in removal rates for the high influent NO_3^--N concentration of 16.1 mg L^{-1} (11.02, 11.36, and 14.14 g N m^{-3} d^{-1} for the 12, 6, and 3 h HRTs, respectively) and the low influent NO_3^--N concentration of 4.5 mg L^{-1} (5.34, 7.71, and 8.02 g N m^{-3} d^{-1} for the 12, 6, and 3 h HRTs, respectively).

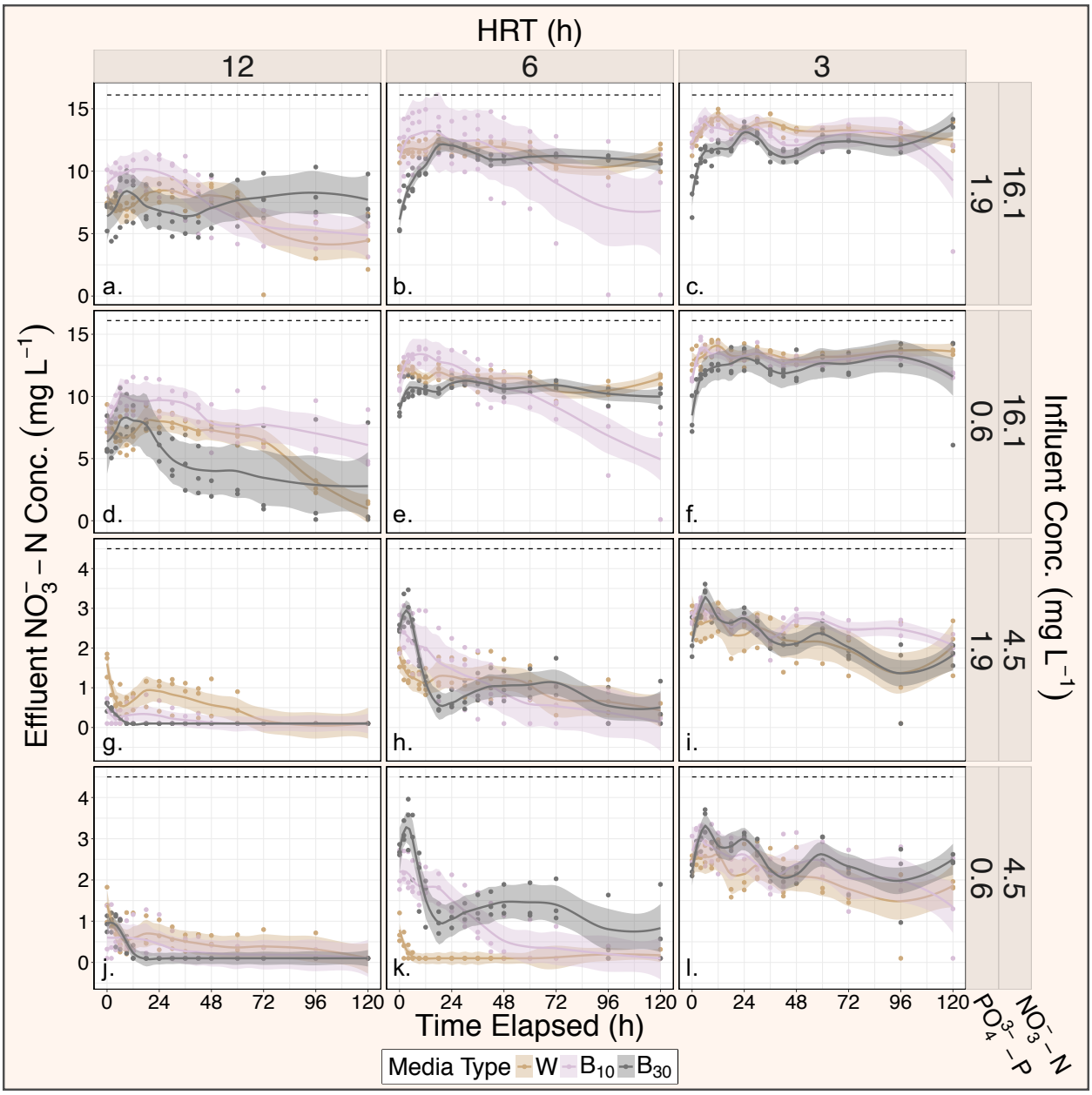

Figure 14 Time series plot of DNBR effluent NO_3^--N concentrations in mg L^{-1}, with each panel representing a different treatment combination of HRT, influent NO_3^--N concentration, and influent PO_4^{3-}-P concentration, and the different colors representing the different media types. The dotted lines on each panel represent influent NO_3^--N concentrations, which are also shown on the right-hand y-axis. A loess smoothing method was used with a span of 0.35. Shading around each loess time series represent the uncertainty associated with the estimated line.

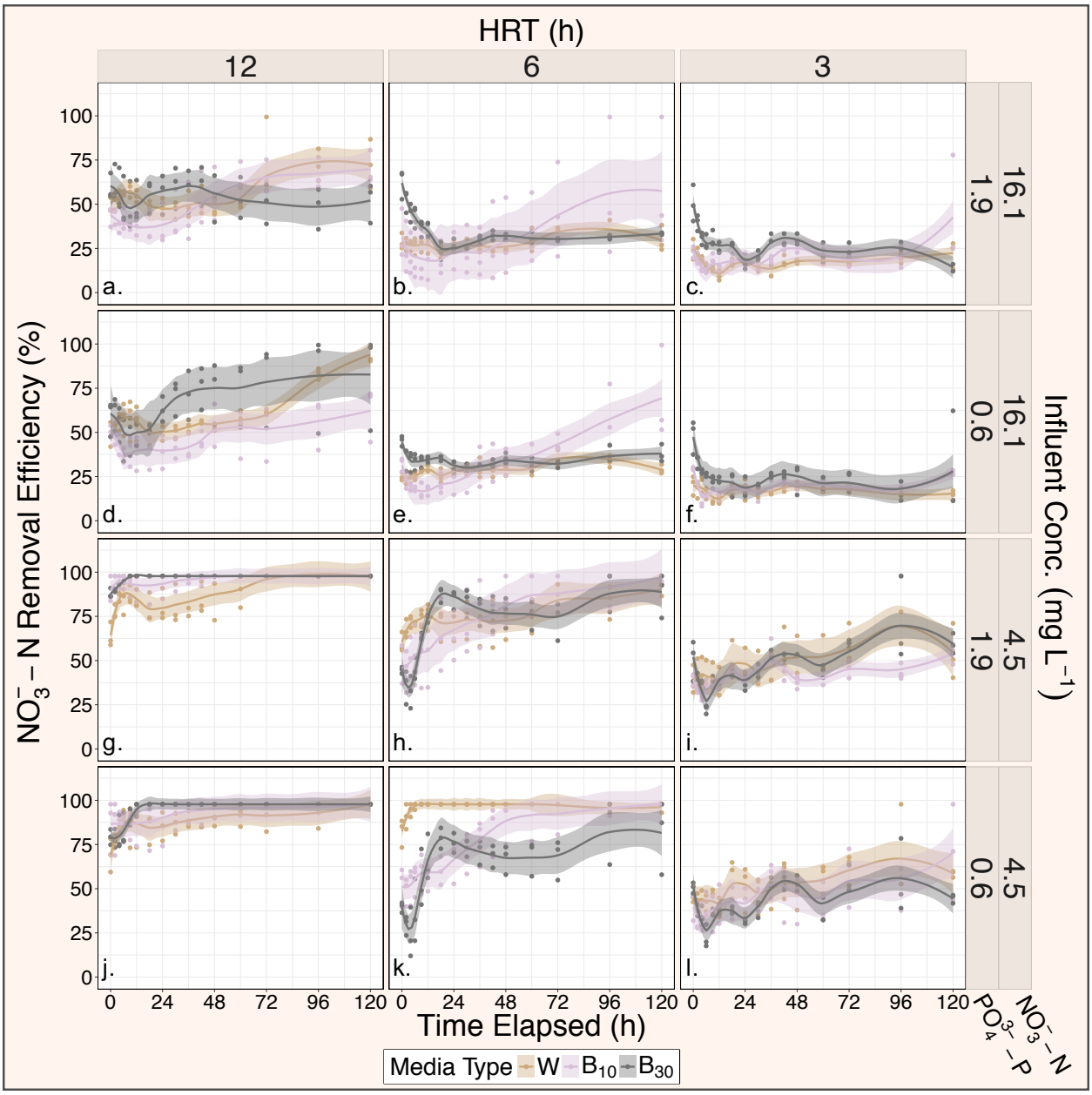

Figure 15 Time series plot of DNBR NO_3^--N % reductions, with each panel representing a different treatment combination of HRT, influent NO_3^--N concentration, and influent PO_4^{3-}-P concentration, and the different colors representing the different media types. A loess smoothing method was used with a span of 0.35. Shading around each loess time series represent the uncertainty associated with the estimated line.

Effect	DFn	DFd	SSn	SSd	F	p
med	2	90	15.689	40.0	17.6	0.000
N.in	1	90	2272.531	40.0	5108.5	0.000
HRT	2	90	231.530	40.0	260.2	0.000
med:N.in	2	90	18.522	40.0	20.8	0.000
med:HRT	4	90	2.298	40.0	1.3	0.279
N.in:HRT	2	90	47.758	40.0	53.7	0.000
med:N.in:HRT	**4**	**90**	**5.922**	**40.0**	**3.3**	**0.014**

Table 3 Output for the ANOVA assessing the effect of media type, influent NO_3^--N concentration, and HRT, and their interactions, on effluent NO_3^--N concentration. DFn represents degrees of freedom for the numerator of the F ratio and DFd represents degrees of freedom for the denominator of the F ratio. P-values in red indicate significance (p-value < 0.05) and bolded rows indicate the highest order significant interactions.

Effect	DFn	DFd	SSn	SSd	F	p
N.in	1	102	2272.531	82.5	2810.8	0.000
HRT	2	102	231.530	82.5	143.2	0.000
N.in:HRT	**2**	**102**	**47.758**	**82.5**	**29.5**	**0.000**

Table 4 Output for the ANOVA assessing the effect of influent NO_3^--N concentration, HRT, and their interaction, on effluent NO_3^--N concentration, independent of media type. DFn represents degrees of freedom for the numerator of the F ratio and DFd represents degrees of freedom for the denominator of the F ratio. P-values in red indicate significance (p-value < 0.05) and bolded rows indicate the highest order significant interactions.

Effect			NO_3^--N Summary Statistics				
			Effluent NO_3^--N Conc. (mg L^{-1})			NO_3^--N Removed (%)	NO_3^--N Removed (g N m^{-3} d^{-1})
HRT (h)	Media	Influent NO_3^--N Conc. (mg L^{-1})	Mean	SD	Q_{50}	Mean	Mean
3	W	4.5	2.41	0.42	2.47	46.4	11.02
3	B_{10}	4.5	2.67	0.40	2.74	40.7	8.94
3	B_{30}	4.5	2.64	0.42	2.68	41.4	7.75
6	W	4.5	0.74	0.63	0.70	83.6	9.93
6	B_{10}	4.5	1.57	0.81	1.69	65.0	7.14
6	B_{30}	4.5	1.71	0.92	1.39	62.0	5.81
12	W	4.5	0.73	0.42	0.68	83.8	4.98
12	B_{10}	4.5	0.35	0.35	0.16	92.2	5.06
12	B_{30}	4.5	0.29	0.32	0.10	93.7	4.38
3	W	16.1	13.37	0.69	13.41	16.9	14.40
3	B_{10}	16.1	13.08	0.78	13.19	18.8	14.74
3	B_{30}	16.1	11.65	1.44	11.77	27.7	18.52
6	W	16.1	11.76	0.58	11.71	26.9	11.45
6	B_{10}	16.1	12.17	1.83	12.64	24.4	9.60
6	B_{30}	16.1	10.40	1.45	10.74	35.4	11.86
12	W	16.1	7.58	0.95	7.49	52.9	11.25
12	B_{10}	16.1	9.04	1.63	9.34	43.9	8.62
12	B_{30}	16.1	6.63	2.04	6.79	58.8	9.85

Table 5 Summary statistics for NO_3^--N experimental data, binned by HRT, media, and influent NO_3^--N concentration effect. Influent PO_4^{3-}-P concentration was omitted because the NO_3^--N ANOVA indicated that none of the interactions containing influent PO_4^{3-}-P concentration significantly affected outflow NO_3^--N concentration. Q_{50} refers to the 50th percentile, or median effluent concentration.

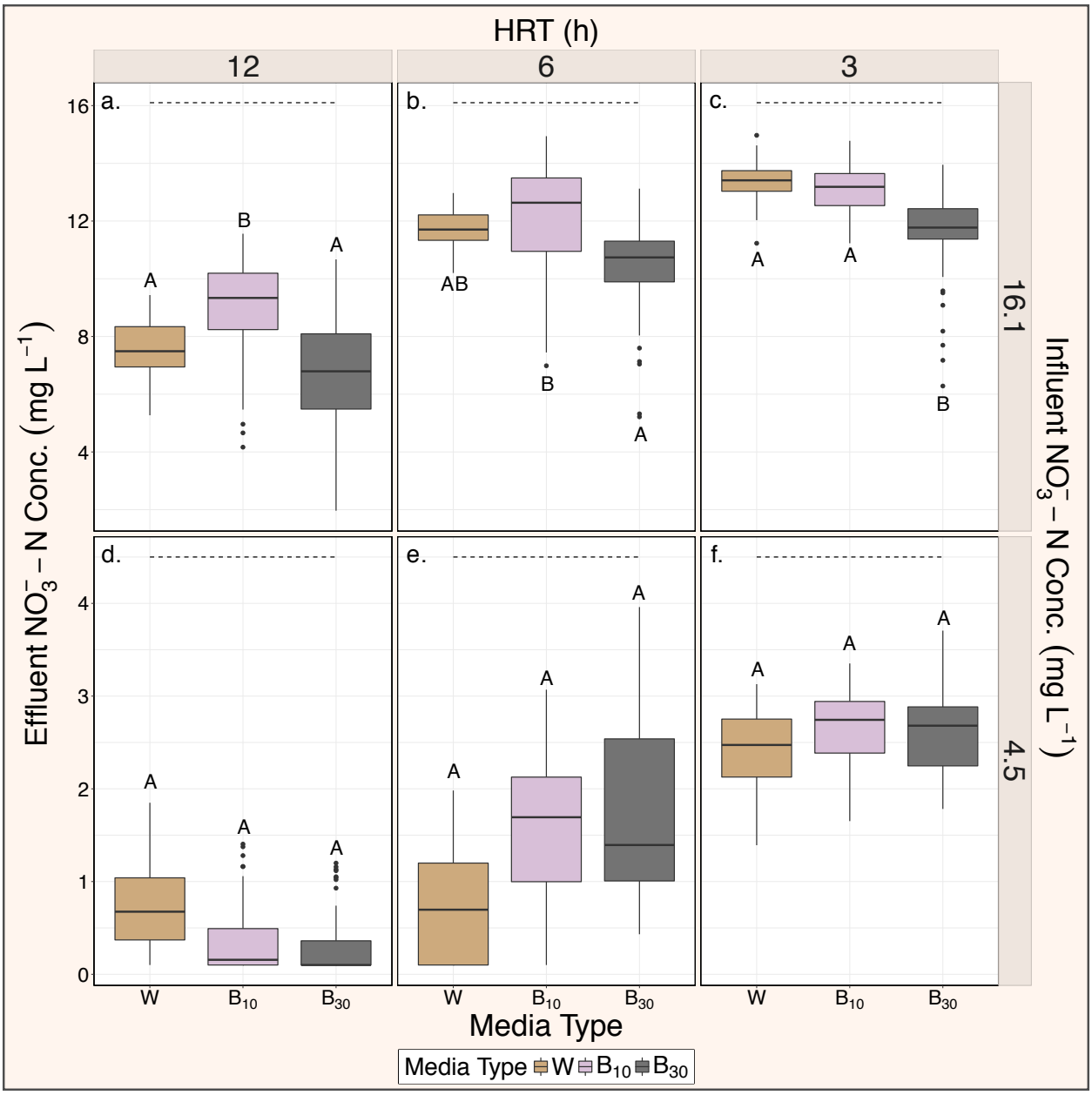

Figure 16 Interaction plot of NO_3^--N experimental data, binned by HRT, media, and influent NO_3^--N concentration. Treatments within a concentration level with the same letter are not significantly different as determined by a Tukey's HSD test at $\alpha \leq 0.05$.

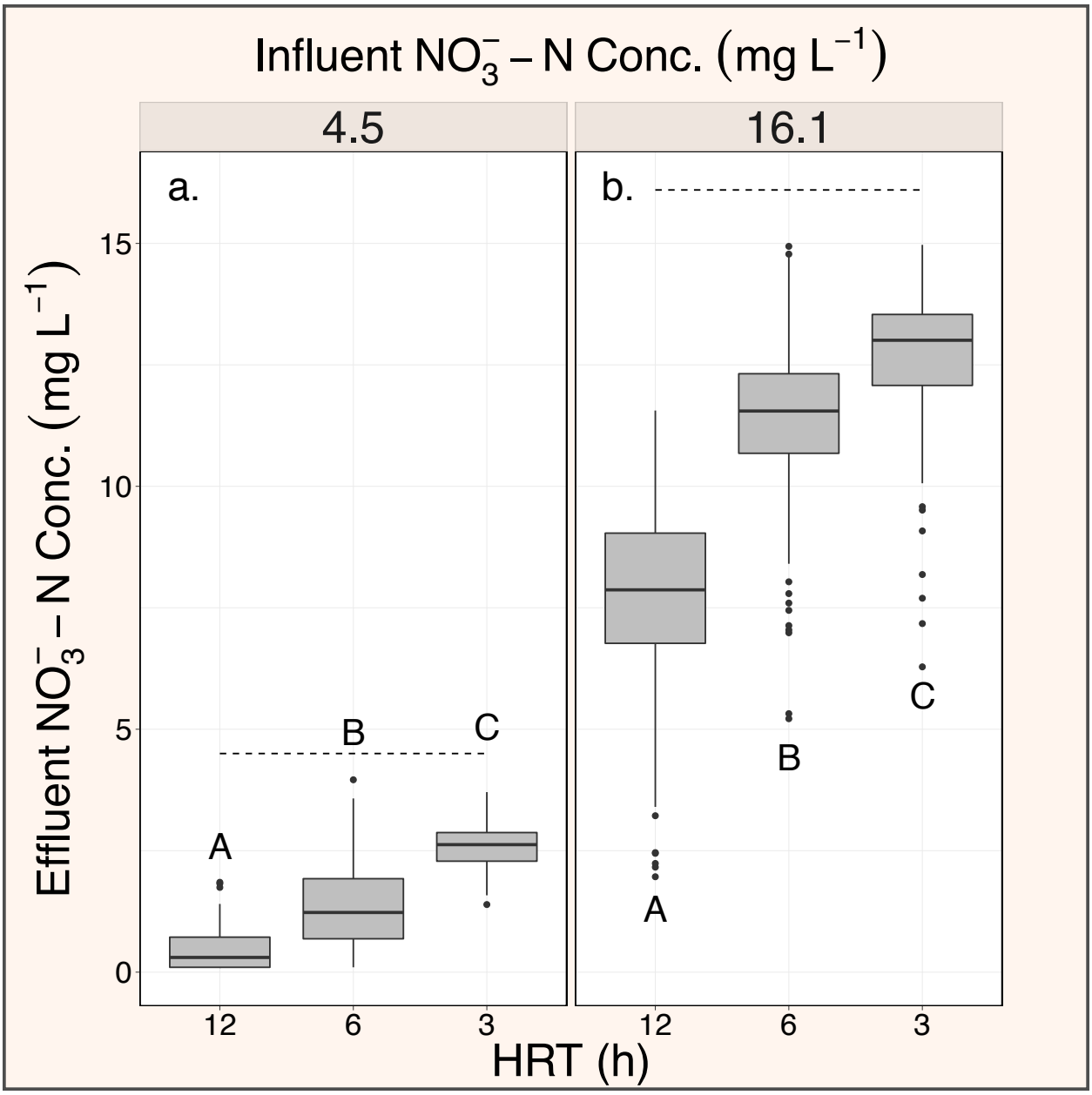

Figure 17 Interaction plot of NO_3^--N concentration, binned by HRT and influent NO_3^--N concentration. Treatments within a concentration level with the same letter are not significantly different as determined by a Tukey's HSD test at $\alpha \leq 0.05$.

4.2 Phosphate

Times series of DNBR effluent PO_4^{3-}-P concentrations (Figure 18) and corresponding removal efficiencies (Figure 19) reveal that the treatments were generally less successful in their ability to support PO_4^{3-}-P removal than they were at supporting NO_3^--N removal, with the majority of the treatments exporting PO_4^{3-}-P. The first, larger PO_4^{3-}-P ANOVA containing all possible explanatory predictors (Table 6) revealed the following interactions to be significant predictors of effluent PO_4^{3-}-P concentration: (1) influent NO_3^--N concentration x influent PO_4^{3-}-P concentration x HRT, (2) media type x influent PO_4^{3-}-P concentration x HRT, and (3) media type x influent NO_3^- concentration.

Based on the output of the first PO_4^{3-}-P ANOVA, a summary statistics table was created for the PO_4^{3-}-P experimental data set, with every combination of HRT, media type, influent PO_4^{3-}-P concentration and influent NO_3^--N concentration represented (Table 7). At the low influent PO_4^{3-}-P concentration of 0.6 mg L^{-1}, regardless of media type, HRT, or influent NO_3^--N concentration, mean PO_4^{3-}-P removal efficiencies and rates ranged from -122.0-74.9% and -1.16-1.67 g P m^{-3} d^{-1}, respectively. At the high influent PO_4^{3-}-P concentration of 1.9 mg L^{-1}, mean PO_4^{3-}-P removal efficiencies and rates ranged from -29.9%-27.5% and from -1.20-0.78 g P m^{-3} d^{-1}. It is also interesting to note that while there is considerable variation in media performance, the W treatment never exported PO_4^{3-}-P, while both the B_{10} and B_{30} treatments did.

The interaction plots with Tukey's HSD test results (Figure 20) for effluent PO_4^{3-}-P concentrations reveal that under the combination of the high influent PO_4^{3-}-P concentrations, high influent NO_3^--N concentration, and the 12 hour HRT (Figure 20a), the media types were significantly different from one another in their ability to remove PO_4^{3-}-P, but these differences disappeared at the lower HRTs (Figure 20b, c). At the high PO_4^{3-}-P concentration, low influent NO_3^--N concentration and the 12 hour HRT (Figure 20d), W was significantly better than B_{10} and B_{30} at removing PO_4^{3-}-P, which were not significantly different from one another, and the same pattern was present at the 3 hour HRT (Figure 20f). At the 6 hour HRT, however, the media types were not significantly different from one another in their ability to remove PO_4^{3-}-P. The patterns

under low influent PO_4^{3-}-P concentrations were the same across HRTs, regardless of influent NO_3^--N concentration. At the 12 hour HRT, the media types were all different from one another in their ability to remove PO_4^{3-}-P (Figure 20g, j), and, at the 6 hour HRT, W was not significantly different from B_{10}, and both removed significantly more PO_4^{3-} than did B_{30} (Figure 20h, k). At the 3 hour HRT, W outperformed B_{10} and B_{30}, which were statistically not different from one another (Figure 20i, l).

Woodchips removed significantly more PO_4^{3-}-P than either B_{10} and B_{30} for 7 of the 12 treatment combinations (Figure 20a, d, g, j, f, i, l). In fact, for many HRTs and influent concentrations, the biochar amendments resulted in PO_4^{3-}-P export (Figure 20a, b, c, d, e, f, j for B_{30} and Figure 20a, c, d, e, f, h, h, I, j, k, l for B_{10}) with median outflow concentrations that were above inflow concentrations of 1.9 or 0.6 mg L^{-1}. Unlike with the NO_3^--N results, regardless of media type, the HRTs at each influent PO_4^{3-}-P concentration and influent NO_3^--N concentration supported effluent PO_4^{3-}P concentrations that were not significantly different from one another (Figure 21).

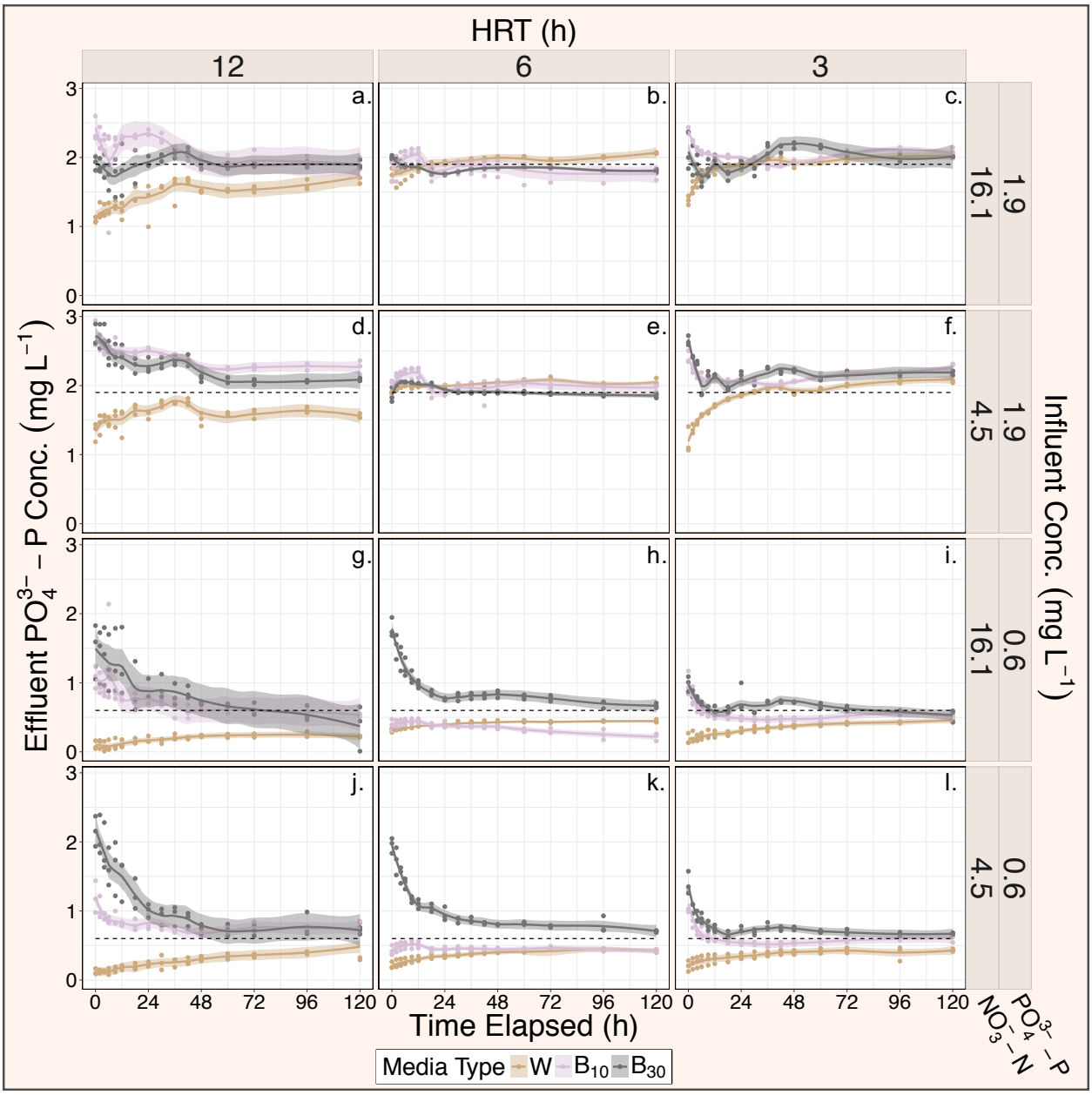

Figure 18 Time series plot of DNBR effluent NO_3^--N concentrations in mg L^{-1}, with each panel representing a different treatment combination of HRT, influent NO_3^--N concentration, and influent PO_4^{3-}-P concentration, and the different colors representing the different media types. The dotted lines on each panel represent influent PO_4^{3-}-P concentrations, which are also shown on the right-hand y-axis. A loess smoothing method was used with a span of 0.35. Shading around each loess time series represent the uncertainty associated with the estimated line.

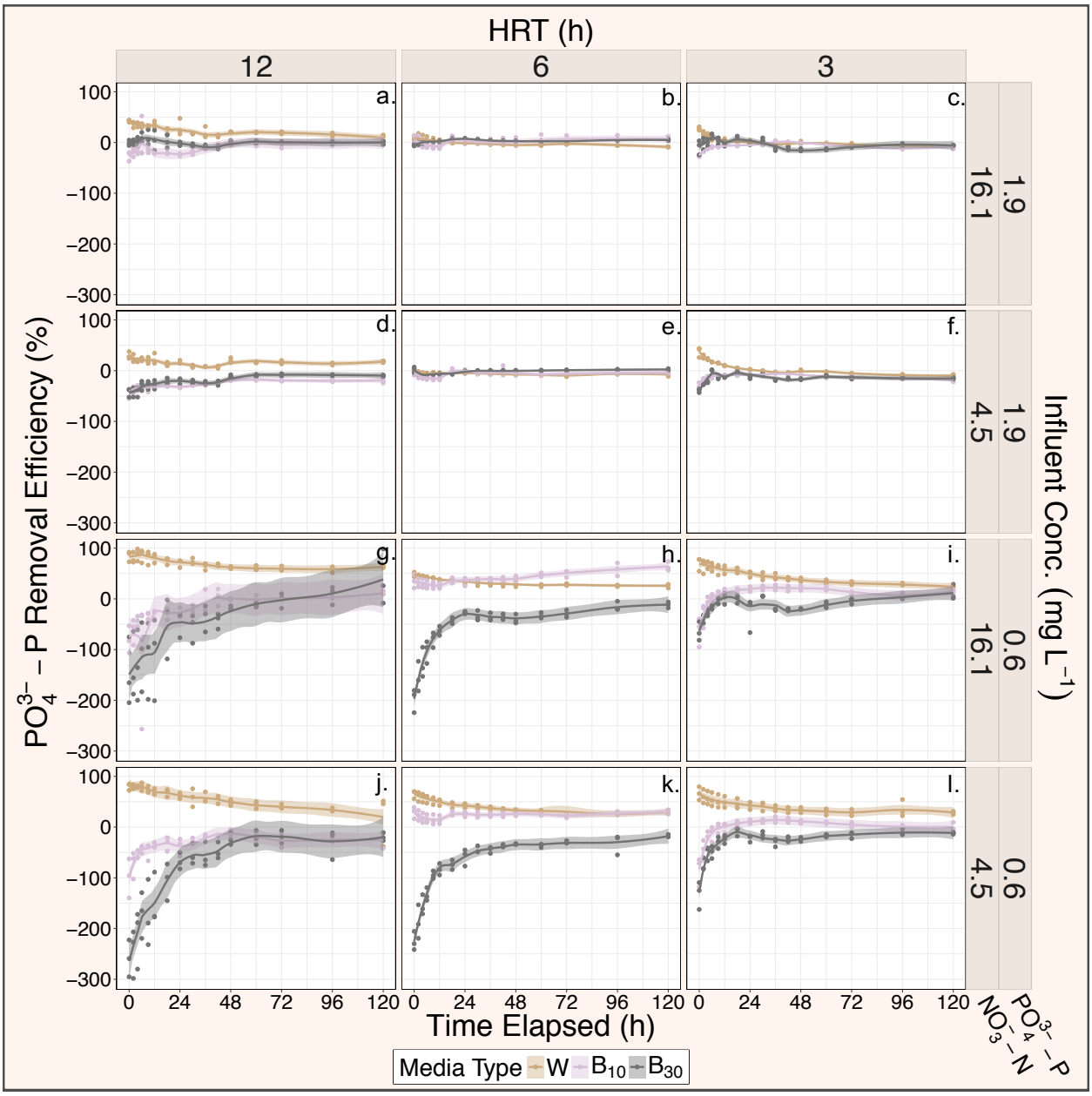

Figure 19 Time series plot of DNBR PO_4^{3-}-P % reductions, with each panel representing a different treatment combination of HRT, influent NO_3^--N concentration, and influent PO_4^{3-}-P concentration, and the different colors representing the different media types. A loess smoothing method was used with a span of 0.35. Shading around each loess time series represent the uncertainty associated with the estimated line.

Effect	DFn	DFd	SSn	SSd	F	p
med	2	72	5.405	0.4	487.3	0.000
N.in	1	72	0.439	0.4	79.1	0.000
P.in	1	72	47.122	0.4	8497.0	0.000
HRT	2	72	0.171	0.4	15.5	0.000
med:N.in	**2**	**72**	**0.146**	**0.4**	**13.2**	**0.000**
med:P.in	2	72	1.254	0.4	113.0	0.000
N.in:P.in	1	72	0.062	0.4	11.2	0.001
med:HRT	4	72	1.689	0.4	76.1	0.000
N.in:HRT	2	72	0.132	0.4	11.9	0.000
P.in:HRT	2	72	0.120	0.4	10.8	0.000
med:N.in:P.in	2	72	0.004	0.4	0.4	0.702
med:N.in:HRT	4	72	0.042	0.4	1.9	0.120
med:P.in:HRT	**4**	**72**	**0.409**	**0.4**	**18.5**	**0.000**
N.in:P.in:HRT	**2**	**72**	**0.052**	**0.4**	**4.7**	**0.012**
med:N.in:P.in:HRT	4	72	0.037	0.4	1.6	0.172

Table 6 Output for the ANOVA assessing the effect of media type, influent NO_3^--N concentration, influent PO_4^{3-}-P concentration, and HRT, and their interactions, on effluent PO_4^{3-}-P concentration. DFn represents degrees of freedom for the numerator of the F ratio and DFd represents degrees of freedom for the denominator of the F ratio. P-values in red indicate significance (p-value < 0.05) and bolded rows indicate the highest order significant interactions.

Effect				PO_4^{3-}-P Summary Statistics				
				Effluent PO_4^{3-}-P Conc. (mg L^{-1})			PO_4^{3-}-P Removed (%)	PO_4^{3-}-P Removed (g P m^{-3} d^{-1})
HRT (h)	Media	Influent NO_3^--N Conc. (mg L^{-1})	Influent PO_4^{3-}-P Conc. (mg L^{-1})	Mean	SD	Q_{50}	Mean	Mean
3	W	4.5	0.6	0.32	0.08	0.33	46.3	1.47
3	B_{10}	4.5	0.6	0.64	0.18	0.56	-7.2	-0.21
3	B_{30}	4.5	0.6	0.83	0.20	0.76	-38.6	-0.96
6	W	4.5	0.6	0.32	0.07	0.34	46.6	0.74
6	B_{10}	4.5	0.6	0.47	0.05	0.46	22.3	0.33
6	B_{30}	4.5	0.6	1.16	0.38	1.04	-93.1	-1.16
12	W	4.5	0.6	0.21	0.08	0.19	65.5	0.52
12	B_{10}	4.5	0.6	0.84	0.16	0.80	-40.6	-0.30
12	B_{30}	4.5	0.6	1.33	0.53	1.13	-122.0	-0.76
3	W	16.1	0.6	0.28	0.08	0.29	52.7	1.67
3	B_{10}	16.1	0.6	0.57	0.16	0.51	4.7	0.14
3	B_{30}	16.1	0.6	0.71	0.13	0.71	-18.8	-0.47
6	W	16.1	0.6	0.38	0.04	0.38	36.7	0.58
6	B_{10}	16.1	0.6	0.39	0.05	0.38	35.0	0.51
6	B_{30}	16.1	0.6	1.05	0.33	0.89	-75.0	-0.94
12	W	16.1	0.6	0.15	0.07	0.17	74.9	0.59
12	B_{10}	16.1	0.6	0.80	0.27	0.77	-33.9	-0.25
12	B_{30}	16.1	0.6	1.07	0.39	0.96	-77.7	-0.48
3	W	4.5	1.9	1.71	0.25	1.80	9.8	0.78
3	B_{10}	4.5	1.9	2.11	0.11	2.08	-11.2	-0.89
3	B_{30}	4.5	1.9	2.19	0.20	2.17	-15.2	-1.20
6	W	4.5	1.9	1.99	0.04	2.00	-5.0	-0.20
6	B_{10}	4.5	1.9	2.04	0.13	2.04	-7.4	-0.29
6	B_{30}	4.5	1.9	1.96	0.07	1.97	-3.2	-0.12
12	W	4.5	1.9	1.57	0.15	1.58	17.5	0.35
12	B_{10}	4.5	1.9	2.47	0.15	2.46	-29.9	-0.59
12	B_{30}	4.5	1.9	2.40	0.22	2.39	-26.3	-0.52
3	W	16.1	1.9	1.80	0.18	1.86	5.3	0.42
3	B_{10}	16.1	1.9	2.04	0.14	2.00	-7.3	-0.58
3	B_{30}	16.1	1.9	1.96	0.19	1.96	-3.0	-0.24
6	W	16.1	1.9	1.88	0.11	1.89	1.1	0.04
6	B_{10}	16.1	1.9	1.90	0.14	1.93	0.2	0.01
6	B_{30}	16.1	1.9	1.86	0.07	1.85	2.3	0.09
12	W	16.1	1.9	1.38	0.20	1.38	27.5	0.54
12	B_{10}	16.1	1.9	2.17	0.27	2.26	-14.0	-0.28
12	B_{30}	16.1	1.9	1.90	0.18	1.91	0.2	0.00

Table 7 Summary statistics for PO_4^{3-}-P experimental data, binned by HRT, media, influent NO_3^--N concentration, and influent PO_4^{3-}-P concentration effect. Q_{50} refers to the 50th percentile, or median effluent concentration.

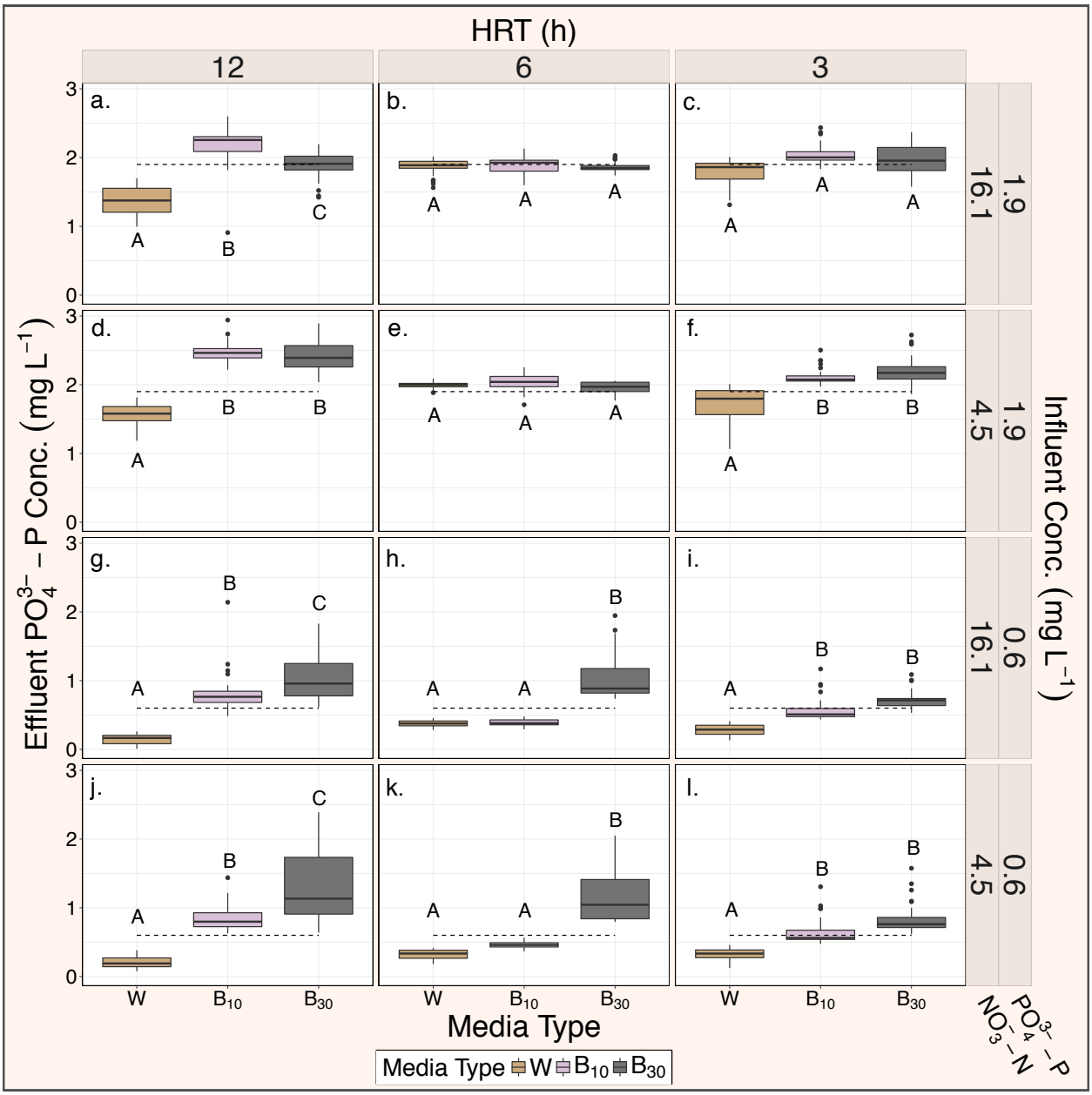

Figure 20 Interaction plot of PO_4^{3-}-P experimental data, binned by HRT, media, influent NO_3^--N concentration, and influent PO_4^{3-}-P concentration. Treatments within a concentration level or HRT with the same letter are not significantly different as determined by a Tukey's HSD test at $\alpha \leq 0.05$.

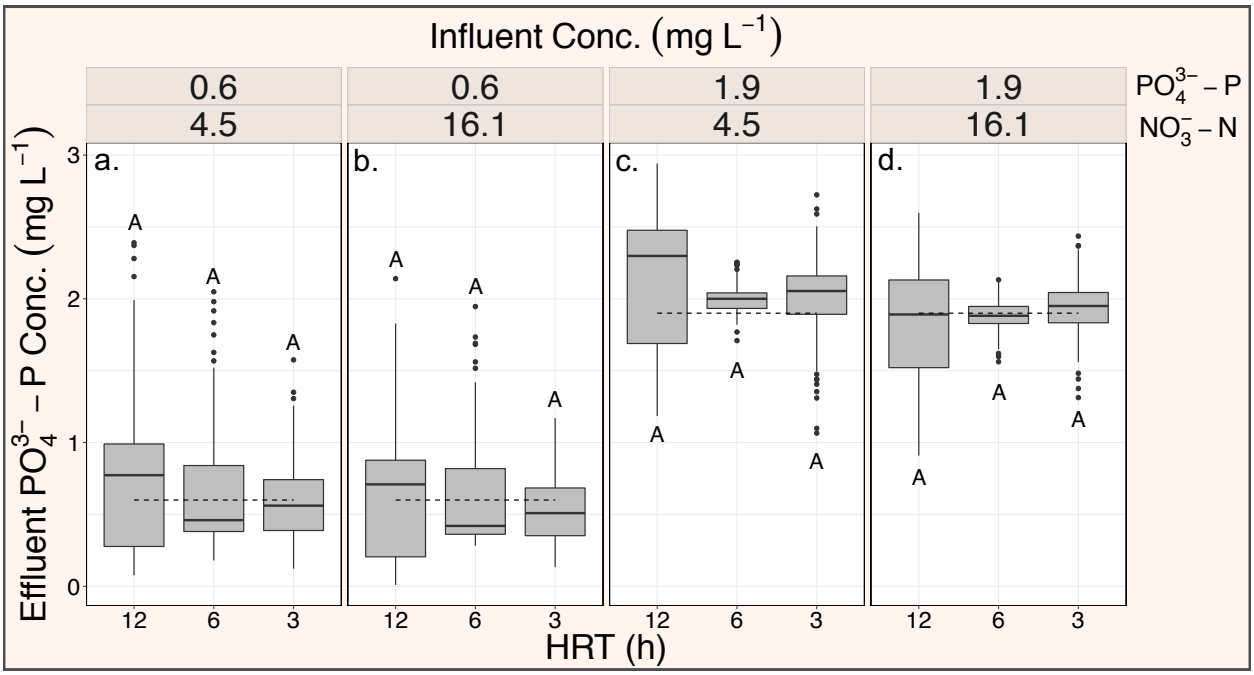

Figure 21 Interaction plot of PO_4^{3-}-P experimental data, binned by HRT and influent NO_3^--N concentration effect, omitting media type. Treatments within a concentration level with the same letter are not significantly different as determined by a Tukey's HSD test at $\alpha \leq 0.05$.

5 Discussion

The results for NO_3^--N and PO_4^{3-}-P are discussed separately below, followed by recommendations regarding media, a discussion of the potential mechanisms contributing to NO_3^--N and PO_4^{3-}-P removal, and suggestions for future work.

5.1 Nitrate

The NO_3^--N removal rates of 4.38-18.52 g N m^{-3} d^{-1} and removal efficiencies of 16.9 - 93.7% reported here are similar to those detailed in other DNBR studies, including the rates of 8.0-18.0 g N m^{-3} d^{-1} and efficiencies of 18-95% at HRTs of 7.2, 18, and 51 h in Christianson et al. (2017), rates of 3.8-15.1 g N m^{-3} d^{-1} with a biochar-amended bioreactor in Hassanpour et al. (2017), and efficiencies ranging from 8% to 55% in bioreactors subjected to HRTs ranging from 1.7 to 21.2 h (Hoover et al., 2016). Our removal rates were also within the range of 2-22 g N m^{-3} d^{-1} reported in the review of Schipper et al. (2010b), well above the mean values for denitrifying beds and laboratory DNBRs reported in the meta-analyses of Addy et al. (2016) (4.7 g N m^{-3} d^{-1} and 3.5 g N m^{-3} d^{-1}, respectively), and close to the mean removal rate of 9.1 g N m^{-3} d^{-1} for beds aged less than 13 months in Addy et al. (2016).

While the Tukey's HSD tests may not have always captured significant differences between the effluent NO_3^--N concentrations for the media types at different HRTs and influent concentrations (Figure 16), it does appear that B_{30} was the best media type for removing NO_3^--N at high influent NO_3^--N concentrations, and this effect appears to be more pronounced at lower HRTs. From these results, it is apparent that biochar amendment in DNBRs may not improve NO_3^--N removal if low influent NO_3^--N concentrations are expected, and careful consideration of expected, site-specific NO_3^--N loads is therefore of utmost importance when installing field-scale DNBRs amended with biochar.

Influent NO_3^--N concentration significantly influenced NO_3^--N removal, and this aligns with the findings of Addy et al. (2016), who found that beds subjected to influent with intermediate NO_3^--N concentrations (10-30 mg L^{-1}) supported significantly higher

NO_3^--N removal rates than beds that were fed lower influent concentrations (<10 mg L^{-1}). The low influent NO_3^--N concentration of 4.5 mg L^{-1} was reduced to mean effluent NO_3^--N concentrations ranging from 0.29 to 2.67 mg L^{-1} (Table 5). The corresponding mean removal efficiencies ranging from 40.7 to 93.7 align with efficiencies reported in similar studies, treating similar influent concentrations, including a 58% removal efficiency for an influent NO_3^--N concentration of 4.8 mg L^{-1} in Robertson and Merkley (2009). Two of the treatments (B_{10}, 12 h HRT and B_{30}, 12 h HRT) supported effluent NO_3^--N concentrations below 0.5 mg L^{-1}, suggesting that these treatments were N-limited (Addy et al., 2016) and therefore there was potential for pollution swapping (Robertson and Merkley, 2009; Shih et al., 2011), which is a phenomenon where a mitigation technology intended to remove one pollutant unintentionally produces another. Furthermore, Easton et al. (2015) showed that while biochar promotes enhanced denitrification, it also encourages SO_4^{2-} reduction, which is a precursor to methyl mercury production, a highly toxic compound to both humans and ecosystems. There are many problems associated with overly long HRTs, such as sulfate reduction, chemical oxygen demand production, and methane production (Fenton et al., 2014) and short HRTs, which can result in nitrite production through incomplete denitrification (Christianson et al., 2017). Although we did not directly measure proxies for pollution swapping in this study, there is a need for more thorough investigation of potential solutions to pollution swapping in DNBRs, as it is concerning and closely linked to HRT, influent NO_3^--N concentration, and biochar amendment.

At both influent NO_3^--N concentrations, the 12 h HRT resulted in significantly greater mean NO_3^--N removal efficiencies, defined as percent reduction in concentration, than did the 6 and 3 h HRTs (Figure 17), and the 6 h HRT mean removal efficiency was significantly greater than the 3 h HRT mean removal efficiency, corroborating laboratory and pilot-scale studies assessing the impact of HRTs on removal in DNBRs (Greenan et al., 2009; Pluer et al., 2016; Hoover et al., 2017). These findings also confirm the meta-analyses of Addy et al. (2016), which revealed that beds subjected to longer HRTs supported significantly higher NO_3^--N removal efficiencies than did beds with shorter HRTs. The opposite trend was true, however, for the mean

NO_3^--N removal rates (Table 5), with the 3 h HRT supporting consistently higher mean NO_3^--N removal rates than did both the 6 and 12 h HRTs, and the 6 h HRT supporting higher mean NO_3^--N removal rates than did the 12 h HRT. This is a common phenomenon in DNBRs (Jaynes et al., 2016; Lepine et al., 2016), and presents a tradeoff in DNBR operation and performance; while the longer HRTs clearly removed more NO_3^--N by percentage, shorter HRTs are technically more efficient, removing more NO_3^--N on a daily basis, since they can treat more bed volumes per day. In the real world, the decision between shorter and longer HRTs should depend on expected flow rates and influent NO_3^--N concentrations. These findings stress the importance of HRT in DNBRs, with there being a clear need to strike a balance between load removal rate and removal efficiency.

At the high influent NO_3^--N concentration of 16.1 mg L^{-1} and HRTs of 3 and 6 h, none of the treatments were able to reduce NO_3^--N concentrations to below the EPA's drinking water standard for NO_3^--N of 10 mg L^{-1}, but all three media types were successful in reducing NO_3^--N concentrations to below 10 mg L^{-1} at the 12 h HRT, suggesting that the 12 h HRT, or HRTs longer than 6 h, may be necessary for sufficient NO_3^--N removal at higher influent concentrations. This supports the findings of Christianson et al. (2013b), which recommended HRTs greater than 8 h for sufficient NO_3^--N removal. While these findings are applicable to DNBRs in environments treating medium to low influent NO_3^--N concentrations, more thorough investigations of NO_3^--N removal at high influent concentrations will need to be conducted to maximize DNBR performance. This is especially important because the kinetics of NO_3^--N removal may change at higher concentrations, and the removal rates recorded here may not be relevant at higher influent concentrations.

Denitrification rates are tightly controlled by Michaelis-Menten kinetics, which describes NO_3^--N removal as being dictated by zero-order kinetics when the influent NO_3^--N concentration is higher than the half-saturation constant (K_m) and first-order kinetics when the influent NO_3^--N concentration is lower than K_m (Ghane et al., 2015). However, the vast majority of DNBRs are subjected to influent with nitrate concentrations that exceed the K_m of denitrifying bacteria (Barton et al., 1999), meaning

a parameter other than influent NO_3^--N concentration is governing the reaction rate (Schipper et al., 2010b), making zero-order kinetics more applicable. Many studies have reported zero-order kinetics (Robertson et al., 2000; Schipper et al., 2005; Robertson, 2010; Warneke et al., 2011b; Schmidt and Clark, 2013), but also first-order kinetics (Elgood et al., 2010; Christianson et al., 2012a), as controlling NO_3^--N removal in DNBRs. More recently, Ghane et al. (2015) successfully modeled woodchip denitrifying bed outflow NO_3^--N concentration with Michaelis-Menten kinetics and Hoover et al. (2016) recorded a decline in the increase of removal rates at higher influent NO_3^--N concentrations (30-50 mg L^{-1}), also supporting Michaelis-Menten kinetics. Hua et al. (2016) reached a similar conclusion, noting a transition from a zero-order reaction to a first-order reaction when the influent NO_3^--N concentration dropped below 3 mg L^{-1}. Jaynes et al. (2016), however, found that simulations of zero-order and first-order removal kinetics for NO_3^--N removal fit their data equally well, using a dual-porosity model. Given these developments, more data is needed to fully explore NO_3^--N removal kinetics in DNBRs, especially since the potential for N limitation needs to be given significant consideration during bioreactor design (Addy et al., 2016). It is worth noting that biochar amendment may have an impact on kinetics, since its ability to promote higher NO_3^--N removal relative to other mediums may lower interior DNBR NO_3^--N concentrations to below the Michaelis-Menten kinetics threshold concentration, thereby shifting from zero-order kinetics to first-order kinetics in N-limited conditions.

5.2 Phosphate

The PO_4^{3-}-P removal rates of -1.20 to 1.67 g P m^{-3} d^{-1} and efficiencies of -122.0% to 74.9% are generally lower than many of the rates reported on DNBRs. For comparison, Goodwin et al. (2015) produced a mean PO_4^{3-}-P reduction from 4.36 mg L^{-1} to 0.16 mg L^{-1}, or a mean removal efficiency of 95.6%, using steel turnings and woodchips in laboratory-scale, column reactors. Christianson et al. (2017) achieved PO_4^{3-}-P removal rates of 25-133 g P m^{-3} d^{-1} and 8.8-48 g P m^{-3} d^{-1} with mine drainage residuals and steel slag P-filters used in conjunction with laboratory-scale woodchip

DNBRs. While these two-stage filters are different systems from DNBRs, and are not directly comparable to the PO_4^{3-}-P removal rates achieved in our DNBRs, they do establish context for what can be achieved by a practice. Gottschall et al. (2016) observed mean PO_3^{3-}-P removal rates of 0.3 g P m^{-3} d^{-1} in woodchip bioreactors and 0.1 g P m^{-3} d^{-1} in woodchips bioreactors amended with alum-based drinking water treatment plant residuals, and these lower rates are closer to what was observed with our experiment.

The insignificant effect of HRT on PO_4^{3-}-P effluent concentration suggests that the primary mechanism for removing PO_4^{3-}-P is a rapid process, such as chemisorption or precipitation. In fact, this evidence suggests that lower HRTs may even be more beneficial for efficient PO_4^{3-}P removal, since higher volumes of drainage can be treated during a given time frame. The evident PO_4^{3-}P export with most of the B_{10} and B_{30} treatments is concerning, and casts doubt on the utility of biochar for improved PO_4^{3-}-P removal in DNBRs. These results contradict a previous study on PO_4^{3-}-P removal with biochar-amended, laboratory-scale DNBRs (Bock et al., 2015), which involved batch experiments, rather than the flow through setup used in these experiments and used a different formulation of biochar. In that study, woodchips amended with biochar supported significantly higher NO_3^--N and PO_4^{3-}-P removal in DNBRs than was observed with the woodchips control, but batch reactor performance likely poorly approximates field conditions. These findings corroborate previous work showing no significant effect of biochar amendment on PO_4^{3-}-P removal in DNBRs (Powers, 2012; Pluer et al., 2016). However, little quantification of PO_4^{3-}-P removal in DNBRs exists in the literature, and even less exists on PO_4^{3-}-P removal with biochar-amended DNBRs. Further work is needed to explore biochar's potential in these systems to invoke simultaneous NO_3^--N and PO_4^{3-}-P removal, especially given the variability of biochar's properties as a function of feedstock, production temperature, particle size, etc. (Lou et al., 2016).

5.3 Media Recommendations

Given the results for NO_3^--N removal in DNBRs, biochar amendment is recommended for promoting higher NO_3^--N removal rates over the traditional woodchip medium, especially in cases when higher influent NO_3^--N concentrations are expected and/or lower HRTs are desired. Given the fact that these results indicate that biochar amendment in DNBR systems may not support higher rates of PO_4^{3-}-P removal, woodchips may be preferred over biochar-amended woodchips if PO_4^{3-}-P removal is a primary goal. In any case, the higher cost of biochar will need to be taken into account, as DNBRs are typically designed to be as inexpensive and cost-effective as possible for practical edge-of-field application.

It should be noted that, aside from the week-long priming periods, the media used in these experiments was fresh, and thus the NO_3^--N removal efficiencies reported here are probably optimal, since there is a tendency for efficiencies to decline with elapsed time, as the carbon media ages, decays, and is consumed during denitrification (Addy et al., 2016; Schipper et al., 2010b; Robertson, 2010). The NO_3^--N removal rates for fresh media are not representative of what can be expected for long-term performance, and mean laboratory NO_3^--N removal rates are, on average, significantly higher than mean NO_3^--N removal rates observed in the field (Addy et al., 2016). Predicting the effect of bed age on PO_4^{3-}-P removal efficiency is much more difficult, and doing so is pure speculation. Given time, perhaps the biochar-amended woodchips would have eventually promoted PO_4^{3-}-P sorption even though, on average, those columns exported PO_4^{3-}-P; the effluent PO_4^{3-}-P concentrations for B_{10} and B_{30} were generally higher than the influent PO_4^{3-}-P concentrations at the beginning of each trial, but sharply decreased during the first few days, reaching steady state by the end of each trial, which did show some removal (Figure 18). This could be due to a first flush type phenomena, whereby the initial, high PO_4^{3-}-P concentrations continue to decline with age, ultimately supporting removal. Indeed, this has been observed in new woodchip bioreactors (Sharrer et al., 2016) and new woodchip bioreactors amended with biochar (Bock et al., 2016; Pluer et al., 2016). More work on the extended

performance of biochar-amended DNBRs is needed, with only a few examples of long-term NO_3^--N removal reported in the literature (Hassanpour et al., 2017), and no known examples for long-term PO_4^{3-}-P removal with biochar-amended DNBRs.

5.4 Potential Biochar Adsorption Mechanisms

Adsorption of pollutants with biochar is the outcome of several processes acting in unison, including complexation reactions, precipitation reactions, and electrostatic attraction, and biochar NO_3^--N and PO_4^{3-}-P sorption and release is still not well understood (Hale et al., 2013). This apparent lack of a consensus is primarily due to the high variance in sorption and desorption properties depending on the feedstock and preparation parameters contributing to biochar production (Morales et al., 2013), such as carbonisation temperatures and reactor residence times (Trazzi et al., 2016). This variability is especially true for NO_3^--N and PO_4^{3-}-P removal (Deng et al., 2017), with some studies showing that certain kinds of biochar have little or no ability to remove NO_3^--N and PO_4^{3-}-P (Yao et al., 2011; Yao et al., 2012; Chen et al., 2010), and others reporting substantial removal of NO_3^--N and PO_4^{3-}-P with various kinds of biochar (Yao et al., 2011; Yao et al., 2013; Bock et al., 2015; Bock et al., 2016; Zhang et al., 2012).

Nitrate adsorption with biochar is believed to be primarily a result of ion exchange mechanisms and electrostatic interactions at the biochar surface via an outer-sphere complexation mechanism, and selecting biochars with higher levels of volatile organic compounds, points of zero charge, and base cation concentrations may facilitate higher sorption rates (Chintala et al., 2013). Biochar amendment is also believed to alter physicochemical soil environments, therefore changing the structure and activity of microbial communities, and affecting N and P cycling as a result (Coumaravel et al., 2011; Anderson et al., 2011). Biochar increases soil surface area and increases the soil water holding capacity, providing greater area for denitrifying bacteria colonization, and more favorable conditions (Coumaravel et al., 2011), a possible mechanism supporting higher NO_3^--N removal under field conditions.

Adsorption of PO_4^{3-}-P ions with biochar is dictated by physical and chemical interactions, including complexation, precipitation, dispersive forces, and electrostatic attraction, and biochars with high surface areas typically are more suitable for promoting adsorption (Ahmad et al., 2014). It may be that the particular variety of biochar used in these experiments, which was sourced from a hardwood feedstock, is not especially advantageous for PO_4^{3-}-P adsorption. Biochar's ability to adsorb anions and cations is highly dependent on the mineral compositions of utilized feedstock (Lou et al., 2016). The vast majority of materials used for P adsorption contain divalent and trivalent metal ions, including magnesium, calcium, aluminum and iron, which are capable of precipitating and complexing with P, removing P in the process (Westholm, 2006). Biochars that do not have an abundance of these metal ions may not provide the ability for P removal, especially when repulsive electrostatic forces exist (Lou et al., 2016). There is evidence to suggest that low calcium content in biochars can promote P release from biochar (Yao et al., 2012; Jung et al., 2015), and since many of the biochar treatments in these experiments supported PO_4^{3-}-P export, perhaps the calcium content of this biochar is simply too low, though calcium content was not directly quantified here. A recent study by Lou et al. (2016) revealed that four different biochars produced from Korean pine (*Pinus koraiensis*) tree sawdust feedstock, subjected to various pyrolysis temperatures and various degrees of steam activation, removed <4% of PO_4^{3-}-P from aqueous solution, and they sited repulsion forces between biochar surfaces and PO_4^{3-}-P ions as the likely culprit contributing to low P adsorption rates; the negatively charged surfaces of this biochar had little ability to adsorb the negatively charged PO_4^{3-}-P ions from solution. Perhaps the pine biochar used here does not have sufficient positively charged surfaces to adsorb negatively charged PO_4^{3-}-P ions.

pH could also be contributing to the lack of PO_4^{3-}-P sorption with this particular kind of biochar. Biochar derived from anaerobically digested sugar beet tailings tested in Yao et al. (2011) achieved its greatest sorption capacity at an approximate pH of 4. Kumar et al. (2010) found similar results, with the greatest sorption capacity for phosphate occurring when aqueous solution pH was below the pH_{pzc} (the pH at the point of zero charge) of the adsorbent. This phenomenon has also been observed in

adsorption experiments with activated carbon, with reported declines in negatively charged dye adsorption in solution where pH > pH_{pzc} (Jayson et al., 1982) and contrasting adsorption of positively charged dyes where pH > pH_{pzc} (Iqbal and Ashiq, 2007). While we did not report pHs here for these experiments, they were collected daily, and were typically close to neutral. The pH_{pzc}s of the biochar used for these experiments were not calculated, but the biochar used in Lou et al. (2016) was similarly derived from pine feedstock at temperatures of 300 and 550 °C, yielding pHs of ~4.87 and ~7.81 and lower pH_{pzc}s of and ~3.91 ~3.49, respectively. The pine biochar in that study removed only ~4% of PO_3^{4-}-P from solution, and, if similar mechanisms are in action with our study, that could explain the low PO_4^{3-}-P removal with biochar.

There is a possibility that the sorption of PO_4^{3-}-P by biochar is being impaired by the presence of other anions that are overwhelming PO_4^{3-}-P anions in competition for binding sites, but little evidence of these phenomena exist in the literature. It is unlikely that NO_3^--N would be contributing to this phenomenon, since there is evidence to suggest that NO_3^--N sorption would likely be limited in the presence of PO_4^{3-}-P and sulfate (Chintala et al., 2013), which is probably not occurring here, since the biochar amended mediums generally improved NO_3^--N removal.

In recent years, several biochar varieties have been proven capable of PO_4^{3-}-P removal. Biochar derived from anaerobically digested sugar beet tailings supported substantial removal rates of 133 mg P g^{-1} of biochar (Yao et al., 2011) and magnesium-modified biochar provided an adsorption capacity over 100 mg P g^{-1} (Yao et al., 2013). Mg-biochar nanocomposites with surface-attached nanosized magnesium oxides (MgO), have been proven to support high P sorption ability (Zhang et al., 2012). Several new methods of production have arisen as well, including steam activation, which increases microporosity by enlarging internal biochar pores (Rajapaksha et al., 2014; Ahmad et al., 2014), and acid activation with hydrochloric acid, which significantly increases the cation-exchange capacity and surface areas of biochars (Chintala et al., 2013).

While this progress of late is substantial, more investigation of NO_3^--N and PO_4^{3-}-P removal with biochar is warranted given wide variation in biochar properties and

performance. Future experiments delineating the advantageous and disadvantageous biochar characteristics for promoting NO_3^--N and PO_4^{3-}-P removal in solution are required, and this is especially important in regards to feedstock and pH. Feedstock with cationic metals and high mineral contents should be targeted. Ideally, optimal biochars will be identified for use in DNBRs.

5.5 Future Work

There are other, emerging approaches that show great promise for simultaneous removal of NO_3^--N and PO_4^{3-}-P from agricultural drainage using DNBRs, and these include other DNBR media amendments, such as alum-based drinking water treatment plant residuals (Gottschall et al., 2016), steel byproducts (Goodwin et al., 2015; Hua et al., 2016; Christianson et al., 2017), and rice straw (Liang et al., 2015), and two-stage filters, such as the one reported in Christianson et al. (2017), which utilized steel slag and acid mine drainage treatment residual filters to sorb PO_4^{3-}-P in conjunction with woodchip bioreactors. There has even been a recent push to utilize alternative DNBR amendments for circumventing the potential shortfalls of pollution swapping, such as the successful use of amorphous iron oxides for avoiding sulfate reduction (Easton et al., 2015). Future work should draw from these inventive approaches to broaden and advance DNBR research to include a wider variety of more effective means for mitigating pollution.

6 Conclusions

Woodchips and both biochar treatments were successful at removing NO_3^--N from the simulated agricultural drainage, with mean NO_3^--N removal efficiencies that ranged from 16.9%-93.7% and removal rates that ranged from 4.38-18.52 g N m^{-3} d^{-1}. Media type did not have a significant effect at low influent NO_3^--N concentrations, but B_{30} was more effective than W and B_{10} at high influent NO_3^--N concentrations. Mean PO_4^{3-}-P removal efficiencies ranged from -122.0% to 74.9% and removal rates ranged from -1.20 to 1.67 g P m^{-3} d^{-1}, with B_{10} and B_{30} both significantly worse than W at removing PO_4^{3-}-P at both influent PO_4^{3-}-P concentrations. HRT significantly influenced NO_3^--N removal efficiencies and rates; removal efficiencies increased as HRTs increased, and removal rates decreased as HRTs increased. HRT had no effect on PO_4^{3-}-P removal.

These findings support DNBRs' utility as mitigation tools for removing NO_3^--N from nutrient-enriched waters at the crossroads of agriculture and the environment, and shed light on key performance factors contributing to DNBR function. Based on this work, appropriate HRTs can be determined for use at the field scale, depending on expected influent concentrations, but site-specific factors will need to be given significant consideration given the expected higher variability of conditions. Future work should examine DNBR NO_3^--N and PO_4^{3-}-P removal at higher influent concentrations, to better determine the limits of DNBR performance, and lower influent concentrations, to examine the unintentional, concerning potential for pollution swapping. Additionally, further work is needed to examine the impact of media aging on long-term phosphate and NO_3^--N removal with both woodchips and biochar at laboratory, pilot, and field scales.

Biochar generally enhanced NO_3^--N removal in these DNBRs, but did not significantly improve PO_4^{3-}P removal, contradicting earlier, similar batch experiments and highlighting the need for further assessment of biochar's ability to potentially reduce NO_3^--N and PO_4^{3-}P export from agricultural systems. Moving forward, more thorough investigation of the underlying mechanisms contributing to NO_3^--N and PO_4^{3-}P removal

with biochar, and how those processes change with different feedstock and production parameters, is warranted. These assessments will need to be performed both on biochar exclusively and on biochar used in DNBRs. Continued research will hopefully determine the optimal biochar characteristics for enhancing DNBR performance, and perhaps more avenues for pollutant removal with biochar will come to the surface. Alternatives for promoting PO_4^{3-}-P removal in conjunction with NO_3^--N removal, such as other amendments and two-stage filters, may also be worth exploring for DNBR optimization.

References

Abusallout, I., & Hua, G. (2017). Characterization of dissolved organic carbon leached from a woodchip bioreactor. *Chemosphere, 183*, 36-43. https://doi.org/10.1016/j.chemosphere.2017.05.066

Addy, K., Gold, A. J., Christianson, L. E., David, M. B., Schipper, L. A., & Ratigan, N. A. (2016). Denitrifying bioreactors for nitrate removal: A meta-analysis. *J. Environ. Qual., 45*(3), 873-881. http://dx.doi.org/10.2134/jeq2015.07.0399

Ahmad, M., Rajapaksha, A. U., Lim, J. E., Zhang, M., Bolan, N., Mohan, D., … Ok, Y. S. (2014). Biochar as a sorbent for contaminant management in soil and water: A review. *Chemosphere*, *99*(Supplement C), 19-33. https://doi.org/10.1016/j.chemosphere.2013.10.071

Alho, C. F. B. V., Cardoso, A. da S., Alves, B. J. R., & Novotny, E. H. (2012). Biochar and soil nitrous oxide emissions. *Pesquisa Agropecuaria Brasileira*, *47*(5), 722-725. https://doi.org/10.1590/S0100-204X2012000500013

Allott, T. E. H., Curtis, C. J., Hall, J., Harriman, R., & Battarbee, R. W. (1995). The impact of nitrogen deposition on upland surface waters in Great Britain: A regional assessment of nitrate leaching. *Water Air Soil Pollut.*, *85*(2), 297-302. https://doi.org/10.1007/BF00476845

Altman, S. J., & Parizek, R. R. (1995). Dilution of nonpoint-source nitrate in groundwater. *J. Environ. Qual., 24*, 707-718. http://dx.doi.org/10.2134/jeq1995.00472425002400040023x

Anbar, A. D., Duan, Y., Lyons, T. W., Arnold, G. L., Kendall, B., Creaser, R. A., . . . Buick, R. (2007). A whiff of oxygen before the Great Oxidation Event? *Science, 317*(5846), 1903-1906. http://dx.doi.org/10.1126/science.1140325

Anderson, C. R., Condron, L. M., Clough, T. J., Fiers, M., Stewart, A., Hill, R. A., & Sherlock, R. R. (2011). Biochar induced soil microbial community change: Implications for biogeochemical cycling of carbon, nitrogen and phosphorus. *Pedobiologia*, *54*(5), 309-320. https://doi.org/10.1016/j.pedobi.2011.07.005

Anderson, C. R., Hamonts, K., Clough, T. J., & Condron, L. M. (2014). Biochar does not

affect soil N-transformations or microbial community structure under ruminant urine patches but does alter relative proportions of nitrogen cycling bacteria. *Agric., Ecosystems Environ.*, *191*, 63-72. https://doi.org/10.1016/j.agee.2014.02.021

Appleford, J. M., Rodriguez, L. F., Cooke, R. A. C., Zhang, Y., Kent, A. D, & Zilles, J. L. (2008). Characterization of microorganisms contributing to denitrification in tile drain biofilters in Illinois. ASABE Paper No. 084583. St. Joseph, MI: ASABE.

Atlas, R. M., & Barthas, R. (1992). *Microbial Ecology: Fundamentals and Applications* (3rd ed.) San Francisco: Benjamin-Cummings Publishing.

Auguie, Baptiste. (2015). gridExtra: Miscellaneous functions for "grid" graphics. R package version 2.0.0. Retrieved from: https://CRAN.R-project.org/package=gridExtra

Averill, B. A., & Tiedje, J. M. (1982). The chemical mechanism of microbial denitrification. *Elsevier Biomedical Press, 138*(1), 9-12. http://dx.doi.org/10.1016/0014-5793(82)80383-9

Ayres, R. U., Schlesinger, W. H., & Socolow, R. H. (1994). Human impacts on the carbon and nitrogen cycles. In *Industrial ecology and global change* (pp. 121-156). Cambridge, MA: Cambridge University Press. Retrieved from http://ebooks.cambridge.org/chapter.jsf?bid=CBO9780511564550&cid=CBO9780511564550A024

Azuara, M., Kersten, S. R. A., & Kootstra, A. M. J. (2013). Recycling phosphorus by fast pyrolysis of pig manure: Concentration and extraction of phosphorus combined with formation of value-added pyrolysis products. *Biomass and Bioenergy*, *49*, 171-180. https://doi.org/10.1016/j.biombioe.2012.12.010

Baker, J. L., Campbell, K. L., Johnson, H. P., & Hanway, A. J. J. (1975). Nitrate, phosphorus, and sulfate in subsurface drainage water. *J. Environ. Qual.*, *4*(3).

Baldock, J. A., & Smernik, R. J. (2002). Chemical composition and bioavailability of thermally altered *Pinus resinosa* (Red pine) wood. *Org. Geochem.*, *33*(9), 1093-1109. https://doi.org/10.1016/S0146-6380(02)00062-1

Barton, L., McLay, C. D. A., Schipper, L. A., & Smith, C. T. (1999). Annual denitrification

rates in agricultural and forested soils: A review. *Aust. J. Soil Res., 37*, 1073–1093. http://doi.org/10.1071/sr99009

Bates, D., Mächler, M., Bolker, B.M., & Walker, S.C. (2015). Fitting linear mixed-effects models using lme4. *J. Stat. Softw., 67*(1), 1-48. http://dx.doi.org/10.18637/jss.v067.i01

Beauchamp, E. G., Trevors, J. T., & Paul J. W. (1989). Carbon sources for bacterial denitrification. *Adv. Soil Sci., 10*, 113-142.

Bedessem, M. E., Edgar, T. V., & Roll, R. (2005). Nitrogen removal in laboratory model leachfields with organic-rich layers. *J. Environ. Qual., 34*, 936-942. http://doi.org/10.2134/jeq2004.0024

Bell, N., Cooke, R. A. C., Olsen, T., David, M. B., & Hudson, R. (2015). Characterizing the Performance of Denitrifying Bioreactors during Simulated Subsurface Drainage Events. *J. Environ. Qual., 44*(5), 1647-1656. https://doi.org/10.2134/jeq2014.04.0162

Berner, R. (2004). *The Phanerozoic carbon cycle: CO_2 and O_2*. Oxford: Oxford University Press.

Berner, R. (2006). Geological nitrogen cycle and atmospheric N_2 over Phanerozoic time. *Geology, 34*(5), 413–415 (2006). http://doi.org/10.1130/G22470.1

Birkeland, K. (1906). On the oxidation of atmospheric nitrogen in electric arcs. *Trans. Faraday Soc., 2*, 98-116. https://doi.org/10.1039%2Ftf9060200098

Blowes, D. W., Robertson, W. D., Ptacek, C. J., & Merkley, C. (1994) Removal of agricultural nitrate from tile-drainage effluent water using in-line bioreactors. *J. Contaminant Hydrology, 15*(3), 207-221. http://dx.doi.org/10.1016/0169-7722(94)90025-6

Bock, E. M., Coleman, B., & Easton, Z. M. (2016). Effect of biochar on nitrate removal in a pilot-scale denitrifying bioreactor. *J. Environ. Qual., 45*, 762-771. http://doi.org/10.2134/jeq2015.04.0179

Bock, E. M., Smith, N., Roger, M., Coleman, B., Reiter, M., Benham, B., & Easton, Z. M. (2015). Enhanced nitrate and phosphate removal in a denitrifying bioreactor with biochar. *J. Environ. Qual., 44*, 605-613. http://doi.org/10.2134/jeq2014.03.0111

Boesch, D. F. (1996). Science and management in four U.S. coastal ecosystems dominated by land-ocean interactions. *J. Coastal Conserv., 2*, 103-114. http://doi.org/10.1007/BF02743044

Bogovski, P., & Bogovski, S. (1981). Animal Species in which N-nitroso compounds induce cancer. *Int. J. Cancer*, *27*(4), 471-474.

Boussaid, F., Martin, G., & Morvan, J. (1988). Denitrification in-situ of groundwaters with solid carbon matter. *Environ. Technol. Letters, 9*, 803-816. http://dx.doi.org/10.1080/09593338809384636

Brewer, C. E. (2012). Biochar characterization and engineering. PhD diss. Ames, Iowa: Iowa State University, Department of Chemical Engineering. Retrieved from http://lib.dr.iastate.edu/cgi/viewcontent.cgi?article=3291&context=etd

Brewer, C. E., Hu, Y.-Y., Schmidt-Rohr, K., Loynachan, T. E., Laird, D. A., & Brown, R. C. (2012). Extent of pyrolysis impacts on fast pyrolysis biochar properties. *J. Environ. Qual.*, *41*(4), 1115-1122. https://doi.org/10.2134/jeq2011.0118

Bridgham, S. D., Updegraff, K., & Pastor, J. (1998). Carbon, nitrogen, and phosphorus mineralization in northern wetlands. *Ecology, 79*(7), 1545-1561. http://dx.doi.org/10.1890/0012-9658(1998)079[1545:CNAPMI]2.0.CO;2

Broda, E. (1977). Two kinds of lithotrophs missing in nature. *Z. Allg. Mikrobiol., 17*, 491-493. http://dx.doi.org/10.1002/jobm.19770170611

Cabrera, A., Cox, L., Spokas, K. A., Celis, R., Hermosín, M. C., Cornejo, J., & Koskinen, W. C. (2011). Comparative sorption and leaching study of the herbicides fluometuron and 4-chloro-2-methylphenoxyacetic acid (MCPA) in a soil amended with biochars and other sorbents. *J.Agric. Food Chem.*, *59*(23), 12550-12560. https://doi.org/10.1021/jf202713q

Camargo, J. A., & Alonso, A. (2006). Ecological and toxicological effects of inorganic nitrogen pollution in aquatic ecosystems: A global assessment. *Environ. Int., 32*(6), 831-849. http://dx.doi.org/10.1016/j.envint.2006.05.002

Cameron, K. C., Di, H. J., & McLaren, R. G. (1997). Is soil an appropriate dumping ground for our wastes? *Aust. J. Soil. Res., 35*, 995-1035. http://doi.org/10.1071/S96099

Cameron, S. G., & Schipper, L. A. (2010). Nitrate removal and hydraulic performance of organic carbon for use in denitrification beds. *Ecol. Eng., 36*, 1588-1595. http://doi.org/10.1016/j.ecoleng.2010.03.010

Canfield, D. E. (1998). A new model for Proterozoic ocean chemistry. *Nature, 396*, 450-453. http://doi.org/10.1038/24839

Canfield, D. E., Glazer, A. N., & Falkowski, P. G. (2010). The evolution and future of Earth's nitrogen cycle. *Science, 330*(6001), 192-196. http://doi.org/10.1126/science.1186120

Canfield, D. E., Poulton, S. W., Knoll, A. H., Narbonne, G. M., Ross, G., Goldberg, T., & Strauss, H. (2008). Ferruginous conditions dominated later Neoproterozoic deep-water chemistry. *Science 321*(5981), 949-952. http://doi.org/10.1126/science.1154499

Canfield, D. E., Rosing, M. T., & Bjerrum, C. (2006). Early anaerobic metabolisms. *Phil. Trans. R. Soc. B, 361*(1474): 1819-1836. https://doi.org/10.1098/rstb.2006.1906

Cao, X., Ma, L., Gao, B., & Harris, W. (2009). Dairy-manure derived biochar effectively sorbs lead and atrazine. *Environ. Sci. Technol. 43*(9), 3285-3291. https://doi.org/10.1021/es803092k

Carmichael, P. A. (1994). Using wood chips as a source of organic carbon in denitrification: A column experiment and field study implementing the funnel and gate designs. MS thesis. Waterloo, Ontario: University of Waterloo, Department of Earth Sciences.

Cayuela, M. L., Sánchez-Monedero, M. A., Roig, A., Hanley, K., Enders, A., & Lehmann, J. (2013). Biochar and denitrification in soils: when, how much and why does biochar reduce N_2O emissions? *Scientific Reports*, *3*, 1732. https://doi.org/10.1038/srep01732

Cayuela, M. L., van Zwieten, L., Singh, B. P., Jeffery, S., Roig, A., & Sánchez-Monedero, M. A. (2014). Biochar's role in mitigating soil nitrous oxide emissions: A review and meta-analysis. *Ag. Ecosys. Environ.*, *191*, 5-16. https://doi.org/10.1016/j.agee.2013.10.009

Cey, E. E., Rudolph, D. L., Aravena, R., & Parkin, G. (1999). Role of the riparian zone in

controlling the distribution and fate of agricultural nitrogen near a small stream in southern Ontario. *J. Contaminant Hydrol., 37*, 45-67. https://doi.org/10.1016/S0169-7722(98)00162-4

Chameides, W. L., & Walker, J. C. G. (1981). Rates of fixation by lightning of carbon and nitrogen in possible primitive atmospheres. *Origins of Life, 11*, 291-302. http://dx.doi.org/10.1007/BF00931483

Chen, B., Chen, Z., & Lv, S. (2011). A novel magnetic biochar efficiently sorbs organic pollutants and phosphate. *Biores. Technol.*, *102*(2), 716-723. https://doi.org/10.1016/j.biortech.2010.08.067

Cheng, C.H., Lehmann, J., Thies, J. E., & Burton, S. D. (2008). Stability of black carbon in soils across a climatic gradient. *J. Geophy. Res.*, *113*(G2), G02027. https://doi.org/10.1029/2007JG000642

Choi, A. L., Weihe, P., Budtz-Jørgensen, E., Jørgensen, P. J., Salonen, J. T., Tuomainen, T.-P., … Grandjean, P. (2009). Methylmercury exposure and adverse cardiovascular effects in Faroese whaling men. *Environ. Health Perspectives, 117*(3), 367-372. https://doi.org/10.1289/ehp.11608

Christianson, L. E., & Helmers, M. (2011a). Woodchip bioreactors for nitrate in agricultural drainage. Iowa State University Extension Publication PMR 1008. Retrieved from: http://lib.dr.iastate.edu/cgi/viewcontent.cgi?article=1083&context=extension_ag_pubs

Christianson, L. E., Bhandari, A., Helmers, M. (2012a). A practice-oriented review of woodchip bioreactors for subsurface agricultural drainage. *Appl. Eng. Agric. 28*(6), 861-874. http://dx.doi.org/10.13031/2013.42479

Christianson, L. E., Bhandari, A., Helmers, M., Kult, K., Sutphin, T., & Wolf, R. (2012b). Performance evaluation of four field-scale agricultural drainage denitrification bioreactors in Iowa. *Trans. Am. Soc. Agric. Eng., 55*(6), 2163–2174.

Christianson, L. E., Castelló, A., Christianson, R., Bhandari, A., & Helmers, M. (2010). Hydraulic property determination of denitrifying bioreactor fill media. *Applied Eng. Agric., 26*(5), 849-854. http://dx.doi.org/10.13031/2013.34946

Christianson, L. E., Christianson, R., Helmers, M., Pederson, C., & Bhandari, A. (2013a). Modeling and calibration of drainage denitrification bioreactor design criteria. *J. Irrig. Drain Eng., 139*(9), 699-709. http://dx.doi.org/10.1061/(ASCE)IR.1943-4774.0000622

Christianson, L. E., Hanly, J. A., & Hedley, M. J. (2011b). Optimized denitrification bioreactor treatment through simulated drainage containment. *Agricultural Water Management, 99*(1), 85-92. http://dx.doi.org/10.1016/j.agwat.2011.07.015

Christianson, L.E., Hedley, M., Camps, M., Free, H., & Saggar, S. (2011c). *Influence of biochar amendments on denitrification bioreactor performance*. Presented at the Adding to the knowledge base for the nutrient manager from the 24th Annual Fertilizer and Lime Research Centre Workshop, Massey University.

Christianson, L. E., Helmers, M., Bhandari, A., & Moorman, T. (2013b). Internal hydraulics of an agricultural drainage denitrification bioreactor. *Ecol. Eng. 52*, 298-307. http://dx.doi.org/10.1016/j.ecoleng.2012.11.001

Christianson, L. E., Lepine, C., Sharrer, K. L., & Summerfelt, S. T. (2016). Denitrifying bioreactor clogging potential during wastewater treatment. *Water Research, 105*, 147-156. http://dx.doi.org/10.1016/j.watres.2016.08.067

Christianson, L. E., Lepine, C., Sibrell, P. L., Penn, C., & Summerfelt, S. T. (2017). Denitrifying woodchip bioreactor and phosphorus filter pairing to minimize pollution swapping. *Water Res.*, *121*, 129-139. https://doi.org/10.1016/j.watres.2017.05.026

Chintala, R., Mollinedo, J., Schumacher, T. E., Papiernik, S. K., Malo, D. D., Clay, D. E., … Gulbrandson, D. W. (2013). Nitrate sorption and desorption in biochars from fast pyrolysis. *Microporous and Mesoporous Materials: The Official Journal of the International Zeolite Association*, 179, 250-257. https://doi.org/10.1016/j.micromeso.2013.05.023

Chintala, R., Schumacher, T. E., McDonald, L. M., Clay, D. E., Malo, D. D., Papiernik, S. K., … Julson, J. L. (2014). Phosphorus sorption and availability from biochars and soil/biochar mixtures. *Clean: Soil, Air, Water*, *42*(5), 626-634. https://doi.org/10.1002/clen.201300089

Chun, J. A., Cooke, R. A., Eheart, J. W., & Kang, M. S. (2009). Estimation of flow and transport parameters for woodchip-based bioreactors: I. laboratory-scale bioreactor. *Biosys. Eng.*, *104*(3), 384-395. https://doi.org/10.1016/j.biosystemseng.2009.06.021

Chun, J. A., Cooke, R. A., Eheart, J. W., & Cho, J. (2010). Estimation of flow and transport parameters for woodchip-based bioreactors: II. field-scale bioreactor. *Biosystems Eng.*, *105*(1), 95-102. https://doi.org/10.1016/j.biosystemseng.2009.09.018

Cloern, J. E. (2001). Review: Our evolving conceptual model of the coastal eutrophication problem. *Mar. Ecol. Prog. Ser., 210*, 223-253. https://doi.org/10.3354/meps210223

Clough, T. J., Bertram, J. E., Ray, J. L., Condron, L. M., O'Callaghan, M., Sherlock, R. R., & Wells, N. S. (2010). Unweathered wood biochar impact on nitrous oxide emissions from a bovine-urine-amended pasture soil. *SSSAJ*, *74*(3), 852-860. https://doi.org/10.2136/sssaj2009.0185

Codispoti, L. A., & Richards, F. A. (1976). An analysis of the horizontal regime of denitrification in the eastern tropical North Pacific. *Limnology and Oceanography, 21*(3), 379-388. http://dx.doi.org/10.4319/lo.1976.21.3.0379

Compeau, G. C., & Bartha, R. (1985). Sulfate-reducing bacteria: Principal methylators of mercury in anoxic estuarine sediment. *Appl. Environ. Microbiol.*, *50*(2), 498-502.

Cooke, R. A., & Bell, N. L. (2014). Protocol and interactive routine for the design of subsurface bioreactors. *Appl. Eng. Agric., 30*(5), 761-771. http://dx.doi.org/10.13031/aea.30.9900

Cooke, R. A., Doheny, A. M., & Hirschi, M. C. (2001). Bioreactors for edge of field treatment of tile outflow. ASAE Paper No. 01-20182001. St. Joseph, MI: ASAE.

Cooper, A. B. (1990). Nitrate depletion in the riparian zone and stream channel of a small headwater catchment. *Hydrobiologia, 202*, 13-26. http://dx.doi.org/10.1007/BF00027089

Correa, P., Haenszel, W., Cuello, C., Tannenbaum, S., & Archer, M. (1975). A model for

gastric cancer epidemiology. *The Lancet*, *2*(7924), 58-60.

Cornelius, O., Matschullat, J., Zurba, K., Zimmermann, F., & Erasmi, S. (2016). Greenhouse gas emissions from soils — A review. *Chemie der Erde, 76*, 327-352. http://dx.doi.org/10.1016/j.chemer.2016.04.002

Cornwell, W. K., Cornelissen, J. H. C., Allison, S. D., Bauhuss, J., Eggleton, P., Preston, C. M., . . . Zanne, A. E. (2009). Plant traits and wood fates across the globe: Rotted, burned, or consumed? *Global Change Biology, 15*, 2431-2449. http://doi.org/10.1111/j.1365-2486.2009.01916.x

Costa, E., Pérez, J., & Kreft, J. U. (2006) Why is metabolic labour divided in nitrification? *Trends Microbiol., 14*(5), 213-219. https://doi.org/10.1016/j.tim.2006.03.006

Coumaravel, K., Santhi, R., Sanjiv Kumar, V., & M. M., Mansour. (2011). Biochar – A promising soil additive - A review. *Agricultural Review*, *32*(2), 134–139. Retrieved from http://www.arccjournals.com/uploads/articles/R3227.pdf

Crutzen, P. J. (1970). The influence of nitrogen oxides on the atmospheric ozone content. *Q.J.R. Meteorol. Soc.*, *96*(408), 320-325. https://doi.org/10.1002/qj.49709640815

Daims, H., Lebedeva, E. V., Pjevac, P., Han, P., Herbold, C., Albertsen, M., . . . Wagner, M. (2015). Complete nitrification by Nitrospira bacteria. *Nature, 528*(7583), 504-509. https://doi.org/10.1038/nature16461

Damaraju, S., Singh, U. K., Sreekanth, D., & Bhandari, A. (2015). Denitrification in biofilm configured horizontal flow woodchip bioreactor: Effect of hydraulic retention time and biomass growth. *Ecohydrology & Hydrobiology*, *15*(1), 39-48. https://doi.org/10.1016/j.ecohyd.2014.11.001

David, C. M. (2014). Evaluating a proposed farm best management practice: Nitrous oxide emissions, in-bed nitrate and carbon monitoring, and hydraulic retention times of denitrifying woodchip bioreactors in Monterey County, California. MS thesis. Seaside, CA: California State University Monterey Bay, Division of

Science and Environmental Policy. Retrieved from http://digitalcommons.csumb.edu/caps_thes

Davis, J. M. (2015). Biochar and pH as drivers of greenhouse gas production in denitrification systems. MS thesis. Blacksburg, VA: Virginia Polytechnic Institute and State University, Department of Biological Systems Engineering.

de Leeuw, F., & Horálek, J. (2009). Assessment of the health impacts of exposure to PM2.5 at a European level. ETC/ACC Technical Paper 2009/1. Retrieved from: http://acm.eionet.europa.eu/docs/ETCACC_TP_2009_1_European_PM2.5_HIA.pdf

DeBoe, G., Bock, E., Stephenson, K., & Easton, Z. (2017). Nutrient biofilters in the Virginia Coastal Plain: Nitrogen removal, cost, and potential adoption pathways. *J. Soil W. Conserv.*, *72*(2), 139-149. https://doi.org/10.2489/jswc.72.2.139

Deenik, J. L., Diarra, A., Uehara, G., Campbell, S., Sumiyoshi, Y., & Antal, M. J., Jr. (2011). Charcoal ash and volatile matter effects on soil properties and plant growth in an acid ultisol. *Soil Sci.*, *176*(7), 336-345. https://doi.org/10.1097/SS.0b013e31821fbfea

DeLuca, T. H., MacKenzie, M. D., & Gundale, M. J. (2009). Biochar effects on soil nutrient transformations. In J. Lehmann & S. Joseph, (Eds.), *Biochar for Environmental Management Science and Technology* (pp. 251-270). London: Earthscan.

Deng, Y., Zhang, T., & Wang, Q. (2017). Biochar adsorption treatment for typical pollutants removal in livestock wastewater: A review. *Engineering Applications of Biochar*. InTech. https://doi.org/10.5772/intechopen.68253

Devol, A. H. (2003). Nitrogen cycle: Solution to a marine mystery. *Nature, 422*(6932), 575-576. https://doi.org/10.1038/422575a

Diaz, R. J., & Rosenberg, R. (1995). Marine benthic hypoxia: A review of its ecological effects and the behavioural response of benthic macrofauna. *Oceanogr. Mar. Biol. Ann. Rev., 33*, 245-303.

Diaz, R. J., & Rosenberg, R. (2008). Spreading dead zones and consequences for

marine ecosystems. *Science, 321*(5891), 926-929. https://doi.org/10.1126/science.1156401

Díaz, R., García, J., Mujeriego, R., & Lucas, M. (2003). A quick, low-cost treatment method for secondary effluent nitrate removal through denitrification. *Environ. Eng. Sci.*, *20*(6), 693-702. https://doi.org/10.1089/109287503770736195

Dicke, C., Andert, J., Ammon, C., Kern, J., Meyer-Aurich, A., & Kaupenjohann, M. (2015). Effects of different biochars and digestate on N_2O fluxes under field conditions. *Sci. Total Environ.*, *524-525*, 310-318. https://doi.org/10.1016/j.scitotenv.2015.04.005

Dinnes, D. L., Karlen, D. L., Jaynes, D. B., Kaspar, T. C., & Hatfield, J. L. (2002). Review and interpretation: Nitrogen management strategies to reduce leaching in tile-drained Midwestern soils. *Agron. J., 94*, 153-171. http://doi.org/10.2134/agronj2002.0153

Doheny, A. (2002). Amelioration of tile nitrate and atrazine using inline biofilters. MS thesis. Urbana-Champaign, IL: University of Illinois at Urbana-Champaign, Agricultural & Biological Engineering.

Downes, M. T., Howard-Williams, C., & Schipper, L. A. (1997). The long and short roads to riparian zone restoration: Nitrate removal efficiency. In N. E. Haycock et al. (Eds.) Buffer zones: Their process and potential in water protection. Oxfordshire, England: Quest Environmental.

Downie, A., Crosky, A., & Munroe, P. (2009). Physical properties of biochar. In *Biochar for environmental management: Science and Technology*. London, UK: Earthscan.

Duarte, C. M. (2009). Coastal eutrophication research: a new awareness. *Hydrobiologia, 629*, 263-269. http://doi.org/10.1007/s10750-009-9795-8

Durand, P., Breuer, L., Johnes, P. J., Billen, G., Butturini, A., Pinay, G., … Wright, R. (2011). Nitrogen processes in aquatic ecosystems. In *The European nitrogen assessment: Sources, effects and policy perspectives* (pp. 126–146). Cambridge: Cambridge University Press.

Easton, Z. M., & Lassiter, E. (2013). Denitrification Management. Retrieved August 15,

2016, from http://www.pubs.ext.vt.edu/BSE/BSE-54/BSE-54-PDF.pdf

Easton, Z. M., Rogers, M., Davis, M., Wade, J., Eick, M., & Bock, E. M. (2015). Mitigation of sulfate reduction and nitrous oxide emission in denitrifying environments with amorphous iron oxide and biochar. *Ecol. Eng., 82*, 605-613. http://dx.doi.org/10.1016/j.ecoleng.2015.05.008

Eldyasti, A., Nakhla, G., & Zhu, J. (2014a). Influence of biofilm thickness on nitrous oxide (N_2O) emissions from denitrifying fluidized bed bioreactors (DFBBRs). *J. Biotechnol.*, 281-290. https://doi.org/10.1016/j.jbiotec.2014.10.008

Eldyasti, A., Nakhla, G., & Zhu, J. (2014b). Mitigation of nitrous oxide (N_2O) emissions from denitrifying fluidized bed bioreactors (DFBBRs) using calcium. *Bioresour. Technol.*, *173*, 272-283. https://doi.org/10.1016/j.biortech.2014.09.121

Elgood, Z., Robertson, W. D., Schiff, S. L., and Elgood, R. (2010). Nitrate removal and greenhouse gas production in a stream-bed denitrifying bioreactor. *Eco. Eng., 36*: 1575-1580. http://dx.doi.org/10.1016/j.ecoleng.2010.03.011

Erisman, J. W., Bleeker, A., Galloway, J., & Sutton, M. S. (2007). Reduced nitrogen in ecology and the environment. *Environ. Pollut., 150*(1), 140-149. http://dx.doi.org/10.1016/j.envpol.2007.06.033

Erisman, J. W., Galloway, J. N., Seitzinger, S., Bleeker, A., Dise, N. B., Petrescu, A. M., . . . de Vries, W. Consequences of human modification of the global nitrogen cycle. *Philos. Trans. R. Soc. Lond. B Biol. Sci., 368*(1621). https://dx.doi.org/10.1098%2Frstb.2013.0116

Erisman, J. W., Sutton, M. A., Galloway, J., Klimont, Z., & Winiwarter, W. (2008). How a century of ammonia synthesis changed the world. *Nat. Geosci., 1*(10), 636-639. http://dx.doi.org/10.1038/ngeo325

Eyde, H. S. (1909). The manufacture of nitrates from the atmosphere by the electric arc - Birkeland-Eyde process. J. Royal Soc. Arts, 57(2949), 568-576.

Falkowski, P. G., & Godfrey, L. V. (2008). Electrons, life and the evolution of Earth's oxygen cycle. *Phil. Trans. R. Soc. B, 363*, 2705-2716. https://dx.doi.org/10.1098%2Frstb.2008.0054

FAO. (2002). The State of Food Insecurity in the World. Rome: Food and Agricultural

Organization.

FAO. (2003). *World agriculture towards 2015/2030: An FAO perspective*. London, UK: Earthscan Publications Ltd. Retrieved from http://www.fao.org/3/a-y4252e.pdf

FAO. (2006). *The State of Food Insecurity in the World*. Rome: FAO.

Farquhar, J., Bao, H., & Thiemens, M. (2000). Atmospheric influence of Earth's earliest sulfur cycle. *Science, 289*(5480), 756-758. http://doi.org/10.1126/science.289.5480.756

Fausey, N., Brown, L., Belcher, H., & Kanwar, R. (1995). Drainage and water quality in Great Lakes and Cornbelt States. *J. Irrig. Drain Eng., 121*(4), 283-288. http://doi.org/10.1061/(ASCE)0733-9437(1995)121:4(283)

Fenton, O., Healy, M. G., Brennan, F., Jahangir, M. M. R., Lanigan, G. J., Richards, K. G., … Ibrahim, T. G. (2014). Permeable reactive interceptors: blocking diffuse nutrient and greenhouse gases losses in key areas of the farming landscape. *J. Agric. Sci.*, *152*(S1), 71-81. https://doi.org/10.1017/S0021859613000944

Feyereisen, G. W., Moorman, T. B., Christianson, L. E., Venterea, R. T., Coulter, J. A., & Tschirner, U. W. (2016). Performance of agricultural residue media in laboratory denitrifying bioreactors at low temperatures. *J. Environ. Qual., 24*, 779-787. http://doi.org/10.2134/jeq2015.07.0407

Field, C. B., Behrenfeld, M. J., Randerson, J. T., & Falkowski, P. (1998). Primary production of the biosphere: Integrating terrestrial and oceanic components. *Science, 281*(5374), 237-240. http://doi.org/10.1126/science.281.5374.237

Fixen, P. E., & West, F. B. (2002). Nitrogen fertilizers: Meeting contemporary challenges. *AMBIO, 31*(2), 169-176. http://dx.doi.org/10.1579/0044-7447-31.2.169

Flewelling, S. A., Herman, J. S., Hornberger, G. M., & Mills, A. L. (2011). Travel time controls the magnitude of nitrate discharge in groundwater bypassing the riparian zone to a stream on Virginia's coastal plain. *Hydrol. Process., 26*, 1242-1253. http://dx.doi.org/10.1002/hyp.8219

Foley, J. A., DeFries, R., Asner, G. P., Barford, C., Bonan, G., Carpenter, S. R., . . . &

Snyder, P. K. Review: Global consequences of land use. *Science, 309*(5734), 570-574. http://dx.doi.org/10.1126/science.1111772

Fox, J. (2003). Effect Displays in R for Generalised Linear Models. *J. Stat. Softw.*, *8*(15), 1-27.

Fox, J., & Weisberg, S. (2011). *An R Companion to Applied Regression, Second Edition* (Vol. 2). SAGE Publications.

Frei, R., Gaucher, C., Poulton, S. W., & Canfield, D. E. (2009). Fluctuations in Precambrian atmospheric oxygenation recorded by chromium isotopes. *Nature, 261*, 250-254. http://dx.doi.org/10.1038/nature08266

Gałecki, A., & Burzykowski, T. (2013). *Linear Mixed-Effects Models Using R: A Step-by-Step Approach*. (G. Casella, S. E. Fienberg, & I. Olkin, Eds.). New York: Springer.

Galloway, J. N., & Cowling, E. B. (2002). Reactive nitrogen and the world: Two hundred years of change. *Ambio., 31*(2), 64-71. https://doi.org/10.1579/0044-7447-31.2.64

Galloway, J. N., Aber, J. D., Erisman, J. W., Seitzinger, S. P., Howarth, R. W., Cowling, E. B., & Cosby, B. J. (2003). The nitrogen cascade. *BioScience, 5*, 341-356. http://dx.doi.org/10.1641/0006-3568(2003)053[0341:TNC]2.0.CO;2

Galloway, J. N., Schlesinger, W. H., Levy, H., Michaels, A., & Schnoor, J. L. (1995). Nitrogen fixation: Anthropogenic enhancement-environmental response. *Global Biogeochemical Cycles*, *9*(2), 235–252. https://doi.org/10.1029/95GB00158

Galloway, J. N., Townsend, A. R., Erisman, J. W., Bekunda, M., Cai, Z., Freney, J. R., . . . Sutton, M. A. (2008). Transformation of the nitrogen cycle: Recent trends, questions, and potential solutions. *Science, 320*, 889–892. http://doi.org/10.1126/science.1136674

Gelman, A., & Hill, J. (2006). *Data Analysis Using Regression and Multilevel/Hierarchical Models* (Vol. 6). Cambridge: Cambridge University Press.

Gerland, P., Raftery, A. E., Sevčíková, H., Li, N., Gu, D., Spoorenberg, T., … Wilmoth, J. (2014). World population stabilization unlikely this century. *Science*, *346*(6206), 234-237. https://doi.org/10.1126/science.1257469

Ghane, E., Fausey, N. R., & Brown, L. C. (2015). Modeling nitrate removal in a denitrification bed. *Water Res.*, *71*, 294-305. https://doi.org/10.1016/j.watres.2014.10.039

Gharabaghi, B., Rudra, R. P., & Whiteley, H. R. (2002). Development of a management tool for vegetative filter strips. In *Best modelling practices for urban water systems* (pp. 289-302).

Gibert, O., Pomierny, S., Rowe, I., & Kalin, R. M. (2008). Selection of organic substrates as potential reactive materials for use in a denitrification permeable reactive barrier (PRB). *Biores. Tech.*, *99*(16), 7587-7596. https://doi.org/10.1016/j.biortech.2008.02.012

Giblin, A. E., Tobias, C. R., Song, B., Weston, N., Banta, G. T., & Rivera-Monroy, V. H. (2013). The importance of dissimilatory nitrate reduction to ammonium (DNRA) in the nitrogen cycle of coastal ecosystems. *Oceanography, 26*(3), 124-131. https://doi.org/10.5670/oceanog.2013.54

Glaser, B., Lehmann, J., Steiner, C., Nehls, T., Yousaf, M., & Zelch, W. (2002). Potential of pyrolysed organic matter in soil amelioration. *Proc. 12th International Soil Conservation (ISCO) Conference*. Beijing, China. Retrieved from: http://www.eprida.com/hydro/ecoss/background/pyrolyzed.pdf

Glaser, B., Wiedner, K., Seelig, S., Schmidt, H.P., & Gerber, H. (2015). Biochar organic fertilizers from natural resources as substitute for mineral fertilizers. *Agron. Sustain. Dev.*, *35*(2), 667-678. https://doi.org/10.1007/s13593-014-0251-4

Gnanadesikan, A. (1999). A simple predictive model for the structure of the oceanic pycnocline. *Science, 283*(5410) 2077-2079. https://doi.org/10.1126/science.283.5410.2077

Godfrey, L. V., & Falkowski, P. G. (2009). The cycling and redox state of nitrogen in the Archaean ocean. *Nature Geoscience, 2*, 725-729. http://doi.org/10.1038/ngeo633

Golea, D. M., Upton, A., Jarvis, P., Moore, G., Sutherland, S., Parsons, S. A., & Judd, S. J. (2017). THM and HAA formation from NOM in raw and treated surface waters. *Water Res.*, *112*, 226-235. https://doi.org/10.1016/j.watres.2017.01.051

Goodwin, G. E., Bhattarai, R., & Cooke, R. (2015). Synergism in nitrate and

orthophosphate removal in subsurface bioreactors. *Ecol. Eng.*, *84*, 559-568. https://doi.org/10.1016/j.ecoleng.2015.09.051

Gottschall, N., Edwards, M., Craiovan, E., Frey, S. K., Sunohara, M., Ball, B., … Lapen, D. R. (2016). Amending woodchip bioreactors with water treatment plant residuals to treat nitrogen, phosphorus, and veterinary antibiotic compounds in tile drainage. *Ecol. Eng.*, *95*, 852-864. https://doi.org/10.1016/j.ecoleng.2016.06.011

Grady, C. P. L., & Lim, H. C. (1980). *Biological wastewater treatment: Theory and applications*. New York, NY: Marcel Dekker.

Grantham, B. A., Chan, F., Nielsen, K. J., Fox, D. S., Barth, J. A., Huyer, A., . . . & Menge, B. A. (2004). Upwelling-driven nearshore hypoxia signals ecosystem and oceanographic changes in the Northeast Pacific. *Nature, 429*, 749-754. http://doi.org/10.1038/nature02605

Greenan, C. M., Moorman, T. B., Kaspar, T. C., Parkin, T.B., & Jaynes, D. B. (2006). Comparing carbon substrates for denitrification of subsurface drainage water. *J. Environ. Qual., 35*(3), 824 - 829. http://doi.org/10.2134/jeq2005.0247

Greenan, C. M., Moorman, T. B., Parkin, T. B., Kaspar, T. C., & Jaynes, D. B. (2009). Denitrification in wood chip bioreactors at different water flows. *J. Environ. Qual., 38*(4), 1664-1671. http://doi.org/10.2134/jeq2008.0413

Groffman, P. M., Altabet, M. A., Böhlke, J. K., Butterbach-Bahl, K., David, M. B., Firestone, M. K., … Voytek, M. A. (2006). Methods for measuring denitrification: diverse approaches to a difficult problem. *Ecol. Appl., 16*(6), 2091-2122. https://doi.org/10.1890/1051-0761(2006)016[2091:MFMDDA]2.0.CO;2

Gruber, N., & Galloway, J. N. (2008). An Earth-system perspective of the global nitrogen cycle. *Nature, 451*, 293-296. http://doi.org/10.1038/nature06592

Gul, S., & Whalen, J. K. (2016). Biochemical cycling of nitrogen and phosphorus in biochar-amended soils. *Soil Biol. Biochem.*, *103*, 1-15. https://doi.org/10.1016/j.soilbio.2016.08.001

Gul, S., Whalen, J. K., Thomas, B. W., Sachdeva, V., & Deng, H. (2015).

Physico-chemical properties and microbial responses in biochar-amended soils: Mechanisms and future directions. *Ag. Ecosys. Environ.*, *206*, 46-59. https://doi.org/10.1016/j.agee.2015.03.015

Haber, F. (1920). The synthesis of ammonia from its elements: Nobel lecture, June 2, 1920. Retrieved from: https://www.nobelprize.org/nobel_prizes/chemistry/laureates/1918/haber-lecture.pdf

Hagmar, L., Bellander, T., Andersson, C., Lindén, K., Attewell, R., & Möller, T. (1991). Cancer morbidity in nitrate fertilizer workers. *Int. Arch. Occup. Environ. Health*, *63*(1), 63-67.

Hagy, J. D., Boynton, W. R., Keefe, C. W., & Wood, K. V. (2004). Hypoxia in Chesapeake Bay, 1950-2001: Long-term change in relation to nutrient loading and river flow. *Estuaries, 27*(4), 634-658.http://dx.doi.org/10.1007/BF02907650

Hale, S. E., Alling, V., Martinsen, V., Mulder, J., Breedveld, G. D., & Cornelissen, G. (2013). The sorption and desorption of phosphate-P, ammonium-N and nitrate-N in cacao shell and corn cob biochars. *Chemosphere*, *91*(11), 1612-1619. https://doi.org/10.1016/j.chemosphere.2012.12.057

Hamm, R. E., & Thompson, T. G. (1941). Dissolved nitrogen in the sea water of the northeast Pacific with notes on the total carbon dioxide and the dissolved oxygen. *J. Mar. Res., 4*, 11-27.

Harter, J., El-Hadidi, M., Huson, D. H., Kappler, A., & Behrens, S. (2017). Soil biochar amendment affects the diversity of nosZ transcripts: Implications for N_2O formation. *Nature: Scientific Reports*, *7*(3338), 1-14. https://doi.org/10.1038/s41598-017-03282-y

Harter, J., Krause, H.M., Schuettler, S., Ruser, R., Fromme, M., Scholten, T., … Behrens, S. (2014). Linking N2O emissions from biochar-amended soil to the structure and function of the N-cycling microbial community. *ISME J.*, *8*(3), 660-674. https://doi.org/10.1038/ismej.2013.160

Hassanpour, B., Giri, S., Pluer, W. T., Steenhuis, T. S., & Geohring, L. D. (2017).

Seasonal performance of denitrifying bioreactors in the Northeastern United States: Field trials. *J. Environ. Manage.*, *202*, 242-253. https://doi.org/10.1016/j.jenvman.2017.06.054

Haumaier, L., & Zech, W. (1995). Black carbon—possible source of highly aromatic components of soil humic acids. *Org. Geochem.*, *23*(3), 191-196. https://doi.org/10.1016/0146-6380(95)00003-W

Haycock, N. E., Pinay, G. (1993). Groundwater nitrate dynamics in grass and poplar vegetated riparian bufferstrips during the winter. *J. Environ. Qual., 22*, 273–278. http://dx.doi.org/10.2134/jeq1993.00472425002200020007x

Healy, M. G., Barrett, M., Lanigan, G. J., João Serrenho, A, Ibrahim, S. F., Rolfe, S. A., . . . Fenton, O. (2015). Optimizing nitrate removal and evaluating pollution swapping trade-offs from laboratory denitrification bioreactors. *Ecol. Eng., 74*, 290-301. http://dx.doi.org/10.1016/j.ecoleng.2014.10.005

Healy, M. G., Ibrahim, T. G., Lanigan, G. J., João Serrenho, A., & Fenton, O. (2012). Nitrate removal rate, efficiency and pollution swapping potential of different organic carbon media in laboratory denitrification bioreactors. *Ecol. Eng., 40*, 198-209. http://doi.org/10.1016/j.ecoleng.2011.12.010

Healy, M. G., Rodgers, M., & Mulqueen, J. (2006). Denitrification of a nitrate-rich synthetic wastewater using various wood-based media materials. *J. Environ. Sci. Health A Tox. Hazard. Subst. Environ. Eng.*, *41*(5), 779-788. https://doi.org/10.1080/10934520600614371

Hedeker, D., & Gibbons, R. D. (2006). *Longitudinal Data Analysis* (pp. 0-334). John Wiley & Sons, Ltd.

Hill, A. R. (1996). Nitrate removal in stream riparian zones. *J. Environ. Qual., 25*, 743-755. http://doi.org/10.2134/jeq1996.00472425002500040014x

Hill, A. R., Devito, K. J., & Vidon, P. G. (2014) Long-term nitrate removal in a stream riparian zone. *Biogeochemistry, 121*, 425-439. http://doi.org/10.1007/s10533-014-0010-2

Hua, G., Kim, J., & Reckhow, D. A. (2014). Disinfection byproduct formation from lignin

precursors. *Water Res.*, *63*, 285-295. https://doi.org/10.1016/j.watres.2014.06.029

Hua, G., Salo, M. W., Schmidt, C. G., & Hay, C. H. (2016). Nitrate and phosphate removal from agricultural subsurface drainage using laboratory woodchip bioreactors and recycled steel byproduct filters. *Water Research, 102*, 180-189. http://dx.doi.org/10.1016/j.watres.2016.06.022

Hüppi, R., Felber, R., Neftel, A., Six, J., & Leifeld, J. (2015). Effect of biochar and liming on soil nitrous oxide emissions from a temperate maize cropping system. *SOIL*, *1*(2), 707-717. https://doi.org/10.5194/soil-1-707-2015

Hurlbert, S.H. (1984). Pseudoreplication and the design of ecological field experiments. *Ecol. Monographs, 54*, 187-211.

Holland, H. D. (1984). *The chemical evolution of the atmosphere and oceans*. Princeton, N.J.: Princeton University Press.

Hoover, N. L., Bhandari, A., Soupir, M. L., & Moorman, T. B. (2016). Woodchip denitrification bioreactors: Impact of temperature and hydraulic retention time on nitrate removal. *J. Environ. Qual., 45*(3), 803-812. http://dx.doi.org/10.2134/jeq2015.03.0161

Hoover, N. L., Soupir, M. L., VanDePol, R. D., Goode, T. R., & Law, J. Y. (2017). Pilot-scale denitrification bioreactors for replicated field research. *Appl. Eng. Agric.*, *33*(1), 83-90. http://dx.doi.org/10.13031/aea.11736

Hothorn, T., Bretz, F., & Westfall, P. (2008). Simultaneous inference in general parametric models. *Biometrical J., 50*(3), 346-363.

Howarth, R. W. (2008). Review: Coastal nitrogen pollution: A review of sources and trends globally and regionally. *Harmful Algae, 8*, 14-20. http://dx.doi.org/10.1016/j.hal.2008.08.015

Hoyos, C. D., Agudelo, P. A., Webster, P. J., & Curry, J. A. (2006). Deconvolution of the factors contributing to the increase in global hurricane intensity. *Science, 312*(5770), 94-97. https://doi.org/10.1126/science.1123560

Howarth, R. W., Anderson, D., Cloern, J., Elfring, C., Hopkinson, C., Lapointe, B., . .

Walker, D. (2000). Nutrient pollution of coastal rivers, bays, and seas. *Issues Ecol., 7*, 1-15.

Hunter, W. J. (2001). Use of vegetable oil in a pilot-scale denitrifying barrier. *J. Contaminant Hydrol., 53*, 119-131. https://doi.org/10.1016/S0169-7722(01)00137-1

Hunter, W. J., Follett R. F., & Cary, J. W. (1997). Use of vegetable oil to remove nitrate from flowing groundwater. *Transactions of the ASAE, 40*(2), 345-353. http://dx.doi.org/10.13031/2013.21279

Ilyas, H., & Masih, I. (2017a). The performance of the intensified constructed wetlands for organic matter and nitrogen removal: A review. *J. Environ. Manage. 198*, 372-383. https://doi.org/10.1016/j.jenvman.2017.04.098

Ilyas, H., & Masih, I. (2017b). Intensification of constructed wetlands for land area reduction: a review. *Environ. Sci. Pollut. Res. Int.*, *24*(13), 12081-12091. https://doi.org/10.1007/s11356-017-8740-z

ILO. (2007). Key indicators of the labour market: Ninth edition. Geneva, Switzerland: International Labour Organization. Retrieved from http://www.ilo.org/wcmsp5/groups/public/---dgreports/---stat/documents/publication/wcms_498929.pdf

Ima, C. S., & Mann, D. D. (2007). Physical properties of woodchip:compost mixtures used as biofilter media. *Agricultural Engineering International: The CIGR Ejournal*, *9*. Manuscript BC 07 005. Vol. IX.

Iowa Natural Resource Conservation Service. (2016). IADentrifyingBioreactor.xlsx v1.0. Retrieved from: https://www.nrcs.usda.gov/wps/portal/nrcs/detail/ia/technical/engineering/?cid=nrcs142p2_008213

IPCC. (2007). Climate change 2007: Synthesis report. Cambridge, UK: Cambridge University Press. Retrieved from: https://www.ipcc.ch/pdf/assessment-report/ar4/syr/ar4_syr.pdf

Iqbal, M. J., & Ashiq, M. N. (2007). Adsorption of dyes from aqueous solutions on

activated charcoal. *J. Hazard. Mater.*, *139*(1), 57-66. https://doi.org/10.1016/j.jhazmat.2006.06.007

Jacobs, T. C., & Gilliam, J. W. (1985). Riparian losses of nitrate from agricultural drainage waters. *J. Environ. Qual., 14*(4), 472 - 478. http://dx.doi.org/10.2134/jeq1985.00472425001400040004x

Jaynes, D. B., Colvin, T. S., Karlen, D. L., Cambardella, C. A., & Meek, D. W. (2000). Nitrate loss in subsurface drainage as affected by nitrogen fertilizer rate. *J. Environ. Qual., 30*(4), 1305-1314. http://doi.org/10.2134/jeq2001.3041305x

Jaynes, D. B., Kaspar, T. C., Moorman, T. B., & Parkin, T. B. (2008). In situ bioreactors and deep drain-pipe installation to reduce nitrate losses in artificially drained fields. *J. Environ. Qual.*, *37*(2), 429-436. https://doi.org/10.2134/jeq2007.0279

Jaynes, D. B., Moorman, T. B., Parkin, T. B., & Kaspar, T. C. (2016). Simulating Woodchip Bioreactor Performance Using a Dual-Porosity Model. *J. Environ. Qual.*, *45*(3), 830-838. https://doi.org/10.2134/jeq2015.07.0342

Jayson, G. G., Lawless, T. A., & Fairhurst, D. (1982). The adsorption of organic and inorganic phosphates onto a new activated carbon adsorbent. *J. Colloid Interface Sci, 86*(2), 397-410. https://doi.org/10.1016/0021-9797(82)90085-6

Jetten, M. S. M., Op den Camp, H. J. M., Kuenen, J. G., & Strous, M. (2010). Description of the order Brocadiales. In *Bergey's manual of systematic bacteriology* (pp. 596-603, Vol. 4). Heidelberg, Germany: Springer.

Jindo, K., Mizumoto, H., Sawada, Y., Sanchez-Monedero, M. A., & Sonoki, T. (2014). Physical and chemical characterization of biochars derived from different agricultural residues. *Biogeosciences*, *11*(23), 6613-6621. https://doi.org/10.5194/bg-11-6613-2014

Johnston, H. (1971). Reduction of stratospheric ozone by nitrogen oxide catalysts from supersonic transport exhaust. *Science*, *173*(3996), 517-522. https://doi.org/10.1126/science.173.3996.517

Jones, C., Brown, B. D., Engel, R., Horneck, D., & Olson-Rutz, K. (2013). *Factors affecting nitrogen fertilizer volatilization* (No. EB0208). Montana State University.

Jørgensen, K. S., & Tiedje, J. M. (1993). Survival of denitrifiers in nitrate-free, anaerobic

environments. *Appl. Environ. Microbiology, 59*(10), 3297-3305.

Jung, K.W., Hwang, M.J., Ahn, K.H., & Ok, Y.S. (2015). Kinetic study on phosphate removal from aqueous solution by biochar derived from peanut shell as renewable adsorptive media. *Int. J. Environ. Sci. Technol.*, *12*(10), 3363-3372. https://doi.org/10.1007/s13762-015-0766-5

Kadlec, R. H., & Wallace, S. D. (2009). *Treatment Wetlands*. Boca Raton, FL: Taylor & Francis Group, LLC.

Kasting, J. F. (1990). Bolide impacts and the oxidation state of carbon in the Earth's early atmosphere. *Origins Life Evol. Biosphere, 20*(3), 199-231. http://doi.org/10.1007/BF01808105

Keiluweit, M., Nico, P. S., Johnson, M. G., & Kleber, M. (2010). Dynamic molecular structure of plant biomass-derived black carbon (biochar). *Environ. Sci. Technol.*, *44*(4), 1247-1253. https://doi.org/10.1021/es9031419

Kellman, L. M. (2005). A study of tile drain nitrate - $\delta^{15}N$ values as a tool for assessing nitrate sources in an agricultural region. *Nutrient Cycling in Agroecosystems, 71*(2), 131-137. http://dx.doi.org/10.1007%2Fs10705-004-1925-0

Kerr, R. A. (2006). Global warming may be homing in on Atlantic hurricanes. *Science, 314*(5801), 910-911. http://doi.org/10.1126/science.314.5801.910

Kerr, R. A. (2008). Hurricanes won't go wild, according to climate models. *Science, 320*(5879), 999. http://doi.org/10.1016/10.1126/science.320.5879.999a

Khan, S., Ahmad, I., Shah, M. T., Rehman, S., & Khaliq, A. (2009). Use of constructed wetland for the removal of heavy metals from industrial wastewater. *J. Environ. Manage.*, *90*(11), 3451-3457. https://doi.org/10.1016/j.jenvman.2009.05.026

Knutson, T. R., Sirutis, J. J., Garner, S. T., Held, I. M., & Tuley, R. E. (2007). Simulation of the recent multidecadal increase of Atlantic hurricane activity using an 18-km-grid regional model. *Bulletin Am. Meteorology Soc., 88*, 1549-1565. https://doi.org/10.1175/BAMS-88-10-1549

Kookana, R. S., Sarmah, A. K., Zwieten, L. V., Krull, E., & Singh, B. (2011). Biochar

application to soil: Agronomic and environmental benefits and unintended consequences. *Adv. Agron. 112*, 103-142. https://doi.org/10.1016/B978-0-12-385538-1.00003-2

Korom, S. F. (1992). Natural denitrification in the saturated zone: A review. *Water Res., 28*, 6, 1657-1668. https://doi.org/10.1029/92WR00252

Kraft, B., Strous, M., & Tegetmeyer, H. E. (2011). Microbial nitrate respiration - genes, enzymes and environmental distribution. *J. Biotechnol., 155*(1), 104-117. http://doi.org/10.1016/j.jbiotec.2010.12.025

Kroeze, C. (1994). Nitrous oxide and global warming. *Sci. Total Environ.*, *143*(2), 193-209. https://doi.org/10.1016/0048-9697(94)90457-X

Kumar, P., Sudha, S., Chand, S., & Srivastava, V. C. (2010). Phosphate removal from aqueous solution using coir-pith activated carbon. Sep. Sci. Technol., 45(10), 1463-1470. https://doi.org/10.1080/01496395.2010.485604

Lachat Instruments. (2012). *Methods List for Automated Ion Analyzers*. Retrieved from http://www.lachatinstruments.com/download/LL022_Methods-List_Rev 6.pdf

Lassiter, E., & Easton, Z. M. (2013). Denitrifying bioreactors: An emerging best management practice to improve water quality. Retrieved August 15, 2016, from https://pubs.ext.vt.edu/BSE/BSE-55/BSE-55-PDF.pdf

Lehmann, J. (2007). A handful of carbon. *Nature, 447*, 143–144.

Lehmann, J., & Joseph, S. (2009). *Biochar for environmental management: Science and technology*. London, UK: Earthscan.

Lehmann, J., da Silva, J. P., Steiner, C., Nehls, T., Zech, W., & Glaser, B. (2003). Nutrient availability and leaching in an archaeological Anthrosol and a Ferralsol of the Central Amazon basin: Fertilizer, manure and charcoal amendments. *Plant Soil*, *249*(2), 343-357. https://doi.org/10.1023/A:1022833116184

Lehmann, J., Gaunt, J., & Rondon, M. (2006). Bio-char sequestration in terrestrial ecosystems - A review. *Mitigation and Adaptation Strategies for Global Change, 11*(2), 403-427. http://doi.org/10.1007/s11027-005-9006-5

Lehmann, J., Liang, B., Solomon, D., Lerotic, M., Luizão, F., Kinyangi, J., … Jacobsen,

C. (2005). Near-edge X-ray absorption fine structure (NEXAFS) spectroscopy for mapping nano-scale distribution of organic carbon forms in soil: Application to black carbon particles. *Global Biogeochem. Cycles*, *19*(1), GB1013. https://doi.org/10.1029/2004GB002435

Lepine, C., Christianson, L. E., Sharrer, K., Summerfelt, S. T. (2016). Optimizing hydraulic retention times in denitrifying woodchip bioreactors treating recirculating aquaculture system wastewater. *J. Environ. Qual. 45*, 813-821. http://doi.org/10.2134/jeq2015.05.0242

Liang, B., Lehmann, J., Solomon, D., Kinyangi, J., Grossman, J., O'Neill, B., … Neves, E. G. (2006). Black Carbon Increases Cation Exchange Capacity in Soils. *Soil Sci. Soc. Am. J.*, *70*, 1719-1730. https://doi.org/10.2136/sssaj2005.0383

Liang, X., Lin, L., Ye, Y., Gu, J., Wang, Z., Xu, L., … Tian, G. (2015). Nutrient removal efficiency in a rice-straw denitrifying bioreactor. *Biores. Technol.*, *198*, 746-754. https://doi.org/10.1016/j.biortech.2015.09.083

Liang, Y., Cao, X., Zhao, L., & Arellano, E. (2014). Biochar- and phosphate-induced immobilization of heavy metals in contaminated soil and water: implication on simultaneous remediation of contaminated soil and groundwater. *Environ. Sci. Pollution Res. Int.*, *21*(6), 4665-4674. https://doi.org/10.1007/s11356-013-2423-1

Libra, J. A., Ro, K. S., Kammann, C., Funke, A., Berge, N. D., Neubauer, Y., … Emmerich, K. H. (2011). Hydrothermal carbonization of biomass residuals: a comparative review of the chemistry, processes and applications of wet and dry pyrolysis. *Biofuels*, *2*(1), 71-106. https://doi.org/10.4155/bfs.10.81

Loehr, R. C. (1984). *Pollution Control for Agriculture*. New York, NY: Academia Press. https://doi.org/10.1017/S0014479700014290

Loh, Y. H., Jakszyn, P., Luben, R. N., Mulligan, A. A., Mitrou, P. N., & Khaw, K.-T. (2011). N-Nitroso compounds and cancer incidence: the European prospective investigation into cancer and nutrition (EPIC)-Norfolk Study. *Am. J. Clin. Nutr.*, *93*(5), 1053-1061. https://doi.org/10.3945/ajcn.111.012377

Long, L. M., Schipper, L. A., Bruesewitz, D. A. (2011). Long-term nitrate removal in a

denitrification wall. *Ag., Ecosystems Env., 140*(3–4), 514-520. http://dx.doi.org/10.1016/j.agee.2011.02.005

Lou, K., Rajapaksha, A. U., Ok, Y. S., & Chang, S. X. (2016). Pyrolysis temperature and steam activation effects on sorption of phosphate on pine sawdust biochars in aqueous solutions. *Chem Spec. Bioavail.*, *28*(1-4), 42-50. https://doi.org/10.1080/09542299.2016.1165080

Lowrance, R. (1992). Groundwater nitrate and denitrification in a coastal plain riparian forest. *J. Environ. Qual., 21*, 401-405. http://dx.doi.org/10.2134/jeq1992.00472425002100030017x

Lu, H., Chandran, K., & Stensel, D. (2014). Microbial ecology of denitrification in biological wastewater treatment. *Water Res., 64*, 237-254. https://doi.org/10.1016/j.watres.2014.06.042

Lyngsie, G., Borggaard, O. K., & Hansen, H. C. B. (2014). A three-step test of phosphate sorption efficiency of potential agricultural drainage filter materials. *Water Research, 51*, 256-265. http://dx.doi.org/10.1016/j.watres.2013.10.061

Madiba, O. F., Solaiman, Z. M., Carson, J. K., & Murphy, D. V. (2016). Biochar increases availability and uptake of phosphorus to wheat under leaching conditions. *Biol. Fertility Soils*, *52*(4), 439-446. https://doi.org/10.1007/s00374-016-1099-3

Maestrini, B., Herrmann, A. M., Nannipieri, P., Schmidt, M. W. I., & Abiven, S. (2014). Ryegrass-derived pyrogenic organic matter changes organic carbon and nitrogen mineralization in a temperate forest soil. *Soil Biol. Biochem.*, *69*, 291-301. https://doi.org/10.1016/j.soilbio.2013.11.013

Magee, P. N., Montesano, R., & Preussmann, R. (1976). N-Nitroso compounds and related carcinogens. In *Chemical Carcinogens* (pp. 491-625). New York: American Chemical Society.

Mancinelli, R. L., & McKay, C. P. (1988). The evolution of nitrogen cycling. *Orig Life Evol Biosph. 18*, 311-325. http://dx.doi.org/10.1007/BF01808213

Mansouri, A, & Lurie, A. A. (1993). Concise review: Methemoglobinemia. *Am. J. Hemotol, 41*(1), 7-12. http://dx.doi.org/10.1002/ajh.2830420104

McCarty, G. W., & Bremner, J. M. (1992). Availability of carbon for denitrification of nitrate in subsoils. *Biol. Fertil Soils 14*, 219–222. http://dx.doi.org/10.1007/BF00346064

McLaughlan, R. G., & Al-Mashaqbeh, O. (2009). Simple models for the release kinetics of dissolved organic carbon from woody filtration media. *Biores. Technol.*, *100*(9), 2588-2593. https://doi.org/10.1016/j.biortech.2008.12.002

McLaughlin, H., Anderson, P. S., Shields, F. E., & Reed, T. B. (2009). All biochars are not created equal, and how to tell them apart. *Proc. North American Biochar, Boulder, CO*, pp 1-36.

Metcalf and Eddy. (2003). *Wastewater Engineering Treatment and Reuse* (4th ed.). New York, N.Y.: McGraw-Hill.

Mikhail, S., & Sverjensky, D. (2014). Nitrogen speciation in upper mantle fluids and the origin of Earth's nitrogen-rich atmosphere. *Nature Geoscience, 7*, 816-819. http://dx.doi.org/10.1038/ngeo2271

Milliman, J. D., & Meade, R. H. (1983). World-wide delivery of river sediment to the ocean. *J. Geol., 91*(1), 1-21. https://doi.org/10.1086/628741

Mirvish, S. S. (1995). Role of N-nitroso compounds (NOC) and N-nitrosation etiology of gastric, esophageal, nasopharyngeal and bladder cancer and contribution to cancer of known exposures to NOC. *Cancer Lett, 93*, 17-48.

Mississippi River/Gulf of Mexico Watershed Nutrient Task Force. (2008). Gulf hypoxia action plan 2008 for reducing, mitigating, and controlling hypoxia in the Northern Gulf ofMexico and improving water quality in the Mississippi River Basin. EPA. Retreived from https://www.epa.gov/ms-htf/gulf-hypoxia-action-plan-2008

Mitsch, W. J., Bernal, B., & Hernandez, M. E. (2015). Ecosystem services of wetlands. *Int. J. Biodivers. Sci. Eco. Srvcs. Mgmt.*, *11*(1), 1-4. https://doi.org/10.1080/21513732.2015.1006250

Moir, J. W. B. (2011). *Nitrogen cycling in bacteria: Molecular analysis*. Norfolk, UK: Caister Academic Press.

Molina, M. J., & Rowland, F. S. (1974). Stratospheric sink for chlorofluoromethanes:

chlorine atom-catalysed destruction of ozone. *Nature*, *249*, 810-812. https://doi.org/10.1038/249810a0

Moorman, T. B., Parkin, T. B., Kaspar, T. C., Jaynes, D. B. (2010). Denitrification activity, wood loss, and N_2O emissions over 9 years from a wood chip bioreactor. *Eco. Eng., 36*(11), 1567-1574. http://dx.doi.org/10.1016/j.ecoleng.2010.03.012

Moorman, T. B., Tomer, M. D., Smith, D. R., & Jaynes, D. B. (2015). Evaluating the potential role of denitrifying bioreactors in reducing watershed-scale nitrate loads: A case study comparing three Midwestern (USA) watersheds. *Ecol. Eng.*, *75*, 441-448. https://doi.org/10.1016/j.ecoleng.2014.11.062

Morales, M. M., Comerford, N., Guerrini, I. A., Falcão, N. P. S., & Reeves, J. B. (2013). Sorption and desorption of phosphate on biochar and biochar–soil mixtures. *Soil Use and Management*, *29*(3), 306-314. https://doi.org/10.1111/sum.12047

Morley, J. (1927). Following through with grass seeds. *The National Greenkeeper, 1*(1), 15.

Mosier, A., Kroeze, C., Nevison, C., Oenema, O., Seitzinger, S., & van Cleemput, O. (1998). Closing the global N_2O budget: Nitrous oxide emissions through the agricultural nitrogen cycle. *Nutrient Cycling in Agroecosystems, 52*, 225-248. http://dx.doi.org/10.1023/A:1009740530221

Mukherjee, A., & Zimmerman, A. R. (2013). Organic carbon and nutrient release from a range of laboratory-produced biochars and biochar–soil mixtures. *Geoderma*, *193*, 122-130. https://doi.org/10.1016/j.geoderma.2012.10.002

Mulder, A., van de Graaf, A. A., Robertson, L. A., & Kuenen, J. G. (1995). Anaerobic ammonium oxidation discovered in a denitrifying fluidized bed reactor. *FEMS Microbiol. Ecol., 16*(3), 177-183. http://dx.doi.org/10.1111/j.1574-6941.1995.tb00281.x

Murray, P. J., Hatch, D. J., Dixon, E. R., Stevens, R. J., Laughlin, R. J., & Jarvis, S. C. (2004). Denitrification potential in a grassland subsoil: effect of carbon substrates. *Soil Biol. Biochem., 36*(3), 545–547. http://dx.doi.org/10.1016/j.soilbio.2003.10.020

Muscutt, A. D., Harris, G. L., Bailey, S. W., & Davies, D. B. (1993). Buffer zones to

improve water quality: a review of their potential use in UK agriculture. *Agric. Ecosyst. Environ.*, *45*(1), 59-77. https://doi.org/10.1016/0167-8809(93)90059-X

Myrold, D. D., & Tiedje, J. M. (1985). Diffusional constraints on denitrification in soil. *Soil Sci. Soc. Am. J., 49*, 651-657. http://dx.doi.org/10.2136/sssaj1985.03615995004900030025x

Namasivayam, C., & Sangeetha, D. (2004). Equilibrium and kinetic studies of adsorption of phosphate onto $ZnCl_2$ activated coir pith carbon. *J. Colloid Interface Sci.*, *280*(2), 359-365. https://doi.org/10.1016/j.jcis.2004.08.015

Nelder, J. A. (1977). A Reformulation of Linear Models. *J. R. Stat. Soci. Ser. A* , *140*(1), 48-77. https://doi.org/10.2307/2344517

Nelder, J. A. (1994). The statistics of linear models: back to basics. *Stat. Comput.*, *4*(4), 221-234. https://doi.org/10.1007/BF00156745

Nelson, N. O., Agudelo, S. C., Yuan, W., & Gan, J. (2011). Nitrogen and phosphorus availability in biochar-amended soils. *Soil Sci.*, *176*(5), 218-226. https://doi.org/10.1097/SS.0b013e3182171eac

Ngatia, L. W., Hsieh, Y. P., Nemours, D., Fu, R., & Taylor, R. W. (2017). Potential phosphorus eutrophication mitigation strategy: Biochar carbon composition, thermal stability and pH influence phosphorus sorption. *Chemosphere*, *180*, 201-211. https://doi.org/10.1016/j.chemosphere.2017.04.012

Nixon, S. W. (1995). Coastal marine eutrophication: A definition, social causes, and future concerns. *Ophelia, 41*(1), 199-219. http://dx.doi.org/10.1080/00785236.1995.10422044

Nixon, S. W. (2003). Replacing the Nile: Are anthropogenic nutrients providing the fertility once brought to the Mediterranean by a great river? *Ambio, 32*(1), 30-39. http://dx.doi.org/10.1579/0044-7447-32.1.30

Nixon, S. W., Ammerman, J. W., Atkinson, L. P., Berounsky, V. M., Billen, G., Boicourt, W. C., . . . Seitzinger, S. P. (1996). The fate of nitrogen and phosphorus at the land-sea margin of the North Atlantic Ocean. *Biogeochemistry 35*(1), 141-180. http://dx.doi.org/10.1007/BF02179826

Nriagu, J. O., & Dell, C. I. (1974). Diagenetic formation of iron phosphates in recent lake

sediments. *Am. Mineralogist, 59*, 934-946.

Oakley, S. M., Gold, A. J., & Oczkowski, A. J. (2010). Nitrogen control through decentralized wastewater treatment: Process performance and alternative management strategies. *Ecol. Eng., 36*, 1520–1531. http://dx.doi.org/10.1016/j.ecoleng.2010.04.030

Obia, A., Cornelissen, G., Mulder, J., & Dörsch, P. (2015). Effect of soil pH increase by biochar on NO, N_2O and N_2 production during denitrification in acid soils. *PloS One*, *10*(9), e0138781. https://doi.org/10.1371/journal.pone.0138781

Ormerod, S. J., & Durance, I. (2009). Restoration and recovery from acidification in upland Welsh streams over 25 years. *J. Ecol., 46*(1), 164-174. http://dx.doi.org/10.1111/j.1365-2664.2008.01587.x

Parkin, T. B., & Meisinger, J. J. (1989). Denitrification below the crop rooting zone as influenced by surface tillage. *J. Environ. Qual., 18*, 12–16.

Perry, R. H., Green, D. W., & Maloney, J.O. (1984). *Perry's Chemical Engineer's Handbook*. New York, NY: McGraw-Hill.

Peterjohn, W. T., & Correll, D. L. (1984). Nutrient dynamics in an agricultural watershed: Observations on the role of a riparian forest. *Ecology, 65*, 1466–1475. https://doi.org/10.2307/1939127

Petersen, J. B., Neves, E., & Heckenberger, M. J. (2001). Gift from the past: Terra Preta and prehistoric Amerindian occupation in Amazonia. In *Unknown Amazonia* (pp. 86-105). London, UK: British Museum Press.

Petter, F. A., de Lima, L. B., Marimon Júnior, B. H., Alves de Morais, L., & Marimon, B. S. (2016). Impact of biochar on nitrous oxide emissions from upland rice. *J. Environ. Management*, *169*, 27-33. https://doi.org/10.1016/j.jenvman.2015.12.020

Pimentel, D., Berger, B., Filberto, D., Newton, M., Wolfe, B., Karabinakis, E., . . . Nandagopal, S. (2004). Water resources: Agricultural and environmental issues. *BioScience, 54*(10), 909-918. https://doi.org/10.1641/0006-3568(2004)054[0909:WRAAEI]2.0.CO;2

Pimentel, D., & Pimentel, M. (2006). Global environmental resources versus world

population growth. *Ecol. Economics, 59*(2): 195-198. https://doi.org/10.1016/j.ecolecon.2005.11.034

Pingali, P.L. (2012). Green Revolution: Impacts, limits, and the path ahead. *PNAS, 103*(31), 12302-12308. https://doi.org/10.1073/pnas.0912953109

Pinheiro, J.C., & Bates, D.M. (2000). *Mixed-effects models in S and S-PLUS*. New York: New York: Springer-Verlag New York, Inc. Retrieved from: http://verde.esalq.usp.br/~jorge/cursos/modelos_longitudinais/Mixed%20Effects%20Models%20in%20S%20and%20S-Plus.pdf

Pinheiro, J., Bates, D., DebRoy, S., Sarkar, D., & R Core Team. (2017). nlme: Linear and nonlinear mixed effects models. R package version 3.1-131. Retrieved from: https://CRAN.R-project.org/package=nlme

Portmann, R. W., Daniel, J. S., & Ravishankara, A. R. (2012). Stratospheric ozone depletion due to nitrous oxide: influences of other gases. *Philos. Trans. R. Soc. Lond. B Biol. Sci.*, *367*(1593), 1256-1264. https://doi.org/10.1098/rstb.2011.0377

Powlson, D. S., Addiscott, T. M., Benjamin, N., Cassman, K. G., de Kok, T. M., van Grinsven, H., . . . van Kessel, C. (2008). When does nitrate become a risk for humans? *J. Environ. Qual., 37*, 291-295. http://dx.doi.org/10.2134/jeq2007.0177

Preiser, R. F. (2005). Living within our environmental means: Natural resources and an optimum human population. Retrieved from http://www.jayhanson.org/page50.htm

Preussmann, R. (1984). Carcinogenic N-nitroso compounds and their environmental significance. *Die Naturwissenschaften*, *71*(1), 25-30.

R Core Team. (2016). R: A language and environment for statistical computing. Vienna, Austria: R Foundation for Statistical Computing. Retrieved from: https://www.R-project.org/

Rabalais, N. N. (2004). Chapter 21: Eutrophication. In A. R. Robinson, J. McCarthy, & B. J. Rothschild (Eds.), *The Global Coastal Ocean: Multiscale Interdisciplinary Processes*. (Vol. 13, pp. 819-865). Cambridge, MA: Harvard University Press.

Rabalais, N. N., Turner, R. E., Díaz, R. J., & Justić, D. (2009). Global change and

eutrophication of coastal waters. *ICES J. Mar. Sci., 66*(7), 1528-1537. https://doi.org/10.1093/icesjms/fsp047

Rabalais, N. N., Turner, R. E., & Scavia, D. (2002). Beyond science into policy: Gulf of Mexico hypoxia and the Mississippi River. *BioScience, 52*(2), 129-142. https://doi.org/10.1641/0006-3568(2002)052[0129:BSIPGO]2.0.CO;2

Rabalais, N. N., Wiseman, W. J., Turner, R. E., Sen Gupta, B. K., & Dortch, Q. (1996). Nutrient changes in the Mississippi River and system responses on the adjacent continental shelf. *Estuaries, 19*, 386-407. http://dx.doi.org/10.2307/1352458

Rajapaksha, A. U., Vithanage, M., Zhang, M., Ahmad, M., Mohan, D., Chang, S. X., & Ok, Y. S. (2014). Pyrolysis condition affected sulfamethazine sorption by tea waste biochars. *Bioresour. Technol.*, *166*(Supplement C), 303-308. https://doi.org/10.1016/j.biortech.2014.05.029

Ranalli, A. J., & Macalady, D. L. (2010). The importance of the riparian zone and in-stream processes in nitrate attenuation in undisturbed and agricultural watersheds - A review of the scientific literature. *J. Hydrol.*, *389*(3-4), 406-415. https://doi.org/10.1016/j.jhydrol.2010.05.045

Ravishankara, A. R., Daniel, J. S., & Portmann, R. W. (2009). Nitrous oxide (N_2O): The dominant ozone-depleting substance emitted in the 21st century. *Science, 326*(5949), 123-125. http://dx.doi.org/10.1126/science.1176985

Reddy, K. R., & Patrick, W. H. (1984). Nitrogen transformations and loss in flooded soils and sediments. *CRC Critical Rev. Environ. Control, 13*(4), 273-309.

Revell, L. E., Bodeker, G. E., Smale, D., Lehmann, R., Huck, P. E., Williamson, B. E., … Struthers, H. (2012a). The effectiveness of N_2O in depleting stratospheric ozone. *Geophys. Res. Lett.*, *39*(15), L15806. https://doi.org/10.1029/2012GL052143

Revell, L. E., Bodeker, G. E., Huck, P. E., Williamson, B. E., & Rozanov, E. (2012b). The sensitivity of stratospheric ozone changes through the 21st century to N_2O and CH_4. *Atmos. Chem. Phys.*, *12*(23), 11309–11317. https://doi.org/10.5194/acp-12-11309-2012

Rice, D. C., Schoeny, R., & Mahaffey, K. (2003). Methods and rationale for derivation of

a reference dose for methylmercury by the U.S. EPA. *Risk Anal., 23*(1), 107-115. http://dx.doi.org/10.1111/1539-6924.00294

Richards, F. A. (1965). Chemical observations in some anoxic, sulfide-bearing basins and fjords. In *Advances in water pollution research* (Vol. 3, pp 215-232). London, U.K.: Pergamon Press Inc.

Richards, J. E., & Webster, C. P. (1999). Denitrification in the subsoil of the Broadbalk continuous wheat experiment. *Soil Biol. Biochem. 31*(5), 747-755. http://dx.doi.org/10.1016/S0038-0717(98)00174-6

Robertson, W. D. (2010). Nitrate removal rates in woodchip media of varying age. *Eco. Eng., 36*, 1581-1587. http://dx.doi.org/10.1016/j.ecoleng.2010.01.008

Robertson, W. D., & Anderson, M. R. (1999). Nitrogen removal from landfill leachate using an infiltration bed coupled with a denitrification barrier. *Ground Water Monitoring & Remediation, 19*(4), 73-80. http://dx.doi.org/10.1111/j.1745-6592.1999.tb00242.x

Robertson, W. D., & Cherry, J. A. (1992). Hydrogeology of an unconfined sand aquifer and its effect on the behavior of nitrogen from a large-flux septic system. *Appl. Hydrogeology, 1*, 32-44. http://doi.org/10.1007/PL00010960

Robertson, W. D., & Cherry, J. A. (1995). In situ denitrification of septic-system nitrate using reactive porous media barriers: Field trials. *Groundwater, 33*(1), 99-111. http://doi.org/10.1111/j.1745-6584.1995.tb00266.x

Robertson, W. D., & Merkley, L. C. (2009). In-stream bioreactor for agricultural nitrate treatment. *J. Environ. Qual., 38*, 230-237. http://doi.org/10.2134/jeq2008.0100

Robertson, W. D., Blowes, D. W., Ptacek, C. J., & Cherry, J. A. (2000). Long-term performance of in situ reactive barriers for nitrate remediation. *Ground Water, 38*(5), 689-695. http://doi.org/10.1111/j.1745-6584.2000.tb02704.x

Robertson, W. D., Cherry, J. A., & Sudicky, E. A. (1991). Ground-water contamination from two small septic systems on sand aquifers. *Ground Water, 29*, 82-92. http://doi.org/10.1111/j.1745-6584.1991.tb00500.x

Robertson, W. D., Ford, G. I., & Lombardo, P. S. (2005a). Wood-based filter for nitrate

removal in septic systems. *Tran. ASAE*, *48*(1), 121-128. http://doi.org/10.13031/2013.17954

Robertson, W. D., Vogan, J. L., & Lombardo, P. S. (2008). Nitrate removal rates in a 15-year-old permeable reactive barrier treating septic system nitrate. *Groundwater Monitoring & Remediation, 28*(3), 65-72. http://doi.org/10.1111/j.1745-6592.2008.00205.x

Robertson, W. D., Yeung, N., VanDriel, P. W., & Lombardo, P. S. (2005b). High-permeability layers for remediation of ground water; go wide, not deep. *Ground Water*, *43*(4), 574-581. https://doi.org/10.1111/j.1745-6584.2005.0062.x

Rochette, P., Angers, D. A., Chantigny, M. H., Gasser, M.-O., MacDonald, J. D., Pelster, D. E., & Bertrand, N. (2013). NH3 volatilization, soil concentration and soil pH following subsurface banding of urea at increasing rates. *Canadian J. Soil Sci.*, *93*(2), 261-268. https://doi.org/10.4141/cjss2012-095

Rock, C. A., Irrinki, S., & Pinkham, P. S. (1990). Elimination of ground-water contamination by septic-tank effluent. Proc. *NATO Adv. Workshop on Nitrate Contamination, Exposure, Consequences and Control*, Lincoln, NE: NATO.

Rodríguez, M. T. (2010). Biochar as a strategy for sustainable land management, poverty reduction and climate change mitigation/adaptation? PhD diss. Amsterdam, Netherlands: VU University Amsterdam, Institute of Environmental Studies.

Rogers, M., Lassiter, E., & Easton, Z. (2014). Mitigation of Greenhouse Gas Emissions in Agriculture. Retrieved August 15, 2016, from https://pubs.ext.vt.edu/BSE/BSE-105/BSE-105-PDF.pdf

Rosen, T., & Christianson, L.E. (2017). Performance of denitrifying bioreactors at reducing agricultural nitrogen pollution in a humid subtropical coastal plain climate. *Water*, *9*(2), 112. https://doi.org/10.3390/w9020112

Rosenfield, J. E., Douglass, A. R., & Considine, D. B. (2002). The impact of increasing carbon dioxide on ozone recovery. *J. Geophys. Res.*, *107*(D6), 1-9. https://doi.org/10.1029/2001JD000824

Saarnio, S., Heimonen, K., & Kettunen, R. (2013). Biochar addition indirectly affects

N_2O emissions via soil moisture and plant N uptake. *Soil Biol. Biochem.*, *58*, 99-106. https://doi.org/10.1016/j.soilbio.2012.10.035

Sadeq, M., Moe, C. L., Attarassi, B., Cherkaoui, I., ElAouad, R., & Idrissi, L. (2008). Drinking water nitrate and prevalence of methemoglobinemia among infants and children aged 1-7 years in Moroccan areas. *Int. J. Hygiene Environ. Health, 211*(5-6), 546-554. http://dx.doi.org/10.1016/j.ijheh.2007.09.009

Saliling, W. J. B., Westerman, P. W., & Losordo, T. M. (2007). Wood chips and wheat straw as alternative biofilter media for denitrification reactors treating aquaculture and other wastewaters with high nitrate concentrations. *Aquacultural Eng.*, *37*(3), 222-233. https://doi.org/10.1016/j.aquaeng.2007.06.003

Sánchez-García, M., Roig, A., Sánchez-Monedero, M. A., & Cayuela, M. L. (2014). Biochar increases soil N_2O emissions produced by nitrification-mediated pathways. *Front. Environ. Sci. Eng. China*, *2*. https://doi.org/10.3389/fenvs.2014.00025

Santiago, A., & Santiago, L. (1989). Charcoal chips as a practical substrate for container horticulture in the humid tropics. *Acta Horticulturae, 238*, 141-147. https://doi.org/10.17660/ActaHortic.1989.238.16

Schink, B. (1999). Ecophysiology and ecological niches of prokaryotes. In J.W. Lengeler, G. Drews, & H.G. Schlegel (Eds.), *Biology of the Prokaryotes* (pp. 723-763). New York, USA: Blackwell Science.

Schipper, L. A., Barkle, G. F., & Vojvodić-Vuković, M. (2005). Maximum rates of nitrate removal in a denitrification wall. *J. Environ. Qual., 34*(4), 1270-1276. http://dx.doi.org/10.2134/jeq2005.0008

Schipper, L. A., & McGill, A. (2008). Nitrogen transformation in a denitrification layer irrigated with dairy factory effluent. *Water Research, 42*, 2457-2464. http://dx.doi.org/10.1016/j.watres.2008.01.033

Schipper, L. A., Cameron, S. C., & Warneke, S. (2010a). Nitrate removal from three different effluents using large-scale denitrification beds. *Ecol. Eng. 36*(11), 1552-1557. http://dx.doi.org/10.1016/j.ecoleng.2010.02.007

Schipper, L. A., Robertson, W. D., Gold, A. J., Jaynes, D. B., & Cameron, S. C. (2010b).

Denitrifying bioreactors—An approach for reducing nitrate loads to receiving waters. *Eco. Eng., 36*(11), 1532-1543. http://dx.doi.org/10.1016/j.ecoleng.2010.04.008

Schipper, L. A., & Vojvodić-Vuković, M. (1998). Nitrate removal from groundwater using a denitrification wall amended with sawdust: Field trial. *J. Environ. Qual., 27*(3), 664-668.http://doi.org/10.2134/jeq1998.00472425002700030025x

Schipper L. A., & Vojvodić-Vuković, M. (2000). Nitrate removal from groundwater and denitrification rates in a porous treatment wall amended with sawdust. *Ecol. Eng., 14*(3), 269-278. http://doi.org/10.1016/S0925-8574(99)00002-6

Schipper, L. A., & Vojvodić-Vuković, M. (2001). Five years of nitrate removal, denification and carbon dynamics in a denitrification wall. *Water Resources, 35*(14), 3473-3477.

Schmidt, C. A., & Clark, M. W. (2012). Evaluation of a denitrification wall to reduce surface water nitrogen loads. *J. Environ. Qual., 41*, 724-731. http://doi.org/10.2134/jeq2011.0331

Schmidt, J. P., Dell, C. J., Vadas, P. A., & Allen, A. L. (2007). Nitrogen export from Coastal Plain field ditches. *J. Soil Water Conser.*, *62*(4), 235-243.

Scott, C., Lyons, T. W., Bekker, A., Shen, Y., Poulton, S. W., Chu, X., & Anbar, A. D. (2008). Tracing the stepwise oxygenation of the Proterozoic ocean. *Nature, 452*, 456-459. http://doi.org/10.1038/nature06811

Seitzinger, S. P. (1988). Denitrification in freshwater and coastal marine ecosystems: ecological and geochemical significance. *Limnology and Oceanography 33*, 702-724.

Seitzinger, S., Harrison, J. A., Böhlke, J. K., Bouwman, A. F., Lowrance, R., Peterson, B., . . . Van Drecht, G. (2006). Denitrification across landscapes and waterscapes: A synthesis. *Ecol. Appl., 16*(6), 2064-2090. http://dx.doi.org/10.1890/1051-0761(2006)016[2064:DALAWA]2.0.CO;2

Sharrer, K. L., Christianson, L. E., Lepine, C., & Summerfelt, S. T. (2016). Modeling and

mitigation of denitrification “woodchip” bioreactor phosphorus releases during treatment of aquaculture wastewater. *Ecol. Eng.*, *93*, 135-143. https://doi.org/10.1016/j.ecoleng.2016.05.019

Shih, R., Robertson, W. D., Schiff, S. L., & Rudolph, D. L. (2011). Nitrate controls methyl mercury production in a streambed bioreactor. *J. Environ. Qual., 40*, 1586-1592. http://dx.doi.org/10.2134/jeq2011.0072

Shindo, H. (1991). Elementary composition, humus composition, and decomposition in soil of charred grassland plants. *Soil Sci. Plant Nutr.*, *37*(4), 651-657. https://doi.org/10.1080/00380768.1991.10416933

Sikora, L. J., & Keeney, D. R. (1976). Denitrification of nitrified septic tank effluent. *J. Water Pollution Control Fed., 48*, 2018-2025.

Sims, J. T., Simard, R. R., & Joern, B. C. (1997). Phosphorus loss in agricultural drainage: Historical perspective and current research. *J. Environ. Qual., 27*(2), 277-293. http://doi.org/10.2134/jeq1998.00472425002700020006x

Skaggs, R. W., & van Schilfgaarde, J. (1999). Drainage for Agriculture, Monograph No. 38. Madison, WI: American Society of Agronomy.

Skaggs, R. W., Fausey, N. R., & Evans, R. O. (2012). Drainage water management. *J. Soil Water Conserv.*, *67*(6), 167A-172A. https://doi.org/10.2489/jswc.67.6.167A

Skjemstad, J. O., Clarke, P., Taylor, J. A., Oades, J. M., & Mcclure, S. G. (1996). The chemistry and nature of protected carbon in soil. *Soil Res.*, *34*(2), 251-271. https://doi.org/10.1071/sr9960251

Smil, V. (1999). Nitrogen in crop production: An account of global flows. *Global Biogeochemical Cycles, 13*(2), 647-662. http://doi.org/10.1029/1999GB900015

Smil, V. (2002). Nitrogen and food production: Proteins for human diets. *AMBIO: J. Human Environ., 31*(2), 126-131. https://doi.org/10.1579/0044-7447-31.2.126

Smith, D. R., King, K. W., Johnson, L., Francesconi, W., Richards, P., Baker, D., & Sharpley, A. N. (2015). Surface runoff and tile drainage transport of phosphorus in the midwestern United States. *J. Environ. Qual.*, *44*(2), 495-502. https://doi.org/10.2134/jeq2014.04.0176

Sombroek, W., Ruivo, M. L., Fearnside, P. M., Glaser, B., & Lehmann, J. (2003).

Amazonian dark earths as carbon stores and sinks. In: *Amazonian Dark Earths: Origin, Properties, Management.* (pp. 127-140). Netherlands: Kluwer Academic Publishers. Retrieved from: http://carbon-negative.us/docs/ADEasCarbonSink.pdf

Sotomayor, D., and Rice, C. W. (1996). Denitrification in soil profiles beneath grassland and cultivated soils. *Soil Sci. Soc. Am. J., 60*(6), 1822–1828. http://doi.org/10.2136/sssaj1996.03615995006000060030x

Spiegelhalder, B., Eisenbrand, G., & Preussmann, R. (1976). Influence of dietary nitrate on nitrite content of human saliva: Possible relevance to in vivo formation of N-nitroso compounds. *Food Cosmet. Toxicol.*, *14*(6), 545-548. https://doi.org/10.1016/S0015-6264(76)80005-3

Spielvogel, S., Prietzel, J., & Kögel-Knabner, I. (2008). Soil organic matter stabilization in acidic forest soils is preferential and soil type-specific. *Eur. J. Soil Sci.*, *59*(4), 674-692. https://doi.org/10.1111/j.1365-2389.2008.01030.x

Starr, R. C., & Cherry, J. A. (1994). In situ remediation of contaminated ground water: The funnel and gate system. *Ground Water, 32*, 465-476. http://doi.org/10.1111/j.1745-6584.1994.tb00664.x

Starr, R. C., & Gillham, R. W. (1993). Denitrification and organic carbon availability in two aquifers. *Groundwater, 33*(6), 934-947. http://doi.org/10.1111/j.1745-6584.1993.tb00867.x

Stephany, R. W., & Schuller, P. L. (1980). Daily dietary intakes of nitrate, nitrite and volatile N-nitrosamines in the Netherlands using the duplicate portion sampling technique. *Oncology*, *37*(4), 203-210.

Stewart, W. M., Dibb, D. W., Johnston, A. E., & Smyth, T. J. (2005). The contribution of commercial fertilizer nutrients to food production. *Agron. J., 97*(1), 1-6 http://doi.org/10.2134/agronj2005.0001

Stolarski, R. S., & Cicerone, R. J. (1974). Stratospheric chlorine: possible sink for ozone. *Can. J. Chem.*, 52, 1610-1615.http://doi.org/10.1139/v74-233

Stolarski, R. S., Douglass, A. R., Oman, L. D., & Waugh, D. W. (2015). Impact of future

nitrous oxide and carbon dioxide emissions on the stratospheric ozone layer. *Environ. Res. Lett.*, *10*(3), 034011. https://doi.org/10.1088/1748-9326/10/3/034011

Stoltzenberg, D. (2005). Fritz Haber: Chemist, Nobel Laureate, German, Jew. *Angew. Chem. Int. Ed., 44*, 3957-3961. http://doi.org/10.1002/anie.200485206

Strous, M., Fuerst, J. A., Kramer, E. H., Logemann, S., Muyzer, G., van de Pas-Schoonen, K. T., . . . Jetten, M. S. (1999). Missing lithotroph identified as new planctomycete. *Nature, 400*(6743), 446-449. https://doi.org/10.1038/22749

Svensson, H. (2014). Characterization, toxicity and treatment of wood leachate generated outdoors by the wood-based industry. PhD diss. Sweden: Linnaeus University, Department of Biology and Environmental Science.

Svensson, H., Marques, M., Kaczala, F., & Hogland, W. (2014). Leaching patterns from wood of different tree species and environmental implications related to wood storage areas. *Water Environ. J.*, *28*(2), 277-284. https://doi.org/10.1111/wej.12034

Tanner, C. C., Sukias, J. P. S., Headley, T. R., Yates, C. R., & Stott, R. (2012). Constructed wetlands and denitrifying bioreactors for on-site and decentralised wastewater treatment: Comparison of five alternative configurations. *Ecol. Eng.*, *42*, 112-123. https://doi.org/10.1016/j.ecoleng.2012.01.022

Thomas, D. S. G., & Middleton, N. J. (1993). Salinization: New perspectives on a major desertification issue. *J. Arid Environ., 24*, 95-105. http://doi.org/10.1006/jare.1993.1008

Tiedje, J. M. (1988). Ecology of denitrification and dissimilatory nitrate reduction to ammonium. In A. J. B. Zehnder (Ed.), *Biology of Anaerobic Microorganisms* (pp. 179-244). New York, USA: John Wiley & Sons.

Tiedje, J. M., Simkins, S., & Groffman, P. M. (1989). Perspectives on measurement of denitrification in the field including recommended protocols for acetylene based methods. *Plant Soil, 115*(2), 261-284. http://doi.org/10.1007/BF02202594

Trazzi, P. A., Leahy, J. J., Hayes, M. H. B., & Kwapinski, W. (2016). Adsorption and

desorption of phosphate on biochars. *J. Environ. Chem. Eng., 4*(1), 37-46. https://doi.org/10.1016/j.jece.2015.11.005

Tricker, A. R., & Preussmann, R. (1991). Carcinogenic N-nitrosamines in the diet: Occurrence, formation, mechanisms and carcinogenic potential. *Mutat. Res., 259*, 277-89.

Trimble, W. H. (1851). On charring wood. *Plough, the Loom and the Anvil, 3*, 513-516.

Trimmer, M., Engström, P., & Thamdrup, B. (2013). Stark Contrast in Denitrification and Anammox across the Deep Norwegian Trench in the Skagerrak. *Appl. and Environ. Microbiol.*, *79*(23), 7381-7389. https://doi.org/10.1128/AEM.01970-13

Turner, R. E., & Rabalais, N. N. (1994). Coastal eutrophication near the Mississippi river delta. *Nature, 368*, 619-621. http://doi.org/10.1038/368619a0

UNEP. (2007a). Global environmental outlook 4: Environment for development. Valetta, Malta: Progress Press Ltd. Retrieved from: http://pardee.du.edu/sites/default/files/GEO-4_Report_Full_en.pdf

UNEP. (2007b). Reactive nitrogen in the environment: Too much or too little of a good thing.

USEPA. (2017). Greenhouse gas emissions. Retrieved from: https://www.epa.gov/ghgemissions/overview-greenhouse-gases

Uzoma, K. C., Inoue, M., Andry, H., Zahoor, A., & Nishihara, E. (2011). Influence of biochar application on sandy soil hydraulic properties and nutrient retention. *J. Food Agric. Environ., 9*(3-4), 1137-1143.

Vadas, P. A., Srinivasan, M. S., Kleinman, P. J. A., Schmidt, J. P., & Allen, A. L. (2007). Hydrology and groundwater nutrient concentrations in a ditch-drained agroecosystem. *J. Soil Water Conserv., 64*(4), 178-188.

van de Graaf, A. A., Mulder, A., de Bruijn, P., Jetten, M. S., Robertson, L. A., & Kuenen, J. G. (1995). Anaerobic oxidation of ammonium is a biologically mediated process. *Appl. Environ. Microbiol., 61*(4), 1246-1251.

van den Berg, E. M., Boleij, M., Gijs Kuenen, J., Kleerebezem, R., & van Loosdrecht, M.

C. M. (2016). DNRA and denitrification coexist over a broad range of acetate/N-NO_3^- ratios, in a chemostat enrichment culture. *Front. Microbiol., 7*, 1842. https://dx.doi.org/10.3389%2Ffmicb.2016.01842

van den Berg, E. M., Rombouts, J. L., Gijs Kuenen, J., Kleerebezem, R., & van Loosdrecht, M. C. M. (2017). Role of nitrite in the competition between denitrification and DNRA in a chemostat enrichment culture. *AMB Expr., 7*, 91. https://dx.doi.org/10.1186/s13568-017-0398-x

van Driel, P. W., Robertson, W. D., & Merkley, L. C. (2006). Upflow reactors for riparian zone denitrification. *J. Environ. Qual.*, *35*(2), 412-420. https://doi.org/10.2134/jeq2005.0027

van Kessel, M. A., Speth, D. R., Albertsen, M., Nielsen, P. H., Op den Camp, H. J., Kartal, B., . . . , Lücker, S. (2015). Complete nitrification by a single microorganism. *Nature, 528*(7583), 555-559. https://dx.doi.org/10.1038/nature16459

van Loon, M. (2014). *Mixed effects models: The basic theory and application in R*. Studierichting Business Analytics.

van Niftrik, L., & Jetten, M. S. M. (2012). Anaerobic ammonium-oxidizing bacteria: Unique microorganisms with exceptional properties. *Microbiol. Mol. Biol. Rev., 76*(3), 585-596. http://dx.doi.org/10.1128/MMBR.05025-11

Verma, S., Bhattarai, R., Goodwin, G., & Student, G. (2010). Evaluation of Conservation Drainage Systems in Illinois – Bioreactors. *Proc. 2010 ASABE Annual International Meeting*. Pittsburgh, Pennsylvania: ASABE.

Verstraete, W., & Alexander, M. (1973). Heterotrophic nitrification in samples of natural ecosystems. *Envir. Sci. Technol., 7*(39), 39-42. http://dx.doi.org/10.1021/es60073a007

Vitousek, P. M., & Matson, P. A. (1993). Agriculture, the global nitrogen cycle, and trace gas flux. In *The biogeochemistry of global change: Radiative trace gases* (pp. 193-208). Springer: Boston, MA.

Vitousek, P. M., Mooney, H. A., Lubchenco, J., & Melillo, J. M. (1997). Human

domination of Earth's ecosystems. *Science, 277*, 494-499. http://dx.doi.org/10.1126/science.277.5325.494

Vogan, J. L. (1993). The use of emplaced denitrifying layers to promote nitrate removal from septic effluent. M.Sc. thesis. Waterloo, Ontario: University of Waterloo.

Volokita, M., Abeliovich, A., & Soares, M. I. M. (1996a). Denitrification of groundwater using cotton as energy source. *Water Sci. Technol., 34*(1-2), 379-385. https://doi.org/10.1016/0273-1223(96)00527-6

Volokita, M., Belkin, S., Abeliovich, A., & Soares, M. I. M. (1996b). Biological denitrification of drinking water using newspaper. *Water Resour., 30*(4), 965-971. https://doi.org/10.1016/0043-1354(95)00242-1

von Ahnen, M., Pedersen, P. B., Hoffmann, C. C., Dalsgaard, J. (2016). Optimizing nitrate removal in woodchip beds treating aquaculture effluents. *Aquaculture, 458*, 47-54. http://dx.doi.org/10.1016/j.aquaculture.2016.02.029

von Mutius, E. (2000). The environmental predictors of allergic disease. *J. Allergy Clin. Immunol., 105*(1), 9-19. http://doi.org/10.1016/S0091-6749(00)90171-4

WaiBER. (2012). Retrieved November 15, 2017, from https://waiber.com/projects/denitrifying-bioreactors/

Wakatsuki, T., Esumi, H., & Omura, S. (1993). High performance and N & P-removable on-site domestic waste water treatment system by multi-soil-layering method. *Water Sci. Technol., 27*, 1, 31-40. http://doi.org/10.2965/jswe1978.14.709

Walker, J. C. G., Hays, P. B., & Kasting J. F. (1981). A negative feedback mechanism for the long-term stabilization of Earth's surface temperature. *J. Geophysical Res., 86*(10), 9776-9782. http://doi.org/10.1029/JC086iC10p09776

Wang, W., Tian, W., Dhomse, S., Xie, F., Shu, J., & Austin, J. (2014). Stratospheric ozone depletion from future nitrous oxide increases. *Atmos. Chem. Phys.*, *14*(23), 12967-12982. https://doi.org/10.5194/acp-14-12967-2014

Warneke, S., Schipper, L. A., Bruesewitz, D. A., & Baisden, W. T. (2011a). A comparison of different approaches for measuring denitrification rates in a nitrate removing bioreactor. *Water Res., 45*(14), 4141-4151. https://doi.org/10.1016/j.watres.2011.05.027

Warneke, S., Schipper, L. A., Bruesewitz, D. A., McDonald, I., & Cameron, S. (2011b). Rates, controls and potential adverse effects of nitrate removal in a denitrification bed. *Ecol. Eng., 37*(3), 511-522. https://doi.org/10.1016/j.ecoleng.2010.12.006

Warneke, S., Schipper, L. A., Matiasek, M. G., Scow, K. M., Cameron, S., Bruesewitz, D. A., & McDonald, I. R. (2011c). Nitrate removal, communities of denitrifiers and adverse effects in different carbon substrates for use in denitrification beds. *Water Res., 45*(17), 5463-5475. https://doi.org/10.1016/j.watres.2011.08.007

Watson, S. W., Valos, F. W., & Waterbury, J. B. (1981). The Family Nitrobacteraceae. In Starr, M. B., Stolp, H., Trüper, H. G., Balows, A., & Schlegel, H. G. (Eds.), *The Prokaryotes* (pp. 1005-1022). Berlin, Germany: Springer-Verlag.

Weng, L., Van Riemsqijk, W. H., & Hiemstra, T. (2012). Factors controlling phosphate interaction with iron oxides. *J. Environ. Qual., 41*(3), 628-635. http://doi.org/10.2134/jeq2011.0250

Westholm, L. J. (2006). Substrates for phosphorus removal - Potential benefits for on-site wastewater treatment? *Water Res.*, *40*(1), 23-36. https://doi.org/10.1016/j.watres.2005.11.006

White, M. (2011). Source list and detailed death tolls for the primary megadeaths of the twentieth century. Retrieved from http://necrometrics.com/20c5m.htm

WHO. (2003). Health aspects of air pollution with particulate matter, ozone and nitrogen dioxide. Copenhagen, Denmark: WHO Regional Office for Europe, Copenhagen.

WHO. (2006). WHO air quality guidelines for particulate matter, ozone, nitrogen dioxide and sulphur dioxide, global update 2005: Summary of risk assessment. Geneva, Switzerland: World Health Organization.

WHO. (2008). Health risks of ozone form long-range transboundary air pollution. Copenhagen, Denmark: WHO Regional Office for Europe, Copenhagen.

Wickham, H. (2009). ggplot2: Elegant graphics for data analysis. New York: Springer-Verlag New York, Inc.

Wildman, T. A. (2001). Design of field-scale bioreactors for bioremediation of nitrate in tile drainage effluent. MS thesis. Urbana-Champaign, IL: University of Illinois at Urbana-Champaign, Agricultural & Biological Engineering.

Wilhelm, O. (1902). Improvements in the manufacture of nitric acid and nitrogen oxides. Germany. Patent No. GB190200698.

Wilhelm, O. (1903). Improvements in and relating to the manufacture of nitric acid and oxides of nitrogen. Germany. Patent No. GB190208300.

Williford, J. W., Mckeag, J. A., & Johnston, W. R. (1971). Field techniques for removing nitrates from drainage water. *Trans. ASAE, 14*(1), 167-171. http://doi.org/10.13031/2013.38248

Winogradsky, S. (1892). Contributions a la morphologie des organismes de la nitrification. *Arch. Sci. Biol., 1*, 87-137.

Winter, B. (2011). Pseudoreplication in phonetic research. *Proc. International Congress of Phonetic Science*. pp. 2137-2140. Hong Kong.

Winter, B. (2013). Linear models and linear mixed effects models in R with linguistic applications. arXiv:1308.5499. Retrieved from: http://arxiv.org/pdf/1308.5499.pdf

Woli, K. P., David, M. B., Cooke, R. A., McIsaac, G. F., & Mitchell, C. A. (2010). Nitrogen balance in and export from agricultural fields associated with controlled drainage systems and denitrifying bioreactors. *Ecol. Eng., 36*(11), 1558-1566. https://doi.org/10.1016/j.ecoleng.2010.04.024

Wright, R. F., Alewell, C., Cullen, J. M., Evans, C. D., Marchetto, A., Moldan, F., … Rogora, M. (2001). Trends in nitrogen deposition and leaching in acid-sensitive streams in Europe. *Hydrol. Earth Sys. Sci. Discuss.*, *5*(3), 299-310.

Xu, G., Sun, J., Shao, H., & Chang, S. X. (2014). Biochar had effects on phosphorus sorption and desorption in three soils with differing acidity. *Ecol. Eng.*, *62*, 54-60. https://doi.org/10.1016/j.ecoleng.2013.10.027

Yao, Y., Gao, B., Inyang, M., Zimmerman, A. R., Cao, X., Pullammanappallil, P., & Yang, L. (2011). Removal of phosphate from aqueous solution by biochar derived from anaerobically digested sugar beet tailings. *J. Hazard. Mat.*, *190*(1-3), 501-507. https://doi.org/10.1016/j.jhazmat.2011.03.083

Yao, Y., Gao, B., Zhang, M., Inyang, M., & Zimmerman, A. R. (2012). Effect of biochar

amendment on sorption and leaching of nitrate, ammonium, and phosphate in a sandy soil. *Chemosphere*, *89*(11), 1467-1471. https://doi.org/10.1016/j.chemosphere.2012.06.002

Yeomans, J. C., Bremner, J. M., & McCarty, G. W. (1992). Denitrification capacity and denitrification potential of subsurface soils. *Commun. Soil Sci. Plant Analysis, 23*, 919-927. http://dx.doi.org/10.1080/00103629209368639

Yoo, G., & Kang, H. (2012). Effects of biochar addition on greenhouse gas emissions and microbial responses in a short-term laboratory experiment. *J. Environ. Qual.*, *41*(4), 1193-1202. https://doi.org/10.2134/jeq2011.0157

Young, A. (1804). *The Farmer's Calendar*. London, UK: Cambridge University Press.

Zeileis, A., & Hothorn, T. (2002). Diagnostic checking in regression relationships. *R News, 2*(3), 7-10. Retrieved from: http://CRAN.R-project.org/doc/Rnews/

Zhai, L., CaiJi, Z., Liu, J., Wang, H., Ren, T., Gai, X., … Liu, H. (2015). Short-term effects of maize residue biochar on phosphorus availability in two soils with different phosphorus sorption capacities. *Biol. Fertil. Soils*, *51*(1), 113-122. https://doi.org/10.1007/s00374-014-0954-3

Zhao, L., Cao, X., Mašek, O., & Zimmerman, A. (2013). Heterogeneity of biochar properties as a function of feedstock sources and production temperatures. *J. Hazard. Mat.*, *256-257*, 1-9. https://doi.org/10.1016/j.jhazmat.2013.04.015

Zheng, W., Guo, M., Chow, T., Bennett, D. N, & Rajagopalan, N. (2010). Sorption properties of greenwaste biochar for two triazine pesticides. *J. Hazard. Mat., 181*(1-3), 121-126. https://doi.org/10.1016/j.jhazmat.2010.04.103

Zheng, J., Stewart, C. E., & Cotrufo, M. F. (2012). Biochar and nitrogen fertilizer alters soil nitrogen dynamics and greenhouse gas fluxes from two temperate soils. *J. Environ. Qual.*, *41*(5), 1361-1370. https://doi.org/10.2134/jeq2012.0019

Zornoza, R., Moreno-Barriga, F., Acosta, J. A., Muñoz, M. A., & Faz, A. (2016). Stability, nutrient availability and hydrophobicity of biochars derived from manure, crop residues, and municipal solid waste for their use as soil amendments. *Chemosphere*, *144*, 122-130. https://doi.org/10.1016/j.chemosphere.2015.08.046

Zumft, W. G. (1997). Cell biology and molecular basis of denitrification. *Microbiol Mol*

Biol Rev., 61(4), 533-616.

Appendix A: R Code Used for Statistical Analyses

```
rm(list=ls())

install.packages("car")
install.packages("readxl")
install.packages("ez")
install.packages("lmtest")
install.packages("nlme")
install.packages("ggplot2")
install.packages("RColorBrewer")
install.packages("broom")
install.packages("xlsx")
install.packages("formattable")
install.packages("sjPlot")
install.packages("tidyr")
install.packages("broom")
install.packages("effects")
install.packages("pander")
install.packages("lattice")
install.packages("dplyr")
install.packages("plyr")
install.packages("multcompView")
install.packages("grid")
install.packages("gridExtra")
install.packages("gridGraphics")

library(car)
library(readxl)
library(ez)
library(lmtest)
library(nlme)
library(ggplot2)
library(RColorBrewer)
library(broom)
library(xlsx)
library(formattable)
```

```
library(sjPlot)
library(tidyr)
library(broom)
library(effects)
library(pander)
library(lattice)
library(dplyr)
library(plyr)
library(multcompView)
library(grid)
library(gridExtra)
library(gridGraphics)

# load data and remove rows with missing data points

column.data <- read_excel("column.data.xls")
column.data <- na.omit(column.data)

# set desired levels for plots

column.data$HRT = factor(column.data$HRT, levels = c('12', '6', '3'))
column.data$med = factor(column.data$med, levels = c('w', 'b10', 'b30'))
column.data$P.in = factor(column.data$P.in, levels = c('1.9', '0.6'))
column.data$N.in = factor(column.data$N.in, levels = c('16.1', '4.5'))

# set colors for time series and interaction plots

combocol <- c("tomato", "tan1", "darkolivegreen3", "steelblue")
medcol <- c("burlywood3", "thistle", "gray45")

# set labels for facet grids

label_names_ts <- c(
 '1' = "12",
 '2' = "6",
 '3' = "3",
 '4' = "W",
 '5' = bquote(B[10]),
 '6' = bquote(B[30])
```

```
)

label_names_ts2 <- c(
 '1' = "12",
 '2' = "6",
 '3' = "3",
 'HH' = "HH",
 'HL' = "HL",
 'LH' = "LH",
 'LL' = "LL"
)

label_names_ef <- c(
 '1' = "12",
 '2' = "6 h HRT",
 '3' = "3 h HRT",
 '4' = "W",
 '5' = bquote(B[10]),
 '6' = bquote(B[30])
)

label_names_ef2 <- c(
 '1' = "12",
 '2' = "6",
 '3' = "3",
 '16.1:1.9' = "HH",
 '16.1:0.6' = "HL",
 '4.5:1.9' = "LH",
 '4.5:0.6' = "LL"
)

plot_labeller_ts <- function(variable,value){
 return(label_names_ts[value])
}
plot_labeller_ts2 <- function(variable,value){
 return(label_names_ts2[value])
}
plot_labeller_ef <- function(variable,value){
 return(label_names_ef[value])
```

```
}
plot_labeller_ef2 <- function(variable,value){
 return(label_names_ef2[value])
}

# set custom themes for plots

custom_theme_ts <- theme_linedraw() +
        theme_light() +
        theme_bw() +
             theme(plot.background = element_rect(size = 2, color = "grey30", fill =
 "seashell"),
                   plot.margin = unit(c(.5, 2.5, .5, .5), "lines"),
                   panel.border = element_rect(colour = "black", fill = NA, size = 0.75),

                   plot.title = element_text(size = 30, hjust = 0.5),

                   axis.title.x = element_text(size = 30),
                   axis.title.y = element_text(size = 30),

                   axis.text.x = element_text(color = "black", size = 20),
                   axis.text.y = element_text(color = "black", size = 20),

                   strip.text.x = element_text(size = 20),
                   strip.text.y = element_text(size = 20, angle = 0),
                   strip.background = element_blank(),

                   legend.position = "bottom",
                    legend.text=element_text(size=24),
              legend.title=element_text(size=24),
                   legend.box.background = element_rect(size=0.75)
                   )

custom_theme_ts2 <- custom_theme_ts +
        theme(strip.text.x = element_text(angle = 0, size=30),
                   strip.text.y = element_text(angle = 270, size=30),
                   plot.margin = unit(c(1,4,.5,1), "lines"),
                   strip.background = element_rect(fill = "seashell2", color = "seashell3"))
```

```
custom_theme_int <- custom_theme_ts +
        theme(legend.position = "right",
                plot.margin = unit(c(.5,.5,.5,.5), "lines"),
                legend.background = element_rect(fill = "white"),
                legend.box.background = element_rect(size=0.75),
                legend.key = element_rect(fill = "white")
                )

custom_theme_tukey <- custom_theme_ts +
        theme(plot.margin = unit(c(.5,3,.5,.5), "lines"),
                strip.text.y = element_text(angle = 270),
                legend.title = element_blank(),
                legend.position="none"
                )

# set line segments for addition to plots

N.H.seg.ts <- data.frame(x = 0, y = 16.1, xend = 120, yend = 16.1, N.in = 16.1)
N.L.seg.ts <- data.frame(x = 0, y = 4.5, xend = 120, yend = 4.5, N.in = 4.5)

P.H.seg.ts <- data.frame(x = 0, y = 1.9, xend = 120, yend = 1.9, P.in = 1.9)
P.L.seg.ts <- data.frame(x = 0, y = 0.6, xend = 120, yend = 0.6, P.in = 0.6)

#####################################
### times series plots for N, P, Nred, Pred ###
#####################################

plot.N.out.ts2 <- ggplot(data = column.data, aes(x = time, y = N.out, color = med)) +
 facet_grid(N.in * P.in ~ HRT, scales = "free") +
 geom_point() +
 geom_smooth(span=0.35, aes(fill = med)) +
 ggtitle("HRT (h)") +
 xlab("Time Elapsed (h)") +
 ylab(expression(Effluent~NO[3]^{'-'}-N~Conc.~(mg~L^{-1}))) +
 scale_x_continuous(breaks = 0:120*24) +
 scale_color_manual("Media Type", values = medcol, labels = c("W", bquote(B[10]),
 bquote(B[30]))) +
 scale_fill_manual("Media Type", values = medcol, labels = c("W", bquote(B[10]),
 bquote(B[30]))) +
```

```
 geom_segment(data=N.H.seg.ts,aes(x=x,y=y,yend=yend,xend=xend),inherit.aes=FAL
 SE,linetype=2) +

 geom_segment(data=N.L.seg.ts,aes(x=x,y=y,yend=yend,xend=xend),inherit.aes=FAL
 SE,linetype=2) +
 custom_theme_ts2
plot.N.out.ts2

plot.N.red.ts2 <- ggplot(data = column.data, aes(x = time, y = Nr*100, color = med)) +
 facet_grid(N.in + P.in ~ HRT, scales = "fixed") +
 geom_point() +
 geom_smooth(span=0.35, aes(fill = med)) +
 ggtitle("HRT (h)") +
 xlab("Time Elapsed (h)") +
 ylab(expression(~'%'~NO[3]^{'-'}-N~Removed)) +
 scale_x_continuous(breaks = 0:120*24) +
 scale_y_continuous(breaks = 0:100*25) +
 scale_color_manual("Media Type", values = medcol, labels = c("W", bquote(B[10]),
 bquote(B[30]))) +
 scale_fill_manual("Media Type", values = medcol, labels = c("W", bquote(B[10]),
 bquote(B[30]))) +
 custom_theme_ts2
plot.N.red.ts2

plot.P.out.ts2 <- ggplot(data = column.data, aes(x = time, y = P.out, color = med)) +
 facet_grid(P.in + N.in ~ HRT, scales = "fixed") +
 geom_point() +
 geom_smooth(span=0.35, aes(fill = med)) +
 ggtitle("HRT (h)") +
 xlab("Time Elapsed (h)") +
 ylab(expression(Effluent~PO[4]^{'3-'}-P~Conc.~(mg~L^{-1}))) +
 scale_x_continuous(breaks = 0:120*24) +
 scale_color_manual("Media Type", values = medcol, labels = c("W", bquote(B[10]),
 bquote(B[30]))) +
 scale_fill_manual("Media Type", values = medcol, labels = c("W", bquote(B[10]),
 bquote(B[30]))) +
```

```
 geom_segment(data=P.H.seg.ts,aes(x=x,y=y,yend=yend,xend=xend),inherit.aes=FAL
 SE,linetype=2) +

 geom_segment(data=P.L.seg.ts,aes(x=x,y=y,yend=yend,xend=xend),inherit.aes=FAL
 SE,linetype=2) +
 custom_theme_ts2
plot.P.out.ts2

plot.P.red.ts2 <- ggplot(data = column.data, aes(x = time, y = Pr*100, color = med)) +
 facet_grid(P.in + N.in ~ HRT, scales = "fixed") +
 geom_point() +
 geom_smooth(span=0.35, aes(fill = med)) +
 ggtitle("HRT (h)") +
 xlab("Time Elapsed (h)") +
 ylab(expression(~'%'~PO[4]^{'3-'}-P~Removed)) +
 scale_x_continuous(breaks = 0:120*24) +
 scale_color_manual("Media Type", values = medcol, labels = c("W", bquote(B[10]),
 bquote(B[30]))) +
 scale_fill_manual("Media Type", values = medcol, labels = c("W", bquote(B[10]),
 bquote(B[30]))) +
 custom_theme_ts2
plot.P.red.ts2


# save plots as 15 x 15 pdf files with y2 axes added as grid.text

pdf(file="plot.N.out.ts2.pdf", width=15, height=15)
plot.N.out.ts2
grid.text(unit(0.97,"npc"),0.5,label = expression(Influent~Conc.~(mg~L^{-1})), rot =
 270,gp=gpar(fontsize=30))
grid.text(unit(0.955,"npc"),0.05,label = expression(NO[3]^{'-'}-N), rot =
 300,gp=gpar(fontsize=24))
grid.text(unit(0.92,"npc"),0.05,label = expression(PO[4]^{'3-'}-P), rot =
 300,gp=gpar(fontsize=24))
dev.off()

pdf(file="plot.N.red.ts2.pdf", width=15, height=15)
plot.N.red.ts2
```

```
grid.text(unit(0.97,"npc"),0.5,label = expression(Influent~Conc.~(mg~L^{-1})), rot =
 270,gp=gpar(fontsize=30))
grid.text(unit(0.955,"npc"),0.05,label = expression(NO[3]^{'-'}-N), rot =
 300,gp=gpar(fontsize=24))
grid.text(unit(0.92,"npc"),0.05,label = expression(PO[4]^{'3-'}-P), rot =
 300,gp=gpar(fontsize=24))
dev.off()

pdf(file="plot.P.out.ts2.pdf", width=15, height=15)
plot.P.out.ts2
grid.text(unit(0.97,"npc"),0.5,label = expression(Influent~Conc.~(mg~L^{-1})), rot =
 270,gp=gpar(fontsize=30))
grid.text(unit(0.955,"npc"),0.05,label = expression(PO[4]^{'3-'}-P), rot =
 300,gp=gpar(fontsize=24))
grid.text(unit(0.92,"npc"),0.05,label = expression(NO[3]^{'-'}-N), rot =
 300,gp=gpar(fontsize=24))
dev.off()

pdf(file="plot.P.red.ts2.pdf", width=15, height=15)
plot.P.red.ts2
grid.text(unit(0.97,"npc"),0.5,label = expression(Influent~Conc.~(mg~L^{-1})), rot =
 270,gp=gpar(fontsize=30))
grid.text(unit(0.955,"npc"),0.05,label = expression(PO[4]^{'3-'}-P), rot =
 300,gp=gpar(fontsize=24))
grid.text(unit(0.92,"npc"),0.05,label = expression(NO[3]^{'-'}-N), rot =
 300,gp=gpar(fontsize=24))
dev.off()

# different versions of plots, facet gridded by media type and HRT

N.out.ts.plot <- ggplot(subset(column.data, id %in% c(1:108)), aes(x = time, y = N.out,
 color=combo)) +
                facet_grid(med.cont ~ HRT.cont, labeller = plot_labeller_ts) +
                geom_point() +
                geom_smooth(span=0.35, aes(fill=combo)) +
                ggtitle("HRT (h)") +
        xlab("Time Elapsed (h)") +
                ylab(expression(NO[3]^{'-'}-N~(mg~L^{-1}))) +
        scale_x_continuous(breaks=0:120*24) +
```

```
                scale_color_manual("Influent N/P Conc.",values = combocol) +
                scale_fill_manual("Influent N/P Conc.",values = combocol) +
                custom_theme_ts
N.out.ts.plot
grid.text(unit(0.98,"npc"),0.5,label = "Media Type", rot = 270,gp=gpar(fontsize=30))

P.out.ts.plot <- ggplot(subset(column.data, id %in% c(1:108)), aes(x = time, y = P.out,
 color=combo)) +
                facet_grid(med.cont ~ HRT.cont, labeller = plot_labeller_ts) +
                geom_point() +
                geom_smooth(span=0.35, aes(fill=combo)) +
                ggtitle("HRT (h)") +
                xlab("Time Elapsed (h)") +
                ylab(expression(PO[4]^{'3-'}-P~(mg~L^{-1}))) +
          scale_x_continuous(breaks=0:120*24) +
                scale_color_manual("Influent N/P Conc.",values = combocol) +
                scale_fill_manual("Influent N/P Conc.",values = combocol) +
                custom_theme_ts
P.out.ts.plot
grid.text(unit(0.98,"npc"),0.5,label = "Media Type", rot = 270,gp=gpar(fontsize=30))

N.red.ts.plot <- ggplot(subset(column.data, id %in% c(1:108)), aes(x = time, y =
 100*Nr, color=combo)) +
                facet_grid(med.cont ~ HRT.cont, labeller = plot_labeller_ts) +
                geom_point() +
                geom_smooth(span=0.35, aes(fill=combo)) +
                ggtitle("HRT (h)") +
                xlab("Time Elapsed (h)") +
                ylab(expression('%'~NO[3]^{'-'}-N~Reduced)) +
          scale_x_continuous(breaks=0:120*24) +
          scale_y_continuous(breaks = 0:100*25) +
                scale_color_manual("Influent N/P Conc.",values = combocol) +
          scale_fill_manual("Influent N/P Conc.",values = combocol) +
                custom_theme_ts
N.red.ts.plot
grid.text(unit(0.98,"npc"),0.5,label = "Media Type", rot = 270,gp=gpar(fontsize=30))

P.red.ts.plot <- ggplot(subset(column.data, id %in% c(1:108)), aes(x = time, y = 100*Pr,
 color=combo)) +
```

```
                facet_grid(med.cont ~ HRT.cont, labeller = plot_labeller_ts) +
                geom_point() +
                geom_smooth(span=0.35, aes(fill=combo)) +
                ggtitle("HRT (h)") +
                xlab("Time Elapsed (h)") +
                ylab(expression('%'~PO[4]^{'3-'}-P~Reduced)) +
          scale_x_continuous(breaks=0:120*24) +
          scale_color_manual("Influent N/P Conc.",values = combocol) +
                scale_fill_manual("Influent N/P Conc.",values = combocol) +
                custom_theme_ts
P.red.ts.plot
grid.text(unit(0.98,"npc"),0.5,label = "Media Type", rot = 270,gp=gpar(fontsize=30))

# second versions are facet gridded by conc. combination and HRT

N.out.ts2.plot <- ggplot(data = column.data, aes(x = time, y = N.out, color = med)) +
                facet_grid(combo ~ HRT, scales = "free_y", labeller = plot_labeller_ts2) +
                geom_point() +
                geom_smooth(span=0.35, aes(fill = med)) +
                ggtitle("HRT (h)") +
                xlab("Time Elapsed (h)") +
                ylab(expression(NO[3]^{'-'}-N~(mg~L^{-1}))) +
           scale_x_continuous(breaks = 0:120*24) +
                scale_color_manual("Media Type", values = medcol) +
                scale_fill_manual("Media Type", values = medcol) +
                custom_theme_ts
N.out.ts2.plot
grid.text(unit(0.98,"npc"),0.5,label = "Influent N/P Conc.", rot =
 270,gp=gpar(fontsize=30))
P.out.ts2.plot <- ggplot(data = column.data, aes(x = time, y = P.out, color = med)) +
                facet_grid(combo ~ HRT, scales = "fixed", labeller = plot_labeller_ts2) +
                geom_point() +
                geom_smooth(span=0.35, aes(fill = med)) +
                ggtitle("HRT (h)") +
                xlab("Time Elapsed (h)") +
                ylab(expression(PO[4]^{'3-'}-P~mg~L^{-1})) +
           scale_x_continuous(breaks = 0:120*24) +
                scale_color_manual("Media Type", values = medcol) +
                scale_fill_manual("Media Type", values = medcol) +
```

```
                custom_theme_ts
P.out.ts2.plot
grid.text(unit(0.98,"npc"),0.5,label = "Influent N/P Conc.", rot =
 270,gp=gpar(fontsize=30))

N.red.ts2.plot <- ggplot(data = column.data, aes(x = time, y = Nr*100, color = med)) +
                facet_grid(combo ~ HRT, scales = "fixed", labeller = plot_labeller_ts2) +
                geom_point() +
                geom_smooth(span=0.35, aes(fill = med)) +
                ggtitle("HRT (h)") +
                xlab("Time Elapsed (h)") +
                ylab(expression(~'%'~NO[3]^{'-'}-N~Removed)) +
           scale_x_continuous(breaks = 0:120*24) +
           scale_y_continuous(breaks = 0:100*25) +
                scale_color_manual("Media Type", values = medcol) +
                scale_fill_manual("Media Type", values = medcol) +
                custom_theme_ts
N.red.ts2.plot
grid.text(unit(0.98,"npc"),0.5,label = "Influent N/P Conc.", rot =
 270,gp=gpar(fontsize=30))

P.red.ts2.plot <- ggplot(data = column.data, aes(x = time, y = Pr*100, color = med)) +
                facet_grid(combo ~ HRT, scales = "fixed", labeller = plot_labeller_ts2) +
                geom_point() +
                geom_smooth(span=0.35, aes(fill = med)) +
                ggtitle("HRT (h)") +
                xlab("Time Elapsed (h)") +
                ylab(expression(~'%'~PO[4]^{'3-'}-P~Removed)) +
           scale_x_continuous(breaks = 0:120*24) +
          scale_color_manual("Media Type", values = medcol) +
                scale_fill_manual("Media Type", values = medcol) +
                custom_theme_ts
P.red.ts2.plot
grid.text(unit(0.98,"npc"),0.5,label = "Influent N/P Conc.", rot =
 270,gp=gpar(fontsize=30))

###################################
### old N, P, Nred, Pred interaction plots ###
###################################
```

```
N.out.int.plot <- ggplot(data = column.data, aes(x = interaction(HRT, med.cont, combo),
 y = N.out, fill = med)) +
                facet_grid(.~combo, shrink=T, scales = "free_x") +
                geom_boxplot() +
                ggtitle("Influent N/P Conc.") +
              xlab("HRT (h)") +
                ylab(expression(NO[3]^{'-'}-N~(mg~L^{-1}))) +
           scale_x_discrete(labels=c(rep(c("3", "6", "12"),3))) +
                scale_color_manual("Media Type", values = medcol) +
                scale_fill_manual("Media Type", values = c(medcol)) +
                custom_theme_int
N.out.int.plot

P.out.int.plot <- ggplot(data = column.data, aes(x = interaction(HRT, med.cont, combo),
 y = P.out, fill = med)) +
                facet_grid(.~combo, shrink=T, scales = "free_x") +
                geom_boxplot() +
                ggtitle("Influent N/P Conc.") +
                xlab("HRT (h)") +
                ylab(expression(PO[4]^{'3-'}-P~mg~L^{-1})) +
           scale_x_discrete(labels=c(rep(c("3", "6", "12"),3))) +
                scale_color_manual("Media Type", values = medcol) +
                scale_fill_manual("Media Type", values = c(medcol)) +
                custom_theme_int
P.out.int.plot

N.red.int.plot <- ggplot(data = column.data, aes(x = interaction(HRT, med.cont,
 combo), y = Nr*100, fill = med)) +
                facet_grid(.~combo, shrink=T, scales = "free_x") +
                geom_boxplot() +
                ggtitle("Influent N/P Conc.") +
                xlab("HRT (h)") +
                ylab(expression(~'%'~NO[3]^{'-'}-N~Removed)) +
           scale_x_discrete(labels=c(rep(c("3", "6", "12"),3))) +
                scale_color_manual("Media Type", values = medcol) +
                scale_fill_manual("Media Type", values = c(medcol)) +
            custom_theme_int
N.red.int.plot
```

```
P.red.int.plot <- ggplot(data = column.data, aes(x = interaction(HRT, med.cont, combo),
 y = Pr*100, fill = med)) +
                facet_grid(.~combo, shrink=T, scales = "free_x") +
                 geom_boxplot() +
                ggtitle("Influent N/P Conc.") +
                xlab("HRT (h)") +
                ylab(expression(~'%'~PO[4]^{'3-'}-P~Removed)) +
          scale_x_discrete(labels=c(rep(c("3", "6", "12"),3))) +
                scale_color_manual("Media Type", values = medcol) +
                scale_fill_manual("Media Type", values = c(medcol)) +
                custom_theme_int
P.red.int.plot

##############################
### LME Model Comparisons ###
##############################

# transform variables to factors
# do not want them to be interpreted by the models as continuous

column.data <- read_excel("column.data.xls")
column.data <- na.omit(column.data)

column.data <- within(column.data, {
 trial<-factor(trial)
 column<-factor(column)
 id<-factor(id)
 med<-factor(med)
 combo<-factor(combo)
 HRT <- factor(HRT)
 N.in <- factor(N.in)
 P.in <- factor(P.in)
})

# full lme model for N and subsequent trimmed models

lme.N.full <- lme(N.out~time*med*HRT*N.in*P.in, data=column.data,
        control=ctrl,random=~timelid,correlation = corCAR1(form = ~timelid),
```

```
        method = "ML")
lme.N.drop.time <- lme(N.out~med*HRT*N.in*P.in, data=column.data,
          control=ctrl,random=~timelid,correlation = corCAR1(form = ~timelid),
                method = "ML")
lme.N.drop.med <- lme(N.out~time*HRT*N.in*P.in, data=column.data,
          control=ctrl,random=~timelid,correlation = corCAR1(form = ~timelid),
        method = "ML")
lme.N.drop.HRT <- lme(N.out~time*med*N.in*P.in, data=column.data,
          control=ctrl,random=~timelid,correlation = corCAR1(form = ~timelid),
        method = "ML")
lme.N.drop.N.in <- lme(N.out~time*med*HRT*P.in, data=column.data,
          control=ctrl,random=~timelid,correlation = corCAR1(form = ~timelid),
                method = "ML")
lme.N.drop.P.in <- lme(N.out~time*med*HRT*N.in, data=column.data,
          control=ctrl,random=~timelid,correlation = corCAR1(form = ~timelid),
                method = "ML")

# model comparisons

anova(lme.N.full, lme.N.drop.time)
anova(lme.N.full, lme.N.drop.med)
anova(lme.N.full, lme.N.drop.HRT)
anova(lme.N.full, lme.N.drop.N.in)
anova(lme.N.full, lme.N.drop.P.in)

# full lme model for P and subsequent trimmed models

lme.P.full <- lme(P.out~time*med*HRT*N.in*P.in, data=column.data,
        control=ctrl,random=~timelid,correlation = corCAR1(form = ~timelid),
        method = "ML")
lme.P.drop.time <- lme(P.out~med*HRT*N.in*P.in, data=column.data,
          control=ctrl,random=~timelid,correlation = corCAR1(form = ~timelid),
                method = "ML")
lme.P.drop.med <- lme(P.out~time*HRT*N.in*P.in, data=column.data,
              control=ctrl,random=~timelid,correlation = corCAR1(form = ~timelid),
        method = "ML")
lme.P.drop.HRT <- lme(P.out~time*med*N.in*P.in, data=column.data,
          control=ctrl,random=~timelid,correlation = corCAR1(form = ~timelid),
        method = "ML")
```

```
lme.P.drop.N.in <- lme(P.out~time*med*HRT*P.in, data=column.data,
        control=ctrl,random=~timelid,correlation = corCAR1(form = ~timelid),
              method = "ML")
lme.P.drop.P.in <- lme(P.out~time*med*HRT*N.in, data=column.data,
        control=ctrl,random=~timelid,correlation = corCAR1(form = ~timelid),
              method = "ML")

anova(lme.P.full, lme.P.drop.time)
anova(lme.P.full, lme.P.drop.med)
anova(lme.P.full, lme.P.drop.HRT)
anova(lme.P.full, lme.P.drop.N.in)
anova(lme.P.full, lme.P.drop.P.in)

####################
### Final models ###
####################

lme.N <- lme(N.out~time*med*HRT*N.in*P.in, data=column.data,
      control=ctrl, random=~timelid, correlation = corCAR1(form = ~timelid))

lme.P <- lme(P.out~time*med*HRT*P.in, data=column.data,
      control=ctrl, random=~timelid, correlation = corCAR1(form = ~timelid))

# P models

lme.P.2way <- lme(P.out~(time+med+HRT+N.in+P.in)^2,data=column.data,
      control = ctrl,random=~timelid, correlation = corCAR1(form = ~timelid))
lme.P.2way.time <- lme(P.out~(time+med+HRT+N.in+P.in)^2+
              time:med:HRT+
          time:med:N.in+
              time:med:P.in+
              time:HRT:N.in+
              time:HRT:P.in+
              time:N.in:P.in,
              data=column.data,
              control = ctrl,random=~timelid, correlation = corCAR1(form = ~timelid))
lme.P.3way <- lme(P.out~(time+med+HRT+N.in+P.in)^3,data=column.data,
      control = ctrl,random=~timelid, correlation = corCAR1(form = ~timelid))
```

```
# anovas

anova.lme.N.2way <- round(anova(lme.N.2way, type="marginal"),3)
anova.lme.N.2way.time <- round(anova(lme.N.2way.time, type="marginal"),3)
anova.lme.N.3way <- round(anova(lme.N.3way, type="marginal"),3)

anova.lme.P.2way <- round(anova(lme.P.2way, type="marginal"),3)
anova.lme.P.2way.time <- round(anova(lme.P.2way.time, type="marginal"),3)
anova.lme.P.3way <- round(anova(lme.P.3way, type="marginal"),3)

# summaries

summary.lme.N.2way <- round(summary(lme.N.2way)$tTable,3)
summary.lme.N.2way.time <- round(summary(lme.N.2way.time)$tTable,3)
summary.lme.N.3way <- round(summary(lme.N.3way)$tTable,3)

summary.lme.P.2way <- round(summary(lme.P.2way)$tTable,3)
summary.lme.P.2way.time <- round(summary(lme.P.2way.time)$tTable,3)
summary.lme.P.3way <- round(summary(lme.P.3way)$tTable,3)

# try plotting an effects plots of P.out concentration through time as a function of N.in
 and time

# create excel workbook of model outputs

wb = createWorkbook()

sheet = createSheet(wb, "2way")

addDataFrame(anova.lme.N.2way, sheet=sheet, startColumn=1, startRow=1,
 row.names=TRUE, col.names=T)
addDataFrame(anova.lme.P.2way, sheet=sheet, startColumn=6, startRow=1,
 row.names=TRUE, col.names=T)

sheet = createSheet(wb, "2way.time")

addDataFrame(anova.lme.N.2way.time, sheet=sheet, startColumn=1, startRow=1,
        row.names=TRUE)
```

```
addDataFrame(anova.lme.P.2way.time, sheet=sheet, startColumn=6, startRow=1,
        row.names=TRUE)

sheet = createSheet(wb, "3way")

addDataFrame(anova.lme.N.3way, sheet=sheet, startColumn=1, startRow=1,
        row.names=TRUE)
addDataFrame(anova.lme.P.3way, sheet=sheet, startColumn=6, startRow=1,
        row.names=TRUE)

saveWorkbook(wb, "column.data.lme.output.xlsx")

# check assumptions

plot(fitted(lme.N.2way), resid(lme.N.2way, type = "normalized"))
plot(fitted(lme.N.2way.time), resid(lme.N.2way.time, type = "normalized"))
plot(fitted(lme.N.3way), resid(lme.N.3way, type = "normalized"))

plot(fitted(lme.P.2way), resid(lme.P.2way, type = "normalized"))
plot(fitted(lme.P.2way.time), resid(lme.P.2way.time, type = "normalized"))
plot(fitted(lme.P.3way), resid(lme.P.3way, type = "normalized"))

# effects plots

plot(allEffects(lme.N.2way))
plot(allEffects(lme.N.2way.time))
plot(allEffects(lme.N.3way))

lme.N.2way.effects <- as.data.frame(allEffects(lme.N.2way), lme.N.2way,
 confidence.level = 0.95)
lme.P.effects <- as.data.frame(effect("time*med*HRT*N.in*P.in", lme.P,
 confidence.level = 0.95))

lme.N.effects$HRT = factor(lme.N.effects$HRT, levels=c('12','6','3'))
lme.N.effects$P.in = factor(lme.N.effects$P.in, levels=c('1.9','0.6'))
lme.P.effects$HRT = factor(lme.P.effects$HRT, levels=c('12','6','3'))
lme.P.effects$P.in = factor(lme.P.effects$P.in, levels=c('1.9','0.6'))
```

```
lme.N.effects.plot <- ggplot(lme.N.effects, aes(time, fit, color=med)) +
 geom_point(size=0) +
 xlab("Time Elapsed (h)") + ylab(expression(NO[3]^{'-'}-N~mg~L^{-1})) +
 facet_grid(N.in:P.in~HRT)+custom_theme_int+
 scale_fill_manual(values = c(medcol)) + scale_color_manual(values = medcol) +
 geom_line(aes(linetype = med),size=.75) +
 geom_ribbon(aes(ymin=lower, ymax=upper,x=time, fill=med, linetype=med),
 alpha=0.3, colour =NA)
lme.N.effects.plot

lme.P.effects.plot <- ggplot(lme.P.effects, aes(time, fit, color=med)) +
 geom_point(size=0) +
 xlab("Time Elapsed (h)") + ylab(expression(PO[4]^{'3-'}-P~mg~L^{-1})) +
 facet_grid(N.in:P.in~HRT)+custom_theme_int+
 scale_fill_manual(values = c(medcol)) + scale_color_manual(values = medcol) +
 geom_line(aes(linetype = med),size=.75) +
 geom_ribbon(aes(ymin=lower, ymax=upper,x=time, fill=med, linetype=med),
 alpha=0.3, colour =NA)
lme.P.effects.plot

ggsave('lme.N.effects.plot.pdf', plot=lme.N.effects.plot,width=15.1, height=8.5, unit='in',
 path="/Users/bscoleman/Downloads/column.data.plots")
ggsave('lme.P.effects.plot.pdf', plot=lme.P.effects.plot,width=15.1, height=8.5, unit='in',
 path="/Users/bscoleman/Downloads/column.data.plots")



### effects package for interactions

lme.N.effects <- as.data.frame(effect("time*med*HRT*combo", lme.N, confidence.level
 = 0.95))
lme.P.effects <- as.data.frame(effect("time*med*HRT*combo", lme.P, confidence.level
 = 0.95))

ggplot(lme.N.effects, aes(time, fit, color=med)) + geom_point(size=0) +
 facet_grid(HRT~combo)+custom_theme_int+
 scale_fill_manual(values = c(medcol)) + scale_color_manual(values = medcol) +
 geom_line(aes(linetype = med),size=.75) +
```

```
 geom_ribbon(aes(ymin=lower, ymax=upper,x=time, fill=med, linetype=med),
 alpha=0.1,colour=NA)
ggplot(lme.P.effects, aes(time, fit, color=med)) + geom_point(size=0) +
 facet_grid(HRT~combo)+custom_theme_int+
 scale_fill_manual(values = c(medcol)x) + scale_color_manual(values = medcol) +
 geom_line(aes(linetype = med),size=.75) +
 geom_ribbon(aes(ymin=lower, ymax=upper,x=time, fill=med, linetype=med),
 alpha=0.1,colour=NA)


################
### ezANOVAs ###
################

# read in excel data again, dropping last three time point because of unbalanced data

column.data <- read_excel("column.data.xls")
column.data <- na.omit(column.data)

column.data = column.data[column.data$time!=72 & column.data$time!=96 &
 column.data$time!=120,]

column.data <- within(column.data, {
 trial<-factor(trial)
 column<-factor(column)
 id<-factor(id)
 med<-factor(med)
 HRT<-factor(HRT)
 combo<-factor(combo)
 time<-factor(time)
 P.in<-factor(P.in)
 N.in<-factor(N.in)
})

column.data$HRT = factor(column.data$HRT, levels=c('12','6','3'))
column.data$med = factor(column.data$med, levels=c('w','b10','b30'))

# N ezANOVA
```

```
ezANOVA.N <- ezANOVA(data = column.data,
        dv = N.out,
        wid = id,
        between = .(med,N.in,P.in,HRT),
        detailed = T)
ezANOVA.N # interactions containing P.in not significant, drop P.in from anova

ezANOVA.N <- ezANOVA(data = column.data,
        dv = N.out,
        wid = id,
        between = .(med,N.in,HRT),
        detailed = T,
        return_aov = T)

# P ezANOVA

ezANOVA.P <- ezANOVA(data = column.data,
        dv = P.out,
        wid = id,
        between = .(med,N.in,P.in,HRT),
        detailed = T,
        return_aov = T)
ezANOVA.P

# ezANOVAs for HRT plots regardless of med

ezANOVA.N.drop.med <- ezANOVA(data = column.data,
        dv = N.out,
        wid = id,
         between = .(N.in,HRT),
        detailed = T,
        return_aov = T)
ezANOVA.N.drop.med

ezANOVA.P.drop.med <- ezANOVA(data = column.data,
        dv = P.out,
        wid = id,
         between = .(N.in,P.in,HRT),
        detailed = T,
```

```
        return_aov = T)
ezANOVA.P.drop.med

wb = createWorkbook()
sheet = createSheet(wb, "ezANOVA.N")
addDataFrame(ezANOVA.N$ANOVA, sheet=sheet, startColumn=1, startRow=1,
 row.names=TRUE)
sheet = createSheet(wb, "ezANOVA.P")
addDataFrame(ezANOVA.P$ANOVA, sheet=sheet, startColumn=1, startRow=1,
 row.names=TRUE)
sheet = createSheet(wb, "ezANOVA.N.drop.med")
addDataFrame(ezANOVA.N.drop.med$ANOVA, sheet=sheet, startColumn=1,
 startRow=1, row.names=TRUE)
sheet = createSheet(wb, "ezANOVA.P.drop.med")
addDataFrame(ezANOVA.P.drop.med$ANOVA, sheet=sheet, startColumn=1,
 startRow=1, row.names=TRUE)
saveWorkbook(wb, "column.data.ezanovas.xlsx")

#################
### TukeyHSDs ###
#################

# TukeyHSDs for optimal anovas

tukey.N <- TukeyHSD(ezANOVA.N$aov)
tukey.N

tukey.P <- TukeyHSD(ezANOVA.P$aov)
tukey.P

# TukeyHSDs for optimal anovas, dropped med

tukey.N.drop.med <- TukeyHSD(ezANOVA.N.drop.med$aov)
tukey.N.drop.med

tukey.P.drop.med <- TukeyHSD(ezANOVA.P.drop.med$aov)
tukey.P.drop.med

wb = createWorkbook()
```

```
sheet = createSheet(wb, "tukey.N")
addDataFrame(tukey.N$`med:N.in:HRT`, sheet=sheet, startColumn=1, startRow=1,
 row.names=TRUE)
sheet = createSheet(wb, "tukey.P")
addDataFrame(tukey.P$`med:N.in:P.in:HRT`, sheet=sheet, startColumn=1,
 startRow=1, row.names=TRUE)
sheet = createSheet(wb, "tukey.N.drop.med")
addDataFrame(tukey.N.drop.med$`N.in:HRT`, sheet=sheet, startColumn=1,
 startRow=1, row.names=TRUE)
sheet = createSheet(wb, "tukey.P.drop.med")
addDataFrame(tukey.P.drop.med$`N.in:P.in:HRT`, sheet=sheet, startColumn=1,
 startRow=1, row.names=TRUE)
saveWorkbook(wb, "column.data.tukey.results.xlsx")

############################################################
### interaction plots with significant differences from TukeyHSD plotted ###
############################################################

# N

N.L.seg <- data.frame(x = 1, y = 4.5, xend = 3, yend = 4.5, N.in = "4.5")
N.H.seg <- data.frame(x = 1, y = 16.1, xend = 3, yend = 16.1, N.in = "16.1")

column.data$N.in = factor(column.data$N.in, levels = c('16.1','4.5'))

plot.N.out.tukey.full <- ggplot(data = column.data, aes(x = interaction(med, HRT), y =
 N.out, fill = med)) +
 facet_grid(N.in ~ HRT, shrink = T, scales = "free") +
 geom_boxplot() +
 scale_color_manual("Media Type", values = medcol, labels = c("W", bquote(B[10]),
 bquote(B[30]))) +
 scale_fill_manual("Media Type", values = medcol, labels = c("W", bquote(B[10]),
 bquote(B[30]))) +
 xlab("Media Type") +
 ylab(expression(Effluent~NO[3]^{'-'}-N~Conc.~(mg~L^{-1}))) +
 ggtitle("HRT (h)") +
 scale_x_discrete(labels = c(rep(c("W", bquote(B[10]), bquote(B[30])), 3))) +
```

```
 geom_segment(data=N.L.seg,aes(x=x,y=y,yend=yend,xend=xend),inherit.aes=FALSE
 ,linetype=2) +

 geom_segment(data=N.H.seg,aes(x=x,y=y,yend=yend,xend=xend),inherit.aes=FALS
 E,linetype=2) +
 custom_theme_ts2
plot.N.out.tukey.full

column.data$N.in = factor(column.data$N.in, levels = c('4.5','16.1'))

plot.N.out.tukey.HRT <- ggplot(data = column.data, aes(x = interaction(N.in, HRT), y =
 N.out)) +
 facet_grid(.~N.in, shrink = T, scales = "free") +
 geom_boxplot(fill = c("grey75")) +
 xlab("HRT (h)") +
 ylab(expression(Effluent~NO[3]^{'-'}-N~Conc.~(mg~L^{-1}))) +
 ggtitle(expression(Influent~NO[3]^{'-'}-N~Conc.~(mg~L^{-1}))) +
 scale_x_discrete(labels=c(rep(c("12", "6", "3"),4))) +

 geom_segment(data=N.L.seg,aes(x=x,y=y,yend=yend,xend=xend),inherit.aes=FALSE
 ,linetype=2) +

 geom_segment(data=N.H.seg,aes(x=x,y=y,yend=yend,xend=xend),inherit.aes=FALS
 E,linetype=2) +
 custom_theme_ts2
plot.N.out.tukey.HRT

# P

P.L.seg <-data.frame(x=1,y=0.6,xend=3,yend=0.6, P.in = 0.6)
P.H.seg <-data.frame(x=1,y=1.9,xend=3,yend=1.9, P.in = 1.9)

column.data$P.in= factor(column.data$P.in, levels=c('1.9','0.6'))
column.data$N.in= factor(column.data$N.in, levels=c('16.1','4.5'))

plot.P.out.tukey.full <- ggplot(data = column.data, aes(x = interaction(med, HRT), y =
 P.out, fill=med)) +
 facet_grid(P.in+N.in~HRT, shrink=T, scales = "free_x") +
```

```
 geom_boxplot() +
 xlab("Media Type") +
 ylab(expression(Effluent~PO[4]^{'3-'}-P~Conc.~(mg~L^{-1}))) +
 ggtitle("HRT (h)")+
 scale_x_discrete(labels=c(rep(c("W", bquote(B[10]), bquote(B[30])),3))) +
 scale_color_manual("Media Type", values = medcol, labels = c("W", bquote(B[10]),
 bquote(B[30]))) +
 scale_fill_manual("Media Type", values = medcol, labels = c("W", bquote(B[10]),
 bquote(B[30]))) +

 geom_segment(data=P.H.seg,aes(x=x,y=y,yend=yend,xend=xend),inherit.aes=FALS
 E,linetype=2) +

 geom_segment(data=P.L.seg,aes(x=x,y=y,yend=yend,xend=xend),inherit.aes=FALSE
 ,linetype=2) +
 custom_theme_ts2
plot.P.out.tukey.full

column.data$P.in= factor(column.data$P.in, levels=c('0.6','1.9'))
column.data$N.in= factor(column.data$N.in, levels=c('4.5','16.1'))
column.data$HRT= factor(column.data$HRT, levels=c('12','6','3'))

plot.P.out.tukey.HRT <- ggplot(data = column.data, aes(x = interaction(P.in, N.in, HRT),
 y = P.out)) +
 facet_grid(.~P.in+N.in,shrink=T,scales = "free_x") +
 geom_boxplot(fill=c("grey75")) +
 xlab("HRT (h)") +
 ylab(expression(Effluent~PO[4]^{'3-'}-P~Conc.~(mg~L^{-1})))+
 scale_x_discrete(labels=c(rep(c("12", "6", "3"),4))) +
 ggtitle(expression(Influent~Conc.~(mg~L^{-1}))) +

 geom_segment(data=P.H.seg,aes(x=x,y=y,yend=yend,xend=xend),inherit.aes=FALS
 E,linetype=2) +

 geom_segment(data=P.L.seg,aes(x=x,y=y,yend=yend,xend=xend),inherit.aes=FALSE
 ,linetype=2) +
 custom_theme_ts2 +
 theme(plot.margin = unit(c(.5,7.5,.5,.5), "lines"))
plot.P.out.tukey.HRT
```

```
# save plots

pdf(file="plot.N.out.tukey.full.pdf", width=15, height=15)
plot.N.out.tukey.full
grid.text(unit(0.97,"npc"),0.5,label =expression(Influent~NO[3]^{'-'}-N~Conc.~(mg~L^{-
 1})), rot = 270,gp=gpar(fontsize=30))
dev.off()

pdf(file="plot.N.out.tukey.HRT.pdf", width=10, height=10)
plot.N.out.tukey.HRT
dev.off()

pdf(file="plot.P.out.tukey.full.pdf", width=15, height=15)
plot.P.out.tukey.full
grid.text(unit(0.97,"npc"),0.5,label = expression(Influent~Conc.~(mg~L^{-1})), rot =
 270,gp=gpar(fontsize=30))
grid.text(unit(0.955,"npc"),0.05,label = expression(PO[4]^{'3-'}-P), rot =
 300,gp=gpar(fontsize=24))
grid.text(unit(0.92,"npc"),0.05,label = expression(NO[3]^{'-'}-N), rot =
 300,gp=gpar(fontsize=24))
dev.off()

pdf(file="plot.P.out.tukey.HRT.pdf", width=15, height=8)
plot.P.out.tukey.HRT
grid.text(unit(0.95,"npc"),0.88,label = expression(PO[4]^{'3-'}-P), rot =
 0,gp=gpar(fontsize=24))
grid.text(unit(0.95,"npc"),0.81,label = expression(NO[3]^{'-'}-N), rot =
 0,gp=gpar(fontsize=24))
dev.off()

############################
### Stats table of column.data ###
############################

means.N.out <- aggregate(N.out ~ HRT:med:N.in, column.data, mean)
means.N.out$N.out <- round(means.N.out$N.out, 3)
means.P.out <- aggregate(P.out ~ HRT:med:N.in:P.in, column.data, mean)
means.P.out$P.out <- round(means.P.out$P.out, 3)
```

```
means.Nr <- aggregate(Nr ~ HRT:med:N.in, column.data, mean)
means.Nr$Nr <- round(means.Nr$Nr, 3)
means.Nr$Nr <- means.Nr$Nr * 100
means.Pr <- aggregate(Pr ~ HRT:med:N.in:P.in, column.data, mean)
means.Pr$Pr <- means.Pr$Pr * 100
means.Pr$Pr <- round(means.Pr$Pr, 3)

medians.N.out <- aggregate(N.out ~ HRT:med:N.in, column.data, median)
medians.N.out$N.out <- round(medians.N.out$N.out, 3)
medians.P.out <- aggregate(P.out ~ HRT:med:N.in:P.in, column.data, median)
medians.P.out$P.out <- round(medians.P.out$P.out, 3)

stdev.N.out <- aggregate(N.out ~ HRT:med:N.in, column.data, sd)
stdev.N.out$N.out <- round(stdev.N.out$N.out, 2)
stdev.P.out <- aggregate(P.out ~ HRT:med:N.in:P.in, column.data, sd)
stdev.P.out$P.out <- round(stdev.P.out$P.out, 2)

stat.table <- cbind(means.N.out, means.Nr$Nr, medians.N.out$N.out,
 stdev.N.out$N.out,
        means.P.out, means.Pr$Pr, medians.P.out$P.out, stdev.P.out$P.out)

wb = createWorkbook()

sheet = createSheet(wb, "stat.table")

addDataFrame(stat.table, sheet=sheet, startColumn=1, startRow=1,
 row.names=TRUE)

saveWorkbook(wb, "column.data.stat.table.xlsx")
```